GEOLOGICAL SURVEY OF CANADA

OPEN FILE 1997

PROVENANCE, DIAGENESIS AND GEOCHEMISTRY OF THE ALBERT FORMATION, EASTERN NEW BRUNSWICK

Ali Chowdhury and J.P.A.Noble

Canada

1989

Natural Resources and Energy
New Brunswick

Ressources naturelles et Énergie
Nouveau-Brunswick

Contribution to Canada-New Brunswick Mineral Development Agreement 1984-89, a subsidiary agreement under the Economic and Regional Development Agreement.
Project funded by the Geological Survey of Canada.

Contribution à l'Entente auxiliaire Canada/Nouveau-Brunswick sur l'exploitation minérale 1984-89 faisant partie de l'Entente de développement économique et régional. Ce projet a été financé par la Commission géologique du Canada.

Energy, Mines and Resources Canada

Énergie, Mines et Ressources Canada

GEOLOGICAL SURVEY OF CANADA
OPEN FILE 1997

PROVENANCE, DIAGENESIS AND GEOCHEMISTRY OF THE ALBERT FORMATION, EASTERN NEW BRUNSWICK

Ali Chowdhury and J.P.A.Noble
Department of Geology
University of New Brunswick
P.O. Box 4400
Fredericton, New Brunswick
E3B 5P7

ABSTRACT

The Lower Carboniferous Albert Formation of the Moncton subbasin in southern New Brunswick is an ancient lacustrine and associated fluvial deltaic deposit. It forms the reservoir of the only oil and gas field in onshore Atlantic Canada.

Provenance of the Albert Formation sandstones is a mix of granite/granodiorite and gabbroic complexes, which includes both Westmorland Uplift and the Caledonia complex. Sediments are immature to submature and suffered short transport distances. Chemical parameters suggest both humid and arid climatic conditions during deposition of the Albert Formation.

A detailed diagenetic study has revealed eodiagenetic to late mesodiagenetic burial stages for the Albert Formation. Dominant authigenic minerals occur as porefill and prelining and include calcite, ankerite, quartz overgrowth, chlorite and illite. Carbon and oxygen isotope analyses of carbonate cements and veins suggest inorganic derivation, with minor contribution from bacterial oxidation at shallow depth and skeletal material on deeper burial. From isotope data and cross-cutting relationships of veins, two sets of fractures were established.

Porosity in the Albert Formation sandstones is mainly secondary caused by organic acids derived during maturation of interbedded shales. Dissolution textures in the framework grains show corrosion of specific sites and has been suggested as surface reaction controlled dissolution.

Organic matter type in the eastern part of the subbasin is mainly algal in origin and in the west terrestrial organic matter predominates. Most of the shales in the Albert Formation show "oil-window" maturation. Hydrocarbons are highly paraffinic, show identical API gravity and are derived from the same maturation level.

INTRODUCTION

The Early Carboniferous Albert Formation in the Moncton Subbasin in southern New Brunswick forms the only gas and hydrocarbon reservoir in onshore Atlantic Canada. The Stoney Creek oil and gas field is located on a structural high in the eastern part of the subbasin and was discovered in 1909. Original estimate was 17.7 million barrels of oil worth 2.6 million recoverable (Carter and Shaw, 1979). However, recovery was poor and by 1982 only 782,833 barrels of oil and 28,253,360 mcf of gas have been produced. The source rock of these hydrocarbons primarily is the medial organic ~~rock~~ rich Frederick Brook Member and the fluvial deltaic sandstones for the stratigraphically controlled reservoir.

This report attempts to explain and understand the different processes involved in the diagenesis of the Albert Formation. Petrographic, provenance and depositional environmental studies were undertaken to establish a basin evolution model during Albert time. Organic geochemical aspects of the source rock were also examined to gain a better understanding of the hydrocarbon potential in different parts of the basin.

Geologic Setting

The Albert Formation occurs in the Moncton Subbasin of the southeast New Brunswick within the larger Maritimes basin (Williams, 1974). This subbasin is bounded on the northwest by the pre-Carboniferous basement of the Kingston-Indian Mountain Uplift and in the southeast by the Caledonia Uplift. The eastern end of the basin is bounded and partly bifurcated by the predominantly granitic Westmorland Uplift (Fig. 1). Basement is composed of Precambrian to Devonian, polydeformed and metamorphosed sedimentary, pyroclastic and mafic volcanic strata which contain inclusions

of mafic and felsic plutons (Pickerill et al., 1985).

Age and Stratigraphy

On the basis of plant remains (e.g., Lepidodendron corrugatum, Cyclopteris acadica, Dadxylon antiquius and Allepthoteris helerophylla) the Albert Formation was given a Mississippian age (Dawson, 1969; Bell, 1927, 1929). Later work (Gussow, 1953; Greiner, 1974; Varma, 1969; Hacquebard, 1972) based on the miospore flora and the palynomorphs, however, indicate a late Devonian to Tournaisian and possibly early Visean age. Recently, Utting (1987) on a detailed study of the Albert Formation polynomorph assemblages, suggested a correlation with the Spelaeotciletes pretiosus-Raistrickia clavata (PC) spore zone of Tournaisian, late Tn2 to early Tn3, age of Western Europe.

Oil and gas discoveries and extensive oil shale occurrences resulted in a detailed geologic study on the Albert Formation by Gussow (1953), and subsequent studies by Greiner (1962), Howie (1972), Pickerill and Cantes (1980, 1985) and Smith (1987). A generalized stratigraphic succession of different lithostratigraphic units and their relation to the Albert Formation ~~is~~ has been summarized ~~in Figure 2~~ by Pickerill et al. (1985).

Different stratigraphic nomenclatures have been proposed in an attempt to correlate different lithologic units within the Albert Formation (e.g., Pickerill et al., 1985). Driller sand terminology, based on the classification of the different sand packages, works as a useful guide as a correlation tool within the oil field (Howie, 1968, 1972, 1979). These driller sand packages (e.g., I to VI) also contain a highly oil wet kerogeneous shale (i.e., unit V). Because of the rapid lateral variation of the Albert lithofacies, this classification scheme falls short in

correlation over wide areas and in cases, even within the oilfield (St. Peter, pers. comm.). Also the shortcoming of this scheme developes from the basis of classification - The presence or absence of hydrocarbon producing units (Norman, 1932; Henderson, 1940). Greiner's (1962) three-fold subdivision ~~(Figure 2)~~ of the Albert Formation is preferred by many authors (e.g., Varma, 1969; Greiner, 1974, 1977; Hea, 1974; Pickerill and Carter, 1980; Macauley and Ball, 1982; Macauley et al., 1984) because it works as a better guide in the correlation of the lithofacies in the entire basin. However, Greiner's (1962) scheme is primarily based on the presence of the Frederick Brook shale in the succession and lithologic variation in the individual units. In section where the Frederick Brook Member is missing and the lithology is gradational, differentiation into individual members becomes difficult. Faced with this problem, some authors have rejected the above schemes and simply describe the Albert Formation as a single unit (McCutcheon, 1978; McLeod and Ruitenberg, 1978; McLeod, 1980 and St. Peter, 1982). Macauley et al., (1984) also proposed a classification of the Frederick Brook Member at Albert Mines into laminated marlstone, clay marlstone and dolomitic marlstone. This classification 'scheme' also failed in basin-wide correlation (Wright, 1982).

Recently, with the availability of drilling data of several deep wells in the subbasin, more subsurface stratigraphic information have been revealed. In the Stoney Creek oil field wells and in Irving Chevron Hillsborough-1, in the subsurface three distinct sandstone packages separated by organic rich shales have been observed. In the deep (3000 meters) Irving Chevron Hillsborough-1, at the bottom section another package of sands have been noted. This sand package is not observed in other adjacent wells. The top three sandstone packages are also

correlatable by sand/shale ratios (Foley, pers. comm.). Because of the consistency of occurrence of these sandstone packages in the oil field and as far south as Hillsborough-1, these sandstone packages are named as I, II, III and IV in descending order. The main purpose to float this physical subdivision is to report the existence of such a sequence and its possible use as a local correlation tool, particularly in the oil field and in the south in Hillsborough-1. Further west of Hillsborough or in the east of the oil field this sequence is missing.

The contacts between the lower Memramcook and the overlying Albert is arbitrarily drawn where the grey beds appear dominant as opposed to the bottom red Memramcook Formation. The upper contact is also defined by a colour change from grey Albert to red Weldon (Pickerill et al., 1985). The change in colour in transition from Memramcook to Albert and to Weldon is gradual rather than abrupt. In the adjacent Sackville Subbasin, Martel (1987) suggested that the colour change from redbeds in the Memramcook to grey beds in the Albert Formation could be due to rapid subsidence and lake development, as opposed to changes in the climate. The gradual change in colour, by itself, probably suggest that the level of the water table was the major controlling factor (e.g., oxidation - reduction reactions) in contributing the colour of sediments. Berner (1981) also suggested that in many continental fluviatile sediments due to oxic decomposition of organic matter, ferric oxide minerals are not reduced. As a result, upon burial and diagenesis they are transformed to hematite thus imparting a red colour to the enclosing sediment (van Houten, 1973).

From the above observations, it can be concluded that any generalized stratigraphic nomenclature to describe and correlate stratigraphic sections in the entire Moncton Subbasin is poised with numerous limitations because

of highly diachronous nature and rapid variation in lithofacies.

Depositional Environments

A detailed study on the depositional environments of the Albert Formation have been carried out by numerous authors (Gussow, 1953; Greiner, 1962; Howie, 1973; Pickerill et al., 1985; Carter and Pickerill, 1980; St. Peter, 1981; and many others) and it has been suggested that these sediments were deposited in lacustrine and associated fluvial-deltaic environments. However, no geochemical approaches were undertaken before to substantiate the interpretations based on the lithofacies character and association. Although reconstruction of environments are generally based on interpretations from sedimentary facies and syndepositional structures, the aqueous reservoir that hosts all the incoming detritus, also by its own, leaves behind characteristic chemical imprints in the sediments. In particular, as in the case of the lacustrine Albert Formation, these chemical signatures are of significant importance for they record organic matter habitat, oxic-anoxic levels and the energy conditions in the basin. To understand the lake evolution and the development of the associated facies, vertical and lateral distribution of different kerogen types, organic carbon/sulfur relationships in the autocthonous facies (shales/marlstones) and sedimentary facies characters have been incorporated in this study.

The following observations gathered from surface outcrop and subsurface core studies and the literature, provide some general clues to the nature of the Albert Formation depositional regime:

1) Current formed structures in both coarse and fine sandstone facies are less commonly present. Most common are symmetrical wave ripples and

cross beds are rarely observed. Wave formed ripples parallel the Caledonia Highlands and the Kingston Uplift (Greiner, 1962), also well developed ripple networks were observed in the Boudreau and Norton sections. Norton section also contain oncolite beds (Plate 1) which have been observed also around the margins of the Great Salt Lake, Utah. Symmetrical wave ripples are formed by waves, oscillating in sheltered standing body of waters, such as lakes. These regions possibly reflect the ancient nearshore region of the lake Albert. Crossbedded sandstones observed in the Albert have been interpreted by Greiner (1962) as offshore bars of the littoral zone or buried dunes.

2) The medial Albert is predominantly composed of quiet water lake deposits that include oil shales, shale and marlstones.

3) Conspicuous absence of the current formed structures in both the top and bottom Albert sand units in the subsurface and outcrop may suggest a predominant gravity controlled deposition.

Organic Facies

Organic facies have been constructed (Figure 3) from the particulate organic matter study to observe the degree of biodegradation, the dominance of distribution pattern of the organic matter type, the oxidizing or reducing depositional conditions and establish any correlation between the organic matter distribution and their sedimentology.

Biodegraded terrestrial materials have been observed as a minor component (5≈20%) but the amount is higher in the western than in the eastern part of the basin. Grey amorphous matter exists in abundance in the Albert Mines and in Dover areas which reflects deposition under reducing conditions and in the presence of sulfur reducing bacteria. Under oxidizing

conditions, preservation is poor and only structured terrestrial material and charcoal survive (Masran, 1984; Masran and Pocock, 1981). A high T.O.C. (total organic carbon) value corresponds with a dominance of these amorphous organic facies (Summerhayes, 1981). Picard and High (1981) also suggested that the deep central core of many lakes are generally stagnant, whereas the nearshore is well aerated by wave agitation. As such, the T.O.C. value is high in the offshore than in the nearshore. They cited examples from lake Tahoe with an offshore T.O.C. upto 3.4% and onshore upto 1% (Court et al., 1972). Similarly in Lake Ontario, T.O.C. value is less than 1% in nearshore and upto 4% in the deeper basin.

Cyclicity of occurrence of the organic matter type have been observed in most of the studied boreholes in the western part of the sub basin which indicates a change in the preservation mode of the organic matter, as well as changes in modes of sediment deposition (Summerhayes, 1981).

On the distribution pattern of organic matter, environmental interpretation have been made in many lacustrine basins. In these basins, grey amorphous (Type I) organic facies are commonly observed in the deeper part of the lake and terrestrial matter (Type III) as marginal lacustrine facies (Yang et al., 1985; Tissot and Welte, 1978; Huang et al., 1984; Demaison and Moore, 1980; Powell, 1984a; Dean, 1981). Distribution of the organic facies across the Moncton subbasin suggest that at the onset of the Albert deposition a predominant lacustrine condition prevailed in the entire subbasin. Deep lacustrine conditions existed in Dover-Stoney Creek, Albert Mines and farther east upto St. Joseph. Deep anoxic facies in these areas are also characterized by thick sequences of organic rich shales and marlstones and the presence of oil shales. Presence of minute non-glacial varve like laminations and lack of any significant bioturbation is also

indicative of a persistent lack of water movement. These features indicate that the lake was probably density stratified because of the temperature differences in the epilimnion and the anoxic hypolimnion (Powell, 1986). Shallow nearshore facies predominate the western part of the sub basin with poor development in the east probably because of fault scarp boundary of the ancient lake that controlled the transgression in the east. Cyclicity of the amorphous and the terrestrial organic matter in the vertical sections suggest fluctuations from shallow to short lived deep lacustrine conditions in the boreholes in the western part of the basin.

Mineralogy of these organic rich shales from Dover, Boudreau, Albert Mines and St. Joseph were extensively studied by Smith (1987) and Wright (1981). They found that among the inorganic component, carbonates (e.g., calcite, dolomite and siderite) content is highly variable (0≈50%). Among the carbonates, dolomite constitute the highest percentage (upto 50%). In the Green River oil shales the Mg-enrichment with respect to calcite was proposed due to the preferential concentration of Mg with respect to Ca by blue green algae whose remains released these cations after accumulations on the lake bottoms (Desborough, 1981). Degan (1981) suggested a relationship between the organic carbon and the carbonates, emphasizing that most of the carbonates precipitated are bio-induced by phytoplankton and littoral macrophytes through photosynthetic removal of Co_2. This Co_2 fixed in the plant tissue as organic carbon is released by respiration and decay into the hypolimnion wherein it lowers the pH and thus dissolves at least part of the precipitated $CaCo_3$. ~~Percent organic carbon versus $CaCo_3$ plot show distinct trends (Figure 4).~~ Dover samples show low organic carbon and $CaCo_3$ content whereas Albert Mines samples show high organic carbon and high $CaCo_3$. These observations indicate that a higher organic productivity

would lead to a lower $CaCo_3$ content as seen in Albert Mines area.

Carbon and Sulfur Relationships in Basin Analysis

Organic carbon and sulfur relationships have been widely used as a tool in interpreting depositional conditions during accumulation of organic carbon rich sediments (Leventhal, 1983a, b; Berner and Raiswell, 1983, 1984; Raiswell and Berner, 1985; Gauties et al., 1984; Hatch and Levanthal, 1981; Gibson, 1985). This relationship is based on the covariance of organic carbon and sulfide sulfur which results from the catabolism of organic carbon and concomitant reduction of sulfate (Leventhal, 1987). C/S plots were commonly used to differentiate between ancient freshwater and marine sediments (Berner and Raiswell, 1984) and also oxic from euxinic environments. A zero (origin) intercept suggest an absence of organic matter and resultant oxicity and an intercept of about 1 on the S-axis as euxinic.

Organic carbon and sulfur of shale samples from Shell Apohaqui, Irving Chevron Hillsborough-1, Irving Chevron Lee Brook-1 and UP McLeod Brook-1 have been plotted in Figures 2 to 5. The intercept on the sulfur axis is low in all the plots (< 0.5%). Low intercepts suggest that most of the analyzed sediments were deposited under very low O_2 or anoxic non-sulfidic conditions. This observation is also in agreement with the type of organic matter (Type III) observed and the interpreted shallow lacustrine condition during the deposition of these shales.

The slopes of the C/S line also show some variability which probably indicate different rates of deposition (Goldhaber and Kaplan, 1974). Since the samples were taken from widely separated areas in the basin, the metabolizability of the sulfate reducers, the depth of the water column may

have varied to produce a variable slope and intercept (Leventhal, 1987).

Geochemical Classification of Environments Based on Dissolved Oxygen and Sulfide

Because of the constancy of pH in most subaqueous sediments and lack of measurability of Eh, Berner (1981) proposed a geochemical classification of environments based on the concentration of dissolved oxygen and sulfide which are independent of pH and salinity. Both these parameters strongly affect the ecology of the organisms and the authigenic mineralogy. He classified the environments into:

(1) Oxic ($Co_2 \geq 10^{-6}$)

(2) Anoxic ($Co_2 < 10^{-6}$)

(2a) Anoxic sulfidic ($C_{H_2S} \geq 10^{-6}$) - pyrite, Fe-carbonate, organic matter.

(2b) Anoxic nonsulfidic ($C_{H_2S} < 10\text{-}6$)

(1) Post oxic - Glauconites, Fe silicates and Fe-carbonates, minor organic.

(2) Methanic - Fe-carbonates, sulfide minerals, organic matter.

From C/S relationship and the organic matter type it has already been established that most of the studied shales in the western part of the basin were deposited under anoxic non-sulfidic conditions. Anoxic non-sulfidic conditions have been recognized in many marine and lacustrine sediments (Froelich et al., 1979; Emerson and Wildmer, 1978; Martens et al., 1978) where sufficient metabolizable organic matter consumes all the dissolved oxygen but since the organic matter content is not sufficient enough to bring about sulfidic conditions further organic matter decomposition takes place under post oxic conditions by nitrate, manganese

and iron reduction. After precipitation of Fe-sulfides and pyrites, if iron reduction continues (in absence of H_2S) Fe^{++} in the interstitial water builds up precipitating siderite and vivianite. After cessation of sulfate reduction, further organic matter decomposition results in the formation of highly reducing non-sulfidic methanic environment (Barnes and Goldberg, 1976; Martens and Berner, 1977 and Berner, 1981).

In addition to calcite, dolomite, siderite, pyrite and rich organic matter, Albert shales contain analcite which is the most common diagenetic mineral observed in the lacustrine Green River Formation. However, in the Albert Formation analcite occurrence is erratic (see Smith, 1985, p. 66; also Wright, 1981, p. 45) and since the shales contain abundant Fe-carbonates and some organic matter, it is plausible that these shales may have been deposited under a predominant methanic anoxic environment (Berner, 1981).

DETRITAL ~~DETAILED~~ PETROGRAPHY OF SANDSTONES

Textures

The Albert Formation sandstones are moderately to well sorted, subangular to subrounded with cements and clay matrix. These sandstones are mainly fine grained with a few samples in the lower medium grain size range and are generally moderately to tightly packed. With increasing size of the framework grains, there is a progressive decrease of the primary matrix.

Framework Constituents

Quartz: Monocrystalline quartz grains have mainly straight extinction and are inclusion rich. Inclusions are mainly vermicular chlorites, tourmaline

and fluid vacuoles. Bipyramidal outline is very common and is mainly due to syntaxial overgrowths. Among the quartz population, polycrystalline quartz is very common up to a maximum of 15% of the total quartz. Polycrystalline quartz is mainly recrystallized metamorphic quartz.

Feldspars: The most abundant detrital feldspar is potash feldspar (primarily orthoclase and rarely microcline) with a few plagioclases. Plagioclase shows lamellar or albite-carlsbad twinning. Progressive or oscillatory zoning in the plagioclases is rarely observed. Plagioclases show a greater degree of alteration to clays as compared to potash-feldspars.

Rock Fragments: Rock fragments in Albert Formation sandstones are of three types:- Metamorphic, sedimentary and volcanic. Metamorphic rock fragments include foliated metaquartzites, quartz mica schists and rare felsic grains. Sedimentary rock fragments are mainly carbonate ooids and clasts, pisoliths, chert and fine grained sandstone, siltstone and carbonaceous fragments. Volcanic rock, although rare (less than 1%) are almost ubiquitous throughout the Albert Formation sandstones in the basin. They are mostly plagioclase porphyritic types. The porphyritic grains are composed of acicular to tabular microlites or microphenocrysts of feldspars, quartz and biotite set in an aphanitic, partially chloritized groundmass.

Accessory Minerals: Small mica flakes are always present but rarely reach more than 1% of the rock. Biotite, often altered to chlorite and replaced by calcite, is more common than muscovite. Other minerals such as epidote, apatite, rutile, ilmenite and pyroxene were also observed.

Provenance of the Albert Formation Sandstones

Provenance is a function of a number of variables and includes source rock type, relief climate and source rock location. These factors leave a characteristics compositional and modal trend on the sandstone suites. On the basis of detrital mode of sandstones, various authors (Dickinson, 1985; Dickinson et al., 1983; Dickinson and Suczek, 1979; Ingersoll and Suczek, 1979; Zuffa, 1985; Mack, 1984 and many others) have concluded that provenance types are governed by plate tectonics. Most common tectonic regimes considered from classical QFR diagrams are continental block provenance, magmatic arc provenance and recycled orogen provenance (ibid.). However, Mack (1984) recognized some error populations of sandstones whose interpreted tectonic setting does not coincide with their location on triangular provenance diagrams. Other authors (Bhatia, 1983; Roser and Korsch, 1986, 1988; Argast and Donnely, 1987; Wyburn and Chappel, 1983 and many others) have followed the chemical approach and suggested that variation in element geochemistry reflect distinct sedimentary provenance and tectonic setting.

To unravel the provenance of the Albert Formation sandstones, both the detrital mode (Table 1) and the bulk chemical composition (Table 2) were studied. Detrital mode of the sandstones were obtained by point counts (minimum 300 points) of thin sections, using the classic methods of Dickinson and Suczek (1979) and Ingersoll and Suczek (1979). All points were recalculated as volumetric proportions for QFR and QmPK and SRF/PRF/MRF categories (where Qm = monocrystalline quartz grains, P = Plagioclase feldspars, K = K-feldspars, PRF = Plutonic rock fragments, MRF = Metamorphic rock fragments, SRF = Sedimentary rock fragments, Qp = polycrystalline quartz, Q = Qm + Qp, F = P + K and R = SRF + PRF + MRF). Modal analyses were

Table 1. Composition, average detrital mode and interpreted provenance for the studied sandstones.

Well	Sandstone Composition	Average Detrital Mode	Principal Lithic Components	Provenance (Dickinson & Suczek, 1979)
Irving Chevron - Stoney Creek #1	Mainly sublitharenite, quartz arenite, subarkose, litharenite	$Q_{68}F_{20}L_{12}$	Carbonate clasts, metaquartzite phyllites, chert and pyroxene	Recycled Orogen
Irving-Chevron - East Stoney Cr. #1	Mainly subarkose, sub-litharenite to litharenite	$Q_{80}F_{11}L_{9}$	Carbonate clasts, metaquartzite, phyllites, chert and pyroxene	Mixed-Continental block, recycled orogen
Irving-Chevron Hillsborough-1	Arkose	$Q_{56}F_{40}L_{5}$	Carbonate clasts, chert and pyroxenes	Continental block
Irving-Chevron - Little River-1	Litharenite	$Q_{61}F_{12}L_{27}$	Carbonate clasts, phyllite and metaquartzite	Recycled orogen
ARCO Rosevale-1	Subarkose-sublitharenite	$Q_{80}F_{9}L_{11}$	Carbonate clasts and metaquartzite	Recycled orogen
ARCO Dover-1	Mainly subarkose, quartz arenite, litharenite	$Q_{87}F_{8}L_{5}$	Carbonate clasts and chert	Mixed-Continental block, recycled orogen
GULF Lower Millstream	Mainly sublitharenite, quartz arenite to subarkose	$Q_{90}F_{4}L_{6}$	Plutonic clasts, phyllite and chert	Recycled orogen

Table 2. Major element composition of the Albert Formation sandstones.

L.O.I.	Well	Depth (meters)	SiO_2	Al_2O_3	Fe_2O_3	CaO	MgO	Na_2O	K_2O	TiO_2	MnO	P_2O_5
9.10												
	ARCO											
10.68	Dover-1A	232.95	64.02	11.16	5.23	1.49	2.84	2.45	2.81	0.27	0.05	0.54
6.00		108.69	58.55	12.01	4.85	4.12	1.83	3.46	1.99	0.69	0.10	0.52
14.47		46.29	73.20	8.60	3.15	2.93	1.43	2.34	0.90	0.40	0.06	0.34
6.51		6.73	52.33	8.76	2.18	15.72	1.34	1.86	1.43	0.34	0.11	0.12
6.19		15.72	70.42	9.57	3.89	3.31	1.62	1.94	1.43	0.34	0.05	0.20
	Irving											
7.08	Chevron	901.67	67.70	9.16	2.24	6.63	1.49	2.69	0.95	0.22	0.08	0.07
4.90	Lee	902.60	70.35	9.69	2.50	5.02	1.53	2.92	1.76	0.13	0.29	0.36
9.86	Brook-1	904.04	60.93	8.12	2.22	11.99	1.45	2.43	1.31	0.31	0.16	0.18
	GULF											
4.12	Lower Mill-	19.10	70.15	10.72	5.66	2.62	1.91	1.81	1.56	0.40	0.11	0.47
11.51	stream-1	20.42	59.93	9.46	1.99	11.99	1.40	1.64	0.5	0.29	0.35	0.31
4.35		22.71	73.40	9.81	4.35	2.59	1.70	1.65	1.14	0.36	0.09	0.16
9.50		59.03	60.45	11.82	4.15	6.32	2.01	1.57	2.59	0.34	0.11	0.16
4.01		43.28	76.19	7.96	4.30	3.08	1.47	1.16	0.80	0.33	0.08	0.47
	Irving											
9.75	Chevron	438.97	63.38	13.54	5.81	3.81	2.08	3.51	0.90	0.39	0.08	0.47
5.45	Stoney	442.60	68.60	13.16	3.93	2.94	1.76	3.84	0.88	0.37	0.08	0.47
7.71	Creek-1	680.48	63.99	6.59	2.47	11.66	1.51	1.82	0.74	0.23	0.21	0.50
12.41		689.26	68.23	7.08	3.24	8.36	1.58	1.83	0.78	0.26	0.19	0.45
15.15		961.46	60.33	6.51	3.14	10.26	1.72	1.85	1.11	0.20	0.12	0.07
4.95		967.35	43.18	10.94	4.34	11.24	2.47	3.44	0.89	0.35	0.18	0.40
3.60		988.64	71.38	8.78	3.73	4.53	1.91	2.23	1.06	0.44	0.09	0.40
	Boyd Creek											
14.51	outcrop section	---	48.50	9.82	3.77	16.17	1.46	2.43	2.30	1.10	0.11	0.29
9.40	ARCO	100.30	63.75	10.87	3.40	4.80	1.99	2.39	2.14	0.40	0.10	0.35
8.40	Rosevale-1	145.35	59.99	14.30	4.82	3.15	2.12	2.97	2.91	0.49	0.10	0.29
6.72		297.51	66.55	13.17	3.89	1.50	2.40	3.82	1.37	0.15	0.06	0.16
	Westmorland											
2.07	Uplift	---	65.96	14.53	5.34	1.32	2.01	3.40	4.18	0.58	0.09	0.26

determined on sandstones from fine to lower medium grain size range. In this range, no detectable effect of grain size on compositional variation was observed. The triangular plots (Fig. 6-9) using the above grain parameters suggest a predominant recycled orogen provenance, with minor contributions from continental block provenance. The key source rocks in recycled orogen are uplifted terrains of folded and faulted strata from which recycled detritus of sedimentary and metasedimentary origin are most prominent (Dickinson et al., 1983). In MRF, PRF and SRF triangular representation (Fig. 10, 11), most of the studied sandstones plot in "sedarenite" field (Folk, 1974), suggesting a dominant contribution of sedimentary rock fragments (e.g., siltstones and carbonate clasts). Metaquartzite or volcanic rock fragments are rarely observed. Rock fragments show a distinct distribution pattern both in the east and the western part of the subbasin. Volcanics tend to increase towards the west, but carbonate rock fragments are more or less laterally uniformally distributed, with a restricted vertical occurrence. These siltstones and carbonate rock fragments, probably are derived from Caledonia Complex in the south of the subbasin. But Mack (1984) suggested that since carbonate rocks are highly susceptible to weathering they should provide few detrital grains under humid conditions. Chemical maturity data (Fig. 12) suggest both arid and humid climatic conditions during deposition of these sediments. This observation is in agreement with the general consensus that at the onset of the Albert deposition humid and wet conditions prevailed that progressively became more arid.

Proponents of chemical discrimination of clastic sedimentary components suggests that chemical composition of components are distinctive and the differentiation of sedimentary components result in concomitant

separation of associated elements (Argast et al., 1987; Bhatia, 1986; Roser and Korsch, 1988). By comparing unlithified sediments from the Black Sea and comparable ancient sediments from North America, Argast et al. (1987) showed that burial alteration does not necessarily result in large scale redistribution of the constituent elements. The simple bivariate plot of K_2O/Na_2O and SiO_2 content has been considered of significant value because it shows chemically distinct signatures in the passive continental margins (PM), Active Continental Margins (ACM) and oceanic island arcs (Maynard et al., 1982; Bhatia, 1983; Schwab, 1975). Plots of the Albert Sandstones in K_2O/Na_2O vs. SiO_2 diagram, predominantly fall in the ACM field with a few data points in ARC field. Quartz intermediate sediments are characteristic of ACM derived detritus, also included in this category are materials derived from uplifted areas associated with strike slip faults and deposition in pull-apart basins (Roser and Korsch, 1986). Similarly, Moncton Subbasin has also been proposed as a strike slip and/or pull-apart basin. ACM data also show a decline in K_2O/Na_2O with increasing silica (Fig. 13). Rowe (1980) and Roser (1983) have observed grain size dependent variations in chemical and modal compositions of sediments. Typically K_2O and Al_2O_3 enrich in finer grained phyllosilicate fraction and SiO_2 and Na_2O enrichment in the coarser sand, tectosilicate rich fraction (Argast et al., 1987). Although the studied sandstones are not quartz poor and not volcanogenic, a few data points in the ARC field probably indicate size dependent control on composition.

The provenance of sandstone suites can also be depicted on a $CaO-Na_2O-K_2O$ ternary diagram (Fig. 14) (Bhatia, 1983). On the same diagram average compositions of gabbro, granite and granodiorite from Le Maitre (1976) are plotted for comparison. Most of the studied sandstones show

composition identical to granodiorite-gabbro clan. This compositional trend suggests that the source of these sediments is not from a pure granitic terrain and a mixture of detritus from more than one source (e.g., Westmorland Uplift and Caledonia Complex) cannot be ruled out.

Based on the general absence of volcanic clasts in the Albert sandstones and paleocurrent pattern, Pickerill and Carter (1980) suggested a predominant granitic terrain source for the Albert sandstones, from the south, as far south as Nova Scotia. However, considering the basin geometry, locale of the uplifts and variable paleocurrent pattern (St. Peter, pers. comm.), it's very likely that the sandstones may have been derived from more than one source. Most of the sediments also are immature to submature, which also indicate that the sediments are transported over short distances as opposed to long transportation that would have required if it is sourced in Nova Scotia. Martel (1985) in a study on the adjacent Sackville subbasin showed from seismic stratigraphy that the Westmorland Uplift, a predominantly granitic terrain was a positive area during the Carboniferous and shed detritus to Horton sediments in the Sackville subbasin. Foley (1988) observed a general thickening of the sandstones and shales towards the south from the Westmorland Uplift and a south/southwest paleocurrent direction. From these observations he concluded that the Westmorland Uplift was probably the major source for the Albert sandstones in the Stoney Creek oil field. Based on paleotransport data and compositional trends, St. Peter (1988) suggested that the distribution of Horton facies is largely controlled by the northeast trending faults that influenced the regional tilt of the underlying basement blocks and in turn, the paleodrainage pattern.

All the above observations indicate the various complexities involved

in the interpretation of the provenance for the Albert sandstones. Although Westmorland Uplift is considered as a granitic terrain, its exact chemical composition is unknown. One sample analysed from Westmorland Uplift show a pure granite composition (Fig. 14). At the present stage, the available data indicate that the Albert sandstones in the larger part of the subbasin is derived from a mixed granite/granodiorite and gabbroic complex.

DIAGENESIS OF SANDSTONES

Physical Compaction

Compaction in the studied sandstones is registered in the bent and warped micas around detrital grains, crushed and slipped feldspars across twin planes and strained quartz. Micas show increasing bending in progressively deeper buried sandstones. Sutured and interpenetrant grain boundaries resulting from pressure solution were also observed in quartz. Surprisingly, carbonate rock fragments show any significant compaction.

Paragenesis of Authigenic Minerals

Based on mutual textural relationships of authigenic mineral phases, a paragenetic sequence has been established (Fig. 15). Mineral textures of authigenic origin are: overgrowths especially on quartz, feldspar and calcite, porelining, porefill and grain replacing cements, delicate clay morphology, grain infilling and illite-smectite conversion to illite and also important diagenetic events.

Quartz Diagenesis

Two phases of quartz cementation were observed in the Albert Formation sandstones. Based on textural relationships, quartz cementation can be classified into early and late phases. These cements occur primarily as overgrowth on both mono and polycrystalline detrital quartz grains, with a minor amount of anhedral porefill and rare chert overgrowths. In all the studied samples, overgrowths are preferentially developed on monocrystalline quartz when compared to polycrystalline quartz grains. Within the monocrystalline quartz population the less strained quartz show more overgrowths. Overgrowths on chert and polycrystalline quartz show

different growth habits. Although individual overgrowth crystals are isolated from each other by intercrystalline boundaries, overgrowths on polycrystalline grains were mostly prismatic in contrast to long rhombohedral needles on chert. At the contact between the host grain and the overgrowth, a dust ring of low index isotropic specks was also observed.

A common development of overgrowths is as rhombohedra in optical continuity with the host grain. However, the initial rhomb or prism faces of the overgrowth are partially lost because of the development of compromise boundaries between thick adjacent overgrowth rims (Fig. Plate 2).

Pressure solution effects are also observed in quartz arenites and subarkoses. Although concavo-convex grain contacts were present in relative abundance, sutured contacts with interpenetrant grain boundaries were less common (Fig. Appendix 1).

From textural observations, it has been found that some quartz overgrowths and porefill quartz cement are pre-solution and predate calcite(1) cementation demonstrated to be early in origin (see section on "calcite"). These early quartz cements also occur pre-compaction, in a high minus cement porosity framework but they postdate early chlorite. Quartz also occurs in enlarged secondary pores caused by solution phase(2) and hence is a late phase quartz. Ankerite rhombs (which represent late carbonate cement) were also observed as inclusions in this late phase quartz (Fig. Plate 3 ?).

From thin section point count data, most of the studied sandstones show about 2% quartz cementation. The only disparity observed was in Stoney Creek-1 with substantially high quartz overgrowths (about 4%).

For early quartz phase cementation meteoric water seems to be the most

likely silica source. Fluvial or surface waters in the meteoric regime contain an average 13 ppm silica. However, a large throughflow of water is considered as a pre-requisite for such a cementation (Blatt, 1979; Bjorlykke, 1981; McBride, 1987; Waugh, 1970; Hoyseknecht, 1984). It would be difficult to document exactly the possible sources of late quartz cement. But pressure solution of quartz grains, carbonate replacements of detrital silicate grains, and conversion of mixed layer clays are the most likely processes to contribute silica to late quartz cement.

Carbonate Cement Diagenesis

Several phases of carbonate cementation were observed in the Albert Formation sandstones. Different carbonate cementation phases have been determined based on the mutual textural relationships of diagenetic components, distinct morphology and optical properties. A summary of the paragenetic sequence is outlined in Figure 16. Petrographic descriptions of the carbonate cements, their significance and interpretations are given below:

Fibrous calcite

This type of cement in the studied sandstones is rare and was only observed at a present depth of about 53 meters in borehole GULF Lower Millstream-1. The cement occurs as columnar crystals that are elongated parallel to the c-axis. The crystals are prismatic in shape with rhombic terminations, with a maximum width to length ratio of 6 (Fig. 3 (plate 3 and 4)). Some of the crystals, however, show curved flat ends suggesting that the crystal grew against some obstruction causing growth to cease.

Most commonly this fibrous calcite occur as partial to complete grain

coating (Fig. plate 4 1). The nucleus of this cement type is highly variable and includes detrital clasts of quartz, feldspars and carbonates. Semi-quantitative analyses by scanning electron microscope (SEM) with an attached energy dispersive analyzer, on these calcite cements show that the chemical composition is pure $CaCO_3$.

The fibrous cement in Lower Millstream area was precipitated in the freshwater vadose and possibly in a shallow mudflat setting. Supersaturation with respect to calcite was achieved primarily by degassing of CO_2 combined with evaporation concentration in an arid environment (Hanor, 1978; Muller, 1978; and Watts, 1980). A general arid environment for the Albert Formation was also proposed by Utting (1987) based on the spore types and the paleogeographic position during the Carboniferous time. The absence of fibrous coat on opposite sides of many grains indicate that these incomplete coating may have formed in the water column draped on the lower side of the grains generating a microstalitic form (Purser, 1971; Ward, 1975; Harris et al., 1985). Such microstalitic nature also suggest cementation in a very shallow water column.

Various attempts have been made to establish a relationship between the fluid composition, cement composition, cement crystal habit and morphology (Katz, 1973; Folk, 1974; Lahann, 1978; Blinkey, 1980). Fibers and steep rhombs of calcite cement occurrence in the marine settings have been explained as a result of Mg^{2+} poisoning effect that retards the sideward growth of the calcite allowing growth only parallel to the c-axis (Folk, 1974). Differential charge development on crystal faces was also proposed as an alternative model in morphologic control (Lahann, 1978). Although these models work well in specific cases, it can't be applied to cements of different depositional setting. As such these generalizations

were suggested unsatisfactory and many authors have shown that variable morphologies may occur as compositionally identical cement from nearly identical fluids (Chafetz et al., 1985; Longman, 1980; Binkley et al., 1980). Recently, Given and Wilkinson (1985) considered the kinetics of surface nucleation as most significant in morphology control, as well as amounts of reactants, principally carbonate ions at the growth sites.

The fibrous cement composition in Lower Millstream area suggest that the porewater was locally deficient in Mg and possibly in the range of ON2 (Muller, 1978). This observation is concluded from Mullers (1978) work on lacustrine carbonate cement types from different geographic areas. High surface cation/anion absorption can't also be documented in a freshwater regime. As such it appears that ~~more~~ none of the above factors control the morphology development of individual crystals. Although it's difficult to explain the mechanism of fibrous cement in non-marine setting, it could possibly be said that the growth rate is the singlemost control on fiber calcite precipitation. This could also depend much on the degree of supersaturation of the evaporitic water and the nature of the nucleating margin of the host grain.

Micrite

Microcrystalline calcite constitute a minor percentage (less than 5%) of the total carbonate cements in most of the studied sandstones. This micrite calcite are extremely fine, semi-opaque mud in the light microscope and occur in patches. SEM observations of these micrite crystals show polyhedral to rounded form. In some samples they show a clotted fabric (structure gremeleuse) (Cayeux et al., 1935; Bathurst, 1975). In Lower Millstream area at a present depth of about 53 meters and in Prosser Brook

outcrop section micrite calcite make up about 70% of the cement. This micrite cement is possibly precipitated as a calcrete (Goudie, 1971, 1973; Reeves, 1976; Tandon and Narayan, 1981; James, 1972) near sediment water interface, recording a sub-aerial exposure surface.

Calcisphere cement

Calcisphere cementation was rarely observed. The spheres are composed of numerous pseudorhombic to irregular tiny calcite crystals, resembling pyrite framboids (~~Fig.~~ Plate 6). Their local occurrence in aggregate suggest supersaturation ~~or~~ of porewater in $CaCO_3$ and a rapid crystallization with a large volume of nuclei per unit volume of calcite. These calcispheres show no organic replacement or association.

Displacive Calcite

Displacive calcite cements are observed in association with fibrous grain coat and high micrite matrix. This displacive calcite occurs within textural components (rock fragments and biotite), fractures and matrix. In the biotite, this calcite type occur along the cleavage planes in ~~rectangular~~ lentic to rectangular bodies. This calcite type, typically show an exploded texture that can be visually fitted back together. Displacive growth is also exemplified by wide separation of framework grains by micrite matrix (e.g., floating grain texture) and brecciation of detrital grains (~~Fig.~~ Plate 3) (Saigal et al., 1988; Watts, 1978).

Most of the framework grains in the studied sections of Lower Millstream-1 and Prosser Brook which has been described as calcrete, float in a micrite matrix. Two processes that can possibly form the texture is replacement and/or displacement of detrital grains by calcite. Replacement

etching of the detrital grains is not observed in the studied sections. This was verified by comparing degree of etching of grain edges from upper and lower non-calcretised horizons. Such displacive floating textures was experimentally observed by Plat-Lajoux et al. (1971) in simulated displacive growth of gypsum.

Brecciation of detrital fragment are mainly observed in quartz and biotite. The exploded texture most commonly seen in these cements suggest a displacive origin.

Theoretically, displacive calcite growth was explained due to the presence exerted during crystallization of calcite and Weyl (1959) calculated a force of normal stress of 10 atmospheres for one percent supersaturation by calcite. With higher degree of supersaturation growth rate proportionally increases. Since the free energy increment for nucleation in microspaces and porethroat is minimum (Berner, 1980) it's very likely that supersaturation of porewater with respect to calcite initiates the nucleation along the cleavages of the biotite or in any minute fractures. With progressive calcite growth from the nuclei, the resultant outward pressure caused expansion and formation of "pseudo-anticlines" within a single biotite pack (Plate 3).

On the association of displacive calcite, fibrous calcite and micrite matrix: a common feature of calcrete?

Calcrete or caliche profile in ancient and recent sequences have drawn significant attention by carbonate and clastic sedimentologists because of their importance in the recognition of subaerial exposure surfaces in the geologic record (Watts, 1978, 1980; Harrison, 1977; Saigal, 1988; Buczynski and Chafetz, 1986; Solomon and Walkden, 1985; Tandon and Narayan, 1981; Goudie, 1971, 1973; and Reeves, 1976). Close association of calcretes

and the semi-arid climate, recognition as an exposure surface, provides valuable insight in concomitant shifts in depositional, diagenetic environments and overall paleoclimatic pattern of the studied area.

To test the many macroscopic field observations, petrographic micromorphologic features of different calcrete profiles were studied by many authors (e.g., ibid.). The most significant petrographic criterias that have been proposed include a high micrite matrix (50-60% of the total constituents), floating framework grains, brecciation of the detrital grains, displacive calcite and needle fibrous calcite (Watts, 1978, 1980; Saigal and Walton, 1988; Buczynski and Chafetz, 1986).

In the Albert Formation Lower Millstream and Prosser Brook sections, a close association of micrite matrix (≈ 70%), fibrous calcite grain coat, fracture fill and displacive calcite conclusively suggest existence of a subaerial exposure surface.

Needle fibrous calcite that are commonly seen in many calcrete profiles (Harrison, 1977; Solomon and Walkland, 1980) have been attributed to an indirect activity of microorganisms because of their close association with plant rootlets (Calvet and Julia, 1983; Wright, 1984). Although the contribution from organic processes to the formation of needle fibers have been generally accepted, the dominant crystal growth control is favoured towards an inorganic origin (Solomon and Land, 1980; James, 1972; Bal, 1975; Fitzpatrick, 1971). In Lower Millstream and Prosser Brook areas no needle fibers were observed in transmitted light microscopy. Calvet and Julia (1983) and Knox (1977) observed neomorphic transformations of these fibers to micrite, which is possibly the case for the studied sections. However, displacive as well as grain coat calcite occurs in distinct blocky fibrous forms and no organic association has been observed. A paragenetic

sequence of the cementation pattern in these calcrete profiles is given below ~~in figure~~ .

Environment	Mode of Cementation	Form and Occurrence
Subaerial vadose	Passive	Fibrous grain coat.
	Displacive (1)	Micrite
	Displacive (2)	Fibrous fracture and grain fill.
Meteoric Phreatic(?)	Replacive	Sparry calcite.

Porefill and Replacement Calcites

Both porefill and replacement calcites occur in two phases (1 and 2). In both cases porefill can't be differentiated from the replacement phase of cementation in as much as they don't show any variation in appearance, mineralogy and significantly no textural discontinuity between the replacement and the porefill. Replacement calcite(1) is most commonly seen in plagioclase, polycrystalline quartz, chert and biotite (~~Fig.~~ Plate 6). Replacement texture is variable depending on the nature of the detrital grain being replaced and possibly the degree of alkalinity of the porewater regime. Calcic-plagioclases show greater degree of replacement than more sodic types (~~Fig. ——~~ Plate 6). Replacement is random and rarely along twin planes. However, many polycrystalline quartz show replacement along subcrystal boundaries. In extreme cases of replacement, the parent grain is completely replaced leaving a fine clay lining and iron oxide coating forming a relict

grain boundary (~~Fig~~. Plate 6).

Porefill calcite(1) occur mainly in two forms as fine to coarse spar and blocky mosaic (Plate 5). In most of the studied samples porefill and replacement calcite(1) was observed to be pre-compaction, since framework grains are barely in contact in a groundmass of calcite cement indicating a high minus cement porosity ~~(Fig.)~~. (Plate 5). Texturally, they postdate early diagenetic quartz overgrowth and commonly follow authigenic chlorite coating.

Both replacement and porefill calcite(1) show a dull grey interference colour and a rhombohedral cleavage. Commonly they contain numerous inclusion of clays and iron oxides. Chemically, porefill and replacement calcite(1) is poor in Fe, Mg and Mn (less than 1%) and show no apparent variation related to depth or areal distribution in the basin. ~~(Fig.)~~. Porefill calcite(2) although is similar in chemical composition to that of calcite(1), locally replaces calcite(1) and thus postdates calcite(1). This calcite(2) make up less than 10 percent of total carbonate cements and is generally inclusion free, blocky mosaic with low interference colour (Plate 5). This cementation phase appears not to be associated with any extensive replacement of framework grains as observed in calcite(1). The non-replacing character of this cementation phase probably is due to decline in the alkalinity of the porewater.

Ankerite

Two phases of ankerite cementation were observed in the Albert Formation sandstones. Ankerite(1) is the most common type, occurring as euhedral rhombic crystals in enlarged porespaces (~~Fig~~. Plate 7). Ankerite(2) is volumetrically rare occurring as irregular to pseudorhombic crystals. Ankerite(2) is always associated with partially dissolved ankerite(1) (~~Fig~~. Plate 7

). As such ankerite(1) must be the source of cementation for ankerite(2).

Pattern of ankerite cementation (Fig. 16) indicate that ankeritization progressively increases with burial, suggesting a downward flux of Fe and Mg enriched porewaters. From studies of the many ancient clastic sequences, it has been established that Fe-Mg rich authigenic carbonate phases occur at deeper burial at increasing temperature (Franks and Forester, 1984; Louchs et al., 1980; Lindquist, 1976; Stanton, 1977; Dutton, 1977; Boles and Franks, 1979 and Matsumoto et al., 1980). Thermodynamically ankerite is more stable at high temperature. This is in agreement with the high vitrinite reflectance (Ro = 0.8-1.2) values observed from shales at the same level of ankerite cemented zones. Boles and Franks (1979) also proposed that mixed layer clay reactions may contribute Fe and Mg required for ankerite cementation.

Comparisons of ankerite cemented horizons, vitrinite reflectance values and stratigraphy suggest that when other relevant data are available, ankerite cement zone can be used as a qualitative geothermometer.

Both lateral and stratigraphic distribution of ankerite cement zone is highly variable, which suggest a variable burial history of the Albert Formation across the sub basin. Ankerite cement zone in the east in ARCO Dover 1A and in the south in ARCO Rosevale-1 occurs at shallow depth of 50-150 meters. In both these zones the Albert Formation is cut by an unconformity and is overlain by the Hillsborough and Enrage Formations respectively. Elsewhere, ankerite occurs at much greater depth. In Irving Chevron Lee Brook-1, although very typical ankerite form occur at a depth of about 900 meters, on probe analyses it shows a pure calcite composition. Absence of rhombic calcite in the Moncton subbasin, its occurrence at a depth range

corresponding to ankerite in the adjacent ~~basins~~ wells and an abnormal bottom hole temperature of 150°C, suggest that ankerite has been calcitized. Calcitization of ankerite has been reported from geothermal systems at about 195°C (McDowell and Paces, 1985). In the western part of the sub-basin in the studied boreholes of Kerr McGee Urney-1, Gulf Lower Millstream-1 and shell Apohaqui-1, no ankerite cementation was observed. Such an absence of the ankerite is possibly related to poor mixed layer clay occurrences in this part of the basin.

Replacive Minerals in Carbonate Cements

Both calcite and ankerite cements host a large suite of replacive minerals that include dolomite, albite, rutile and siderite. Their paragenetic sequence has been outlined in figure 17.

Dolomitization of calcite is local in occurrence and their absence in the associated carbonate cement suggest a short transport distance of the solute Mg^{2+} ion. Dolomite crystallization show development of intercrystalline porosity (~~Fig.~~ Plate 8). Increased dolomitization has been observed in association with chlorite cement (~~Fig.~~ Plate 8). Although, numerous dolomitization models particularly on carbonate sequences have been proposed (Badiozamani, 1973; Folk and Land, 1975; McKenzie, 1981; Patterson and Kinsman, 1982; Baker and Kastner, 1981 and Hardie, 1987) dolomitization of calcite cements in non-marine clastic sequences have drawn little attention. In smectite rich Tertiary Gulf coast sections all magnesium rich carbonate cements approach ankerite composition and ankeritization has been explained due to shale diagenesis (Land, 1984; Milliken et al., 1981). Land (1985) also added that low iron dolomite is not a significant product of shale diagenesis.

Authigenic chlorite in most of the Albert Formation sandstones is very rich in Mg and show considerable local dissolution. In this particular case, the parent calcite mosaic is zig-zagged by narrow films of chlorite, poor in Mg content (Plate 8). Absence of any other Mg source nearby suggest that chlorite might have acted as Mg-donor to the dolomitization of calcite. Since replacement dolomite at low temperatures require long reaction times (> 10^4 year) (Hardie, 1987) this close association may explain short mass transport. Siderization of ankerite was observed as a local core replacement of ankerite (Plate 8). These siderite replacements occur as rhombs and show development of intercrystalline porosity. Siderization was possibly carried out by dissolution-precipitation reaction which is petrographically supported by incomplete dissolution of the host ankerite.

$$CaFeMg(CO_3)_2 \rightarrow Ca\ Fe(CO_3)_2 + Mg^{++}$$

Albite replacements is very common in both calcite and ankerite (Plate 8). They most commonly occur as tiny needles or partially euhedral cubes. Albite replacement occur in the same horizons showing pervasive albitization of detrital calcic-plagioclases. The close association of albite replacing carbonate cements and albitization of detrital calcic-plagioclases suggest a mutual genetic relationship. An excess of Na^+ ions from albitization of calcic-plagioclases, possibly contributed to the replacement of the carbonate cements.

$$CaCO_3 + 3H_4SiO_4^\circ + Na^+ Al(OH)_4^- + H^+ = NaAlSi_3O_8 + Ca^{++} + HCo_3^- + H^+$$

$$CaFeMg(Co_3)_2 + 3H_4SiO_4^\circ + Na^+ + Al(OH)_4^- + H^+ = NaAlSi_3O_8 + Ca^{2+} + Fe^{2+} + Mg^{++} + 2HCo_3 + 8H_2O$$

(plate 8)

Pervasive pyrite replacements were observed in the carbonate cements. Pyrite replacements in the carbonate cements may have taken place at least in two phases. Since the Albert Formation is interbedded with organic rich shales, bacterial sulphate reduction was possibly the major source for sulphide. Iron could have been derived from the shale diagenesis and the amorphous iron oxide coat around the grains. The reaction is as follows:

$$CaCo_3 + Fe^{++} + H_2S \rightarrow FeS + Co_3^{--} + Ca^{2+} + 2H^+, FeS + S^\circ \rightarrow FeS_2$$

Isotope Geochemistry of Carbonate Cements

Stable carbon and oxygen isotopes were studied for different generations of carbonate cements observed in the Albert Formation sandstones. The main purpose of this study was to explain the oxygen isotope compositions of the successive carbonate cement phases which is a function of isotope composition of the pore fluids and temperature. Carbon isotope signatures was also used to characterize the carbon source of the cements during successive burial (Anderson and Arthur, 1985; Longstaffe, 1984, 1987; Land, 1984 and Bjorlykke, 1986).

Authigenic carbonate cements were prepared for carbon and oxygen isotopic analyses by reacting organic and carbonate clast free powdered rock samples (< 44μm) in phosphoric acids using the methods of Walthers et al. (1972). No sample was obtained with only calcite(1) or calcite(2) cements, as such isotope values for calcite cements represent both calcite(1) and calcite(2). However, calcite cements were point counted to determine the relative percentage of calcite(1) and calcite(2). ~~Cross plots of calcite(2)/total carbonate cements vs. $\delta^{18}O$ and $\delta^{13}C$ show depleted values in both carbon and oxygen isotopes (Fig. 19a, b).~~ In addition, completely ankerite cemented sandstones were also studied for carbon and

oxygen isotopes. The isotope date are presented in the usual δ notations (Table 3) with respect to both Mean Ocean Water (SMOW) and Pee Dee Belemite (PDB). Carbon vs. Oxygen isotope values are plotted in Figure 19.

Both carbon and oxygen stable isotope data of these cements show distinct trends in rock-porewater reaction. Calcite cements show light carbon isotope values (-4.45‰ to -0.16‰ (PDB)). The low Mg content and light isotope values of these calcite cements indicate a possible mixing of carbon derived from inorganic carbonate and $\delta^{13}C$ depleted organic carbon from the maturation of organic matter (Longstaffe, 1986). Carbon isotope values of the ankerite is heavier (-0.81% to +4.97% (PDB)) than calcite cements. Since most of the ankerites are formed from dissolution of pre-existing calcite, they must have inherited some of the precursor carbon. Ankerites form in deeper burial at increasing temperature as such prograde carbonate solubility would contribute to increasing HCo_3^- and Co_2 from dissolution of different carbonate phases including carbonate clast, plant and fish fragments which are abundantly present in the Albert Formation. This suggest that the carbon source for ankerite formation is primarily skeletal ($\delta^{13}C$ = 0±4, Gross, 1964) with secondary inorganic calcite contribution.

In all the studied wells, oxygen isotope show progressive lighter values with increasing burial. Calcite cements show values in the range +13.61 to +16.50 (SMOW). Such a narrow range of values indicate that both phases of calcite cementation took place at a close temperature range and is possibly separated by a short timing event. However, oxygen isotope values of the ankerite cements show lighter values (+17.60 to +22.22 (SMOW)). In addition to high temperature requirements for ankerite

formation, this variation could also be explained due to cation enrichment as compared to the calcite phase and alkalinity change due to slight anoxicity expected during precipitation of Fe-Mg rich phases (Anderson and Arthur, 1985). Isotope fractionation between the solid carbonate phase and the water is affected by the mass and the size of the crystal. Both these parameters directly control the internal and lattice vibrations that determines amount of isotopic fractionation (Kyser, 1987). Although fractionation factor for ankerite-water has not been studied, oxygen isotope fractionation on dolomite has been experimentally determined. Mathews and Katz (1977) on their experimental studies on dolomitization of calcite observed a progressive lowering in $\delta^{18}0$ that correlates with the change in the Mg/Mg+Ca ratio and Sr/Mg+Ca ratio and concluded that all reactions takes place by solution-reprecipitation through intermediate magnesian rich phases. ~~The variation in $\delta^{18}0$ relative to mole percent Fe and Mg content has been compared in Figure __.~~

Isotope values of the carbonate cements from the Albert Formation sandstones has been compared with other diagenetic carbonate phases from different petroliferous basins (Longstaffe, 1986, 1984; Hutchian, 1985; Bjorlykke, 1986; Milliken et al., 1984 and Land and Dutton, 1978) (Table 4). Hutchion et al. (1985) reported heavy carbon values for carbonate cements and explained it's origin to methane generation and lighter oxygen isotope values to meteoric water circulation and increasing crystallization temperature. They also observed depleted oxygen isotope values in siderite and ankerite phases. In Basal Belly river sandstones both calcite and dolomite precipitate as cements. Calcite cements show a narrow range of values as in the case of the Albert Formation sandstones suggesting that early diagenetic cementation is very rapid and occur in restricted

temperature range. Oxygen and carbon values of dolomite also show higher values than calcite. A mixing of porefluids trapped during sedimentation and low oxygen meteoric groundwater was proposed as the precipitating fluid for the Belly River carbonates (Longstaffe, 1984).

In offshore Norway, in Haltenbanken area, the carbonate cements in the Jurassic sandstones has been reported to show highly negative carbon isotope values and the source was interpreted as carbon dioxide derived from early diagenetic sulfate reduction on later methane oxidation. Oxygen isotope values (0 - -12% SMOW) was also characteristic of an early diagenetic sulphate reduction zone (Bjorlykke et al., 1986).

Longstaffe (1984) reported higher dolomite isotope values than calcite in the Milk River Formation. A low temperature range (<+15°C) was proposed for crystallization of authigenic carbonate phases. The low carbon values of the cements was compared to the CO_2 derived from organic source and low oxygen values were consistent with low temperature crystallization from a mixing groundwater and evolved seawater.

In Frio sandstones, Milliken et al. (1981) calculated a crystallization temperature range of about 75 to 80°C for different carbonate cements, assuming that the oxygen isotope composition of the pore water was similar to seawater. Carbon isotope signatures was also explained due to organic and skeletal contribution. Again, lighter oxygen isotope values of dolomite was observed in respect to co-existing calcite, which was proposed as a result of fractionation between co-existing calcite and dolomite (Land, 1980).

In the Strawn series, Land et al. (1978) reported co-existing ankerite and calcite and observed that the ankerite is approximately 8% enriched in $\delta^{18}O$ relative to Fe-calcite. A temperature range of about 35-65°C was

calculated using the formation water isotopic analyses.

All the above observations of isotope studies on carbonate cements from sediment sequences of different basins show some general trend in isotope signatures. Depositional environment show little influence in terms of isotopic imprints on diagenetic components primarily because over geologic time period there is an inevitable mixing of freshwater and connate water (e.g., seawater/brackish/saline water, etc.).

Since isotope values is a function of crystallization temperature and thus burial depth is reflected in progressive lighter values of oxygen isotopes. However, in almost all the studied basins including Moncton Subbasin, iron and magnesium carbonate phases show some variation in contrast to the above linear trend observed in pure calcite phases. This was explained as a result of fractionation between near equilibrium calcite - ankerite phases and other factors, as previously described. Another problem poised is calculation of paleotemperature of cement formation because of unknown isotopic composition of the initial precipitating fluid. Although marine water did not fluctuate much in its isotopic composition ($\delta^{18}0$ - 0‰) over geologic time period (Anderson and Arthur, 1985) the isotopic composition in many cases is influenced by meteoric freshwater flushing due to tectonic uplifts. Another alternative followed is taking the oxygen isotope values of the formation water as the maximum value at which the carbonate phases were equilibrated. It would be of definite advantage if isotope values could be determined on co-existing mineral pairs which would require no approximation of the porewater composition. However, in sandstones with delicate nature of the diagenetic minerals it's difficult to isolate different components and then analyse by wet chemical methods. A possible solution is the iron probe which is still in its

nascent stage (Schimizu, 1987, pers. comm.). As such it's preferable to use paleotemperature values determined from isotopes in conjunction with paleotemperature values obtained by other methods (Anderson and Arthur, 1985), such as organic metamorphism as being attempted in the case of the Albert Formation (see Chowdhury, in prep.).

Pyrite Diagenesis

Pyrite in the studied sandstones is minor (up to about 1%) and occur in three distinct textural forms. These are 1) Framboids, 2) Euhedral and, 3) Concretions.

Framboids are composed of numerous smaller pyrite crystallites and are variable in size (< 1μm to 10μm). They occur mostly as isolated porefill and in the interstices of authigenic chlorite. SEM close-up views of single framboids show that individual crystals are octahedral in nature.

Euhedral pyrite, most commonly occurs as a replacement of carbonate cements, clasts and veins, feldspars, biotite and clay. They are cubic to octahedral in form and each grain is composed of several smaller microplates. Some of these pyrite also enclose several detrital particles developing a poikilotopic texture (~~Fig~~. Plate 4). In the carbonate veins, profuse pyrite replacement was noted where it occurs preferentially on the surfaces of the organic rich shale clasts included in the vein.

Concretions are mostly elliptical and variable in size (up to a centimeter).

Pyrite authigenesis in organic rich shales and sediments is well known (Berner, 1970, 1981; Love and Murray, 1963; Howarth, 1979; Altschuler et al., 1983). Pyrite generally forms at shallow burial depth by the reaction of H_2S and Fe minerals. Most common source of H_2S is the reduction of

interstitial dissolved sulphate by bacteria using sedimentary organic matter as a reducing agent. The general equation for the reduction of the decomposable organic matter and pyrite formation is as follows (Berner, 1984):

$$2CH_2O + SO_4^{=} \text{ -- } H_2S + 2HCo_3^{-}$$

$$Fe^{++} + H_2S \text{ -- } FeS + 2H^{+}$$

$$FeS + S \text{ -- } FeS_2$$

To explain framboid and euhedral pyrite texture, iron availability, saturation index and reaction of sulphur with respect to the intermediate phases (e.g., mackinawite and greigite) was also proposed (Goldhaber and Kaplan, 1974; Raiswell, 1982).

Different sulphate ions from evaporite deposits may also enrich the porewater. Fe source for pyrite formation could be met by hydrous ferric hydroxides, iron-rich clay minerals, pyroxenes, magnetite and ilmenite.

Albert Formation sandstones are generally interbedded with organic rich shales and these sandstone beds locally contain abundant plant remains. In the top section of the Albert Formation, local evaporite occurrence have also been reported (Pickerill et al., 1984). As such, these sandstones must have been flushed by various sulphate sources over the geologic time period. Besides, pyrite replacement of different framework grains and cements, the sandstones commonly show general presence of larger concretions as compared to the shales. Some of the fractures also show total infilling by pyrite. Most of the bioturbated sandstone section show absence of pyritization.

Main iron source in the Albert Formation sandstones are amorphous hydrous ferric oxides that coat many of the detrital grains and iron rich

chlorite. In the pyritized chlorites Fe/Fe+Mg ratio is considerably lower than in unpyritized chlorites. From textural relationships, it was observed that pyrite formed after the formation of chlorite ~~(Fig.).~~ Here it is suggested that the chlorite served as a source of Fe^{2+} by the substitution of Mg^{2+} into its octahedral site (Morad, 1986). Such a reaction would require a porewater with a high $aMg^{2+}/aH+$ ratio. A high Mg^{2+} in porewater possibly is derived from the adjacent ferro-magnesium silicate minerals (such as biotite). Morad (1986) showed by mass balance calculations that up to 75% of Fe^{2+} needed in pyrite formation could be supplied by this process. The framboid nature of these pyrites also suggest that they are very likely early diagenetic in origin (Raiswell, 1982).

Rutile

Rutile in the studied sandstones is rare and occurs in clusters as a porefill and replacement of carbonate cements. Rutile mostly shows ~~a~~ prismatic or acicular crystal form (~~Fig.~~ Plate 9). Possible sources of titanium ions are biotite and ilmenite. Because of the low solubility of titanium ions it is very likely that the rutile formed in close proximity to the local source (Hutton and Norish, 1974). However, Mossman et al. (1987) reported TiO_2 content in some sandstones as high as 3.28% which they related to the presence of titaniferous oxide deposits in basement rocks at the northeastern edge of the Caledonia Mountain. ~~Since solubility of titanium is low, it's not clearly understood how these ions would transport considerable distances without forming a complex in its pathway.~~ However, the data reported was based on bulk chemical analyses, as such whether the TiO_2 was detrital or diagenetic in origin could not be verified (Mossman, Pers. Comm, 1988).

FRACTURES AND VEIN DIAGENESIS

Two generations of fractures were observed in the Albert Formation from the cross-cutting relationships of fracture fills (e.g., veins) and two distinct sets of clustering of oxygen isotope data points (~~Fig.~~ Plate 10 and Fig. 18). Carbonate mineralized natural fractures in the Albert Formation locally occur in both the sandstone and shale sequences both in the outcrop and core. Fractures in outcrop and subsurface are relatively more common in the east as compared to the western part of the basin. Fractures in the sandstones are commonly oriented perpendicular to the bedding surfaces, completely mineralized and show no evidence of lateral displacement, which indicate that they have been formed by extension. The fractures in the shales are typically inclined at a low angle to bedding and show slickensided surfaces that involves shear involvement in their development. Local brecciation of fracture fills (~~Fig.~~ Plate 10) observed in the subsurface, which are possibly hydraulic in origin. Mineralized fractures also cut across authigenic carbonate cements within the sandstone matrix indicating development and cementation of fractures late in the burial history, following main stages of diagenetic alteration.

Drummond (1964) classified the reservoir fractures into two types: "tectonic" which are directly related to specific structures or as "cryptic" where the origin of the fracture is "obscure". In the Albert Formation both tectonic and cryptic features are observed. Tectonic fractures in the Albert Formation could be related to different sets of fault that criss-cross the basin. Leger and Williams (1986) on their detailed work from the various kinematic indicators suggested two prominent fault (NE and NNW) systems in the southern New Brunswick.

Wayne ~~and Nair~~ et al. (1982) proposed fracture development due to decreasing

effective stress during uplift and erosion of a sedimentary sequence. Erosion of thick overburden of the Albert Formation in and around the basin (as suggested from ankerite cement zone and vitrinite reflectance data) must have accompanied stress relief and consequently caused fracture development. Radial stretching from numerous normal faults in the basin or stress from the bending of the strata was minor, since no significantly folded sequence was observed in the studied sections.

Beach (1980) explained the formation of syntectonic veins from natural hydraulic fracturing in rocks under low grade metamorphic conditions. He also described the geometric features of these veins - length, simple tapering, symmetric and assymetric forking, branching irregular zig-zag traces, en-echelons and explained their geometric relationship to applied stress and fluid pressure. In the Albert Formation, most of the veins studied in thin sections fall in two categories (Beach, 1980): 1) single tapering vein termination, and 2) slight curvature vein termination.

Fractures terminate as a single tapering structure when the minimum stress during crack growth is symmetrically positioned at the crack tip. If the stress at the crack tip is asymmetric then curving and tapering may occur. Phillips (1972) proposed that an abrupt drop in fluid pressure during fracturing may cause bursting apart of the rock into which the solution may permeate under high pressure forming angular breccias. In deeper burial at Hillsborough-1, such brecciated calcite veins was also observed.

From the above observations, it can be concluded that the fractures in the Albert Formation might have been caused by a number of processes including loading-unloading of the sedimentary pile, hydraulic pressure and some tectonic contributions.

Vein Diagenesis

Petrography of Veins

Carbonate veins both from the outcrop and subsurface were petrographically studied to determine different cementation events and mutual textural relationships of fracture filling minerals. Their chemical and isotopic characters were also studied.

Calcite cementation pattern in the veins differ in various parts of the subbasin (Plate II). However, in all the veins two common vein calcite types (1 and 2) were observed. In many cases, vein calcite (1) is completely dissolved out by flushing of agressive acid solutions and they float as clasts in vein calcite(2) (Plate II). Where the calcite(1) is attached with the wall of the fracture and not completely washed away show distinct overgrowths and possibly record a time gap. These two calcite types within the vein can easily be distinguished by the following parameters; as outlined in the following:

Identifying Character	Vein Calcite(1)	Vein Calcite(2)
Pressure Shadows	Present	Generally absent
Twin type	Commonly untwinned	Commonly checkerboard to lamellar
Micro-fracture pattern	Perpendicular to each other	Parallel (if present)
Inclusions	Cloudy, abundant inclusion specks	Clearly, rarely inclusions

Morphologically, these calcites in the fractures occur in the following forms (Plate 11 and 12)

1) Equant to inequant
2) Cornflake
3) Beef
4) Rosette
5) Reticulate irregular

Equant to inequant sparry calcite in the fracture fills mimic the calcite cements in the sandstones. However, these vein calcites have formed later (see description above), as such the similarities could only refer to an identical environment of cementation. The more blocky nature of these vein calcites is possibly a function of larger space availability and rapid rate of crystallization. This is the most common cementation pattern in the veins.

Rhombic calcite is rarely observed (Plate 12). If present, they occur alongside the fracture walls in tiny rhombs and then progressively crystallizing into coarse crystal forms towards the center of the fracture.

Cornflake fabric forms by mutual interference of the various cornflake like calcite crystals (Plate 12). This calcite type is most commonly seen in the organic rich shale sequences. However, no direct association of any skeletal material was observed. This calcite type is progressively coarsely crystalline from the wall of the fractures to the apices of the cones. These calcite crystals are curved and grow inward from the opposite sides of the vein, meeting along a highly jagged plane caused by mutual accommodation of the growing crystals. The apical angle of the subflake (individual "corn" like crystal within a single cornflake) on the average

is about 60°, however, flakes with broad diffuse angle (≈ 120°) is also present. These cornflakes show a radiating internal pattern of cyclic undulose extinction. This calcite type show minor inclusions and include large clasts of matrix material floating in it.

Thin symmetrical fibrous veins are defined as beef (Marshall, 1982). Linear trails of minute opaque intercrystalline inclusions indicate former presence of finely fibrous carbonate (~~Fig.~~ Plate 12). At the fabric discontinuity a marked angular change in crystal growth direction and a sharp increase in inclusion density was also observed. Toward the base of the vein both crystal boundaries and inclusion fibers are sinusoidally curved. Curvature may have been a response to local stress conditions ~~(Fig. 2.22~~

Rosette type calcite is rarely observed (~~Fig.~~ Plate 10). They are composed of acicular calcites radiating from a nucleus. These fibers show different extinction patterns. They are clear and are free of inclusions.

Reticulate irregular calcite is defined here as a network of numerous small columnar calcites cross-cutting each other (~~Fig.~~ Plate 11). These cross-cutting calcite crystals show low interference colour and a variable crystal to crystal extinction pattern. One calcite type cross cutting the other is relatively inclusion free than the other. From the fracture wall toward the center, they show progressive coarse crystallization.

A detailed paragenetic study on the diagenetic minerals of the carbonate veins has been carried out. Mutual interrelationships of different authigenic phases from different areas of the basin is outlined in ~~figure 21, A, B, C, D, E, F and G.~~ Appendix IV

From the paragenetic relationships of the different diagenetic minerals within the vein and their areal variation suggest local changes in porewater evolution in the sub-basin. Some general observations made on the

vein occurrence, the host rock lithology and the mineral fabric are as follows:

1) Fibrous calcite is restricted to veins in organic rich shale sequences (~~Fig~~. Plate 11).

2) Quartz filling veins are more common in organic rich marlstones which are later dissolved and later infilled by calcite (~~Fig~~. Plate 12).

3) All the veins do not record both phases of hydrocarbon migration. Large patches of hydrocarbons coating vein calcite(2) and filling small cracks within it, suggest secondary hydrocarbon migration postdating fracturing events and after precipitation of vein calcite(2) (~~Figures A, B, C~~) (Plate 14).

4) Dissolution phases in all the veins differ suggesting significant control of local water rock interaction in production of acid water ~~(Fig 22)~~.

5) ~~Opaline silica~~ Chalcedony are more common in the veins which were initially cemented by quartz and later substantially dissolved out (~~Fig~~. Plate 12) ~~A, B~~).

6) The most common replacement in the veins are pyrite and barite (~~Figures A, B~~) (Plate 12).

Geochemistry of Veins

Chemical composition of the veins have been determined by atomic absorption spectroscopy (AAS) that show a pure calcite composition with minor Fe and Mg content. ~~Figure 22~~ This composition is similar to the calcite cements observed in the sandstones. Sr content in these veins are also very high (up to 1200 ppm) which indicates that these vein calcites were precipitated from fresh meteoric water flushing (Longstaffe, 1987).

Carbon and oxygen analyses of the veins are shown in Table 3. In some of the wells, as in Stoney Creek-1 or in outcrop sections (e.g., Boudreau), the veins show two sets of oxygen isotope values, that indirectly would record a range of crystallization temperature. The veins near the depocenter of the basin in Hillsborough-1 show one set of oxygen isotope values. Although the data is limited, it can possibly be concluded that areas with overburden erosion show two sets of oxygen isotope values as compared to one where erosion is minimal. This observation suggests a possible interpretation that precipitation of fracture fills continued throughout an episode of decreasing host rock burial (i.e., lower temperature) (Narr and Currie, 1982). As such open fractures could have developed gradually when the overburden was eroded.

Carbon isotope signatures of the veins also show some variation as compared to the isotope values of the cements. The carbon isotope values are generally more negative than the cements but a few analyses show heavy carbon (up to +9.06% PDB). These characteristics of carbon signatures show significant local variation in the porewater evolution trend over the basin. Highly negative (up to -9.2% PDB) carbon values is due to Co_2 derived from decarboxylation of organic matter (-10 to -25% PDB, Irwin and Coleman, 1977) and a mixing of meteoric water which would dilute the existing porewater regime towards more positive values. A general relationship between the lighter carbon isotope and relatively heavier oxygen isotope values observed in most of the outcrops also point toward the fact that these veins formed earlier in the geologic history and at decreasing burial depth, possibly in a decarboxylation zone.

Heavy carbon isotopes (up to 15% PDB) have been reported in clayey organic rich sediments (Murata et al., 1969; Irwin et al., 1977) due to

fermentation reactions or biodegradation of petroleum (up to 14.3‰ PDB) (Dimitrakpoulas, 1987). Heavy carbon isotopes in the Albert Formation veins is generally restricted to the organic rich shales which suggest carbon isotope enrichment due to microbial attack during fermentation reactions. Since most of the carbonate veins ~~post~~re date phases of hydrocarbon migration and as the hydrocarbons show no biodegradation (33-~~53~~35° API), its role in ^{13}C enrichment of the carbonate phases can be neglected. $\delta^{13}C$ and $\delta^{18}C$ signatures of the veins are plotted in figure 20.

Secondary Porosity

Secondary porosity in sandstones is created by subsurface dissolution of detrital grains such as feldspars and cements by undersaturated or agressive porewater with respect to dissolved mineral phases (Bjorlykke, 1981, 1984; Bogli, 1964; Plummer, 1975; Schmidth and McDonald, 1979; Surdam et al., 1984; Giles and Marshall, 1986; ~~Surdam and~~ Crossey et al., 1986; Erdman and Surdam, 1986; Curtis, 1983 and many others). This observation was of significant importance in the discovery of new hydrocarbon bearing sandstone reservoirs at depths which would otherwise not be considered viable.

Albert Formation sandstones independent of composition show significant generation of secondary porosity from dissolution of framework grains and cements ~~and~~ which is mostly restricted in the eastern part of the basin. Dissolution of framework grains include quartz, detrital and diagenetic feldspars, carbonate cements and clays. Three phases of dissolution events have been recognized in the Albert Formation sandstones (Fig. 16) based on the following evidences:

(1) Early dissolution (predating early quartz overgrowth formation) of

feldspars and quartz grains and calcite(1) (~~Figure~~ (Plate 13)).

(2) Intermediate phase of dissolution recorded by incomplete to complete solution stripping of quartz overgrowths (~~Fig.~~ (Plate 14)), corrosion of diagenetic and detrital feldspars (~~Fig.~~ (Plate 14)), calcite cement(2) and diagenetic chlorite (~~Fig.~~ (Plate 14)).

(3) Late dissolution of ankerite (~~Fig.~~ Plate 7).

A mutual paragenetic sequence of these dissolved mineral phases is given in Figure 16.

Albert Formation sandstones, in most parts of the basin are both intra/ and interbedded with thick organic rich shale and marlstone sequences. Within the basin, there is a progressive decrease of the shale content from east to west. Also total organic carbon values is very low in the west of the basin (see "organic geochemistry" section). Secondary porosity is best developed in the Hillsborough, Stoney Creek and Dover areas, with no dissolution observed in the western part of the basin in LeeBrook, Apohaqui and Lower Millstream. With progressively coarser grain sizes, secondary porosity improves. This is probably because of the higher initial permeability of these sandstones permitting more acidic fluids to circulate around the available porenetwork. Maceral studies of these organic rich lithotypes in the Albert Formation suggest that the organic matter is predominantly exinite type (e.g., alginite B, lepdodertinite, Spornite and telalginite in order of relative abundance) with rare fusinites and vitrinites (Smith, 1985, also see section on "organic geochemistry").

The undersaturated or agressive porewater for leaching inorganic mineral phases in a sandstone can be derived from/ :

(1) Meteoric water driven by gravity heads,

(2) Organic acids and CO_2 derived during maturation of organic matter, and

(3) Clay mineral reactions.

Large volumes of meteoric water flushes through most sedimentary basins (Bjorlykke, 1981) effectively. However, leaching capacity of this water was questioned because of attainment of equilibrium with respect to reactive minerals in the initial portion of the flow path and in deeper part due to high temperature that promotes faster reaction rates and hence faster attainment of equilibrium (Giles and Marshall, 1986). Although the Albert Formation must have been flushed by meteoric water from the high groundwater head in Stoney Creek-Dover areas towards the center of the basin, absence of any secondary porosity in the younger outcrop sections suggest that ~~the~~ meteoric water did not have any control on porosity development. xx

Numerous studies were undertaken to understand the organic-inorganic interactions resulting in the production of organic acids and Co_2 in the sandstone/shale sequences. It was observed that different source rocks with varying type of organic matter have differential potential for Co_2 generation. Algal and mixed source rocks as found in the Albert formation, are incapable of producing sufficient Co_2 (Tissot, 1978). On the other hand, Surdam et al. (1984) in their experiments on different kerogen types observed that Type I Kerogen (primarily algal) releases significant amount of oxalic acid during thermal maturation in a water wet system. They also concluded that these oxalic acids are responsible for enhancement of porosity to varying degrees depending on the pH of the interstitial solution, framework and cement mineralogy, fluid flux, sandbody geometry

and sand/shale ratios.

Given the composition and maturation of the organic matter in the Albert Formation, it is postulated that most of the secondary porosity is generated from organic acids derived from lamalginite rich shales (Chowdhury and Noble, 1988). This hypothesis is further supported by the fact that the observed secondary porosity is always associated with sections thick in shale sequences. A low (average 1 to 2) sand/shale ratio and low pH interstitial waters expectable in the Albert Formation lacustrine setting possibly combined to generate the acid porewater environment required for framework and grain dissolution.

Acidic fluids generated during clay mineral reactions is generally buffered by reaction between the fluids and the feldspars and the carbonate present; and thus reducing any significant expelled acid to the reservoir. In the Albert Formation absence of any significant mixed layer clays suggest no contribution of mixed layer clay reactions in generating secondary porosity.

Solution Texture

Development of acid porewater pre-requisite to dissolution of framework grains and cements has been described in the secondary porosity section. Here the solution textures and their formation mechanisms is described.

The following criteria have been used to describe solution pores (Schmidt and McDonald, 1979; Shanmugam, 1984):

a) Oversized pores,

b) Elongate pores,

c) Corroded grains,

d) Remnant cement,

e) Partial dissolution, and

f) Intraconstituent pores.

Oversized pores observed are mostly fabric selective and include: dissolution of calcite cement filling primary pore, calcite replacement of feldspars and dissolution of clay fill (Plate 13)

Elongate pores in the studied sandstones are mostly concave with adjacent corroded grains. This is mainly caused by solution of a suite of minerals, including matrix, intergranular and syntaxial cement (Plate 13).

Corroded grains are very common and proved to be the most important criteria for identification of different solution phases. These are recognized by uneven replacement of the grain boundary margins.

Remnant cement and partial dissolution almost always occur together. Remnant cements were most commonly observed in calcite cements with extensive dissolution.

Intraconstituent pores are most commonly seen in the feldspars, quartz and ankerite.

Detailed studies have been carried out on different dissolution mechanisms and the resultant diagenetic textures of quartz (Williams and Crear, 1985a, 1985b; Berner, 1978; Hurst, 1981; Hurst and Bjorkum, 1986; Schwartzentruber et al., 1987 and many others) and feldspars (AlDahan and Morad, 1987; Petrovic, 1976; Berner and Holdren, 1979; Aagard and Helgeson, 1982; Chou and Wollast, 1985; Busenberg and Clemeney, 1976 and many others).

Dissolution reactions are either controlled by transport of ions to and from the reacting surface or by the reaction at the solid solution interface (Berner, 1978, 1980). Transport controlled dissolution is

characterized by rapid non-specific corrosion and is typical of concentrated solutions or highly soluble minerals. The resultant texture is intense etching and corrosion of all available sites. Surface reaction controlled dissolution by contrast is generally slow and more specific, being typical of slow dissolution of relatively insoluble minerals in solutions of low chemical reactivity and tends to produce distinct crystallographically controlled features such as well defined notches (Burley and Kantorowictz, 1986).

Burley and Kantorowictz (1986) have observed a number of quartz solution features by SEM studies that includes pits or notches, embayments and depressions. Pits are highly irregular shaped in contrast to more uniform V-shaped notches. Embayments are coarse in sizes (>20μm) and form by larger or coalesced pits. Depressions are the final products in the corrosion events where the embayments have considerably enlarged and have removed overgrowth surfaces such that they are no longer recognizable.

SEM studies on the quartz grains in the Albert sandstones show predominant "depression" textures with a few pits and notches suggesting a slow surface reaction control dissolution. Since surface reaction control is dependent more upon the chemistry of the solution rather than its hydrodynamic state, a highly alkaline or a low pH water condition prevailed during dissolution.

Like quartz, different etching patterns in feldspars have also been explained based on the nature of feldspar composition, solution chemistry, porosity-permeability and T-P conditions (Devore, 1959; FitzGerald and McLaren, 1982; Helgeson, 1971; Chou and Wollast, 1984; Petrovic, 1976; Berner and Holdren, 1979 and Holdren and Adams, 1982). Devore (1959) postulated that surface compositions (010, 100 and 001) depends on the

variable proportions of the unsaturated tetrahedra which could result in different reaction rates with pore fluids. Exsolution lamellae may also control dissolution, based on their frequency, arrangement and size (FitzGerald and McLaren, 1982; Yund, 1983; and Ribbe, 1983). On the mechanisms, two main thoughts prevail, whether dissolution occurs by diffusion through a protective layer (Wollast, 1967; Helgeson, 1971; and Chou and Wollast, 1984) or at the surface of the feldspars (Lagache, 1965; Petrovic, 1976; Berner and Holdren, 1979; and Holdren and Adams, 1982). Surface layer formation, if any, possibly does not have any control on feldspar solution (Fung and Sanipelli, 1982; Chou and Wollast, 1984; Holdren and Speyer, 1985; Chou and Wollast, 1985). In the Albert Formation sandstones, dissolution textures observed can be classified into the following types:-

(1) Parallel straight, shallow to deep etch pits (~~Fig.~~ Plate 15).

(2) Parallel curved deep etch pits (~~Fig.~~ Plate 16).

(3) Honeycomb network (~~Fig.~~ Plate 17).

(4) Stepwise in rectangular and irregular patchy network (~~Fig.~~ plate 17).

All the above solution textures suggest a predominant surface reaction control on dissolution (Berner, 1978). At least, two dissolution phases have been observed in the studied feldspars, evidenced by two distinct dissolution textures in diagenetic albite (~~Fig.~~ Plate 14). Since, dissolution is primarily dependent on porewater chemistry, the pH would have a significant control in dissolution. Feldspar dissolution may have been carried out under a low pH in early phase of dissolution and a late phase in a high alkaline (pH $\geq$ 11) condition acquired from the organic molecules during maturation of the interbedded shales.

K-feldspars

The K-feldspars in the Albert Formation sandstones, studied by SEM show a higher degree of variability in its etch pattern, as compared to the plagioclases. K-feldspars may show interlocking patchy skeletal dissolution texture (~~Fig.~~ Plate 1B) with differential dissolution on a single grain. At the center, a deep oval etch pit forms of about 40 μm in size that host the reticulate skeletal pattern bounded by partially dissolved prismatic nods. The pits between the rods is more dissolved along (001) rather than the (010) cleavage planes. Prismatic rods and skeletal fabric may represent two dissolution phases.

K-feldspar dissolution also results in the formation of parallel shallow to deep etch pits that retains partially dissolved crystals with thick rods and spiny terminations (~~Fig.~~ Plate 1B) (compare with AlDahan and Morad, 1987, p. 474). The occurrence of these rods in parallel planes may reflect cross hatched twinning in microcline. In extreme cases of dissolution this microcline show thin skins floating in a pore, which possibly have been carried out as a sheet removal along the grain surface. The sizes of these pits is highly variable and range from 1 to 8 μm.

K-feldspar dissolution with preserved overgrowths was also observed. This type of dissolution show (straight) shallow to deep etch pits. The surface is relatively smooth and forms dissolution steps parallel to (010) cleavage plane. This particular texture mimics albite dissolution texture (compare with AlDahan and Morad, 1987, p. 492). The pits parallel the cleavage plane occupying the space between dissolved out slabs and vary in sizes from 1 to 5 μm (~~Fig.~~ Plate 1A).

In extreme cases of dissolution, K-feldspars also show dissolution parallel to (100) cleavage planes. The preserved undissolved part of the

grain show corrigated pinnacles occurring in stacks. Etch pits vary in sizes from 1 to 2 μm. Typical fragile honeycomb textures representing advanced stages of dissolution was also observed (~~Fig.~~ Plate 17) (compare with Berner and Holdren, 1979, p. 1183). This growth stage might have reached from initial dissolution stage ~~(compare with figure)~~ by coalescence of initial etch pits to produce such a rugged irregular surface. The etched pits are deep and form an interconnected network of micro/macropores ranging in size from 1 μm to 20 μm. Compared with oligoclase prismatic honeycomb dissolution pattern (Berner and Holdren, 1979), K-feldspar dissolution network is highly irregular and maximum dissolution follows (100) plane rather than both (100) and (010) plane in oligoclase.

Albite

Although there is a slight overlapping in solution texture between albite and K-feldspar, albite dissolution texture is relatively smooth and symmetric (~~Fig.~~ Plate 14). The most common albite etch pits observed are preferentially along (001) cleavage planes (~~Fig.~~ Plate 14) (compare with Berner and Holdren, 1979, p. 1181; AlDahan and Morad, 1987, p. 506) with their long axes parallel to the c-axis. This etch pit is highly elongated, generally form smooth sides and show traces of chlorite precipitation. The initial dissolution phase (1) in this albite show highlighting of twins ~~(Fig.)~~. Advanced stages of dissolution also accompany along (100) cleavage planes ~~(Fig.)~~.

Submicron to micron sized etch pits which varies in shape from straight to curved was also obscured on the albite surfaces (~~Fig.~~ Plate 14) (compare with Berner and Holdren, 1979, p. 1176) which represents initial dissolution phases. Later solution textures in the same grain show

curvillinear pattern of solution pits along (010) cleavage planes.

The other pattern of solution texture observed in the albite is rectangular etch pits, stripped by stepwise sheet removals (Fig. Plate 15) (compare with AlDahan and Morad, 1987, p. 490) along the grain surface. The remaining skeleton grain is composed primarily of elongated rods (ditrigonal prisms) and the resultant pits are along (100) cleavage planes.

Oligoclase

Oligoclase dissolution texture is mostly parallel (straight to curvillinear) along (010) cleavage planes. Single oligoclase grains show two phases of solution textures (Fig. Plate 16) suggesting two different solution events. Oligoclase are less intensely dissolved as compared to the albite. Etch pits vary in sizes from 1 μm to 5 μm. In some cases, the etch pits also show infilling by diagenetic chlorite.

Oligoclase also show very fine, micro etch pits (≤ 1 μm) resulting in a sheet removal ~~(Fig.)~~. During sheet removal the grain is cleaved into different smaller grains as in flaky minerals. Oligoclase also commonly show "chatter marks" (~~Folk, 1975~~; Bull, 1979 and Grovener et al., 1978) which are the results of initial dissolution.

The "chatter marks" have been interpreted as mechanical scratching features, produced as a result of initial dissolution. True "chatter marks" have been interpreted as mechanical scratching features as a result of glacial abrasion (ibid.). However, Bull (1977) disputed that these "chatter marks" are dissolution features and represent initial stages of dissolution.

Organic Properties, Facies and Source Rock Potential of the Albert Formation

Significant amount of work has been done on organic geochemical aspects of the Albert shales (Smith and Gibling, 1987; Mossman et al., 1987; Kalkreuth and Macauley, 1984; King, 1963; Macauley et al., 1984) but most of the work so far has been restricted within the Stoney Creek oil field and the oil shale deposits in the south in the Albert Mines area. Lateral distribution of these shales, their source rock quality and maturity in the rest of the basin is virtually unknown. Even within the oil field very little quantitative maturation data is available (Kalkreuth and Macauley, 1984). This study was undertaken to gather more information on the source richness and quality, type of organic matter present and maturity in different parts of the basin.

Organic richness in the source rocks was determined by using total organic carbon (TOC) content of the shale cuttings. The source quality was analysed using Rock eval pyrolysis, maturity by vitrinite reflectance and thermal alteration index (TAI) and kerogen characteristics by transmitted light petrography. These analytical techniques are described in Tissot and Weste (1978), Hunt (1979) and Espitalie (1985).

For Rock eval pyrolysis analyses about 140 shales were samples from Shell Apohaqui-1, McLead Brook-1, Irving Chevron Lee Brook-1 and Irving Chevron Stoney Creek-1. Since most of the studied samples are cuttings, no attempt has been made to establish any relationship between organic content and lithotypes. A log approach has been followed to show source thicknesses and the degree of intercalation of the index-source lithologies.

Rock eval pyrolysis data (Appendix__) in the different parts of the basin show distinct trends in S_1, S_2, S_3, HI and TOC content. The above terminologies are described below (Tissot and Wette, 1978):

S_1 is indicative of light, indigineous or migrated hydrocarbons in a source rock.

S_2 represents how much hydrocarbons could be generated by thermal conversion or organic matter.

Production index (PI) plotted vs. depth indicates "oil window" maturation and the degree of migration and accumulation.

T_{max} indicates different stages of maturation (e.g., diagenesis, catagenesis and metagenesis).

On the basis of the above parameters, organic matter can be characterized into three main types (Tissot and Welte, 1978): Hutton et al., 1980.

1. Type I refers to organic matter with high initial H/C ratio (>1.5) and a low initial O/C ratio (<0.1), commonly characteristics of algal materials.

2. Type II is less rich in hydrogen (atomic H/C ratio 1.4-1.2) than Type I. This class of compound is commonly derived from single macerals such as sporinite and from mixtures of alginite with vitrinite, bituminite or inertinite.

3. Type III has a relatively low initial H/C ratio (less than 1.0) with a high initial O/C ratio and is commonly derived from terrestrial land plants.

Comparison of OI vs. HI (Figs. 19) plots to characterize kerogen types in the studied wells show predominantly Type III organic matter. Organic matter type distribution in the basin as a whole is represented in Figure 20. This study contradicts the general observation that the Albert shales are predominantly composed of Type I organic matter (Macauley et al., 1984;

Smith, 1985 and Mossman et al., 1987). Smith (1985) reported organic matter from Dover-Albert Mines areas with low total carbon content comparable to Type III but concluded that they are mainly caused by mineral matrix effects and low carbon content (Katz, 1983). However, in the present study no such relationship between low organic carbon content and the oxygen indices have been observed. This suggests that the oxygen indices are solely due to the type of organic matter present and not due to the matrix or carbon content. Additional evidence to support this, exists in the predominantly terrestrially derived organic matter composition as revealed by kerogen petrography (~~Fig~~. Plate 19).

Kerogen petrography data is summarized in Table 5 and plotted in Figure 21. Kerogen types are classified after Pocock (1982) and Masran and Pocock (1981).

Structural materials are all recognizable tissues which have a definite organization and could be both marine or terrestrial in origin. Amorphous materials are parts of particulate organic matter which are broken up and altered by mechanical means and with fungi and bacteria. "Grey amorphous" refers to highly degraded organic material with a "grey black" appearance in transmitted light. Inertinite represent more aromatic and oxidized components, also includes remnants of biological oxidation, forest fires or reworked materials from older sediments.

In many lacustrine basins, Type I to Type III organic matter show some distinct gradational trends (Powell, 1986). Given the distribution trends of the organic matter in the basin in Figure 20, it can be concluded that the organic matter in the western part of the basin is gas prone as compared to the predominantly oil prone kerogen in the east. This is also supported by the triangular diagrammatic representation of the organic

matter, where Dover/Albert Mines samples fall in the "oil" zone and the rest of the samples from different wells, including Stoney Creek fall in the "wet gas + condensate" and "Dry Gas" zones (Fig.21). It is surprising that the Stoney Creek samples fall outside the "oil" zone, although it hosts most of the oil field. This raises the probable question of whether the reservoired "oil" is migrated or originated from the interbedded shales. Given the limited number of organic petrographic data and the observation ~~(Fig. , depth vs. S_2/S_3 plot)~~ that most of the organic matter from top to bottom of the section is Type I, either way, no definite conclusions can possibly be made.

Maturity of the studied samples are represented in Table 6 ~~and in Figures 1 and 2~~. Since most of the studied sections are within the "oil-window" maturation and based on the relative abundance of the amorphous materials, maximum hydrocarbon potential exist in the Dover-Albert Mines areas. Amorphous materials represent partial chemical breakdown of the larger complex molecules, as such requires less maturation temperature to convert to hydrocarbons than the "structured" counterparts. Since the amorphous material contain more lipid rich materials per unit volume, each volume of the amorphous material would yield more hydrocarbons than an equal volume of structured material (Pocock, 1982). However, higher maturation levels have been suggested for the onset of oil generation from algal (Type I) rich source rock. In the Paris and Douala Basins (Type II and III) the peak of oil generation was observed at 0.8% to 1.0% reflectance, whereas in the Uinta Basin (Type I) the required reflectance was at about 1.1% (Tissot and Welte, 1978). Since the oil prone source rock in the Albert Formation is primarily algal and of reflectance levels of 0.8% to 0.94%, it can be suggested that the maturity level is close to the peak oil generation.

Oil Analyses

Unpublished data (St. Peter, File 315-84, Chevron (Canada) Ltd.) of four oil analyses have been incorporated in this study (Table 7). All these crude oil samples contain a high alkane and fall into paraffin class in the PNA (Paraffins, Napthenes and aromatics) triangular diagram (Fig. 22). High paraffin content is very characteristic of crude oils derived from continental organic matter particularly in a paralic and/or lacustrine environment. These light waxy crude oils as in the coal of the Carboniferous Albert Formation, has a high pour point (Table 7) and is derived from organic matter which is generally strongly reworked by micro-organisms (Tissot and Welte, 1978). Hedberg (1968) studied extensively this waxy crude oil and observed that they are frequently associated with coal or highly carbonaceous strata and are very common in shale/sandstone sequences.

In the Albert Formation, the most common algae is Botryococcus (Kalkreuth and Macauley, 1984) which beside fatty acids is also composed of olefinic straight chain hydrocarbons (Golpi, 1968). The Albert crude oils show a high percentage of olefins (up to 8%), low sulphur and nickel is prevalent over vanadium. API gravity of these oils are consistent (32-35°) and suggest a possible origin from the same maturation level (Fig. 23).

CONCLUSIONS

1. At the onset of Albert time, a predominantly lacustrine condition prevailed in the Moncton subbasin. East of the subbasin (e.g., Dover, Albert Mines and St. Joseph areas) was under deep-lacustrine conditions and while to the west, shallow and marginal lacustrine conditions prevailed.

2. Carbon and oxygen isotope analyses of carbonate cements and veins show a high degree of homogeneity in the entire basin. Carbon precursor in carbonate cements and veins was primarily inorganic with contributions from bacterial oxidation at shallow depths and skeletal material in deeper sections.

3. Provenance of sandstones is from mixed granitic/granodiorite and gabbroic complexes - a mix of Caledonian and Westmorland Uplift sources.

4. Porosity is mainly caused by acid dissolution of framework grains and cements during the maturation of the shales. Dissolution textures suggest surface reaction controlled dissolution.

5. Organic matter type in the Albert Formation is both algal and terrestrial in origin. Algal materials which predominate in the east of the subbasin serve as sources of oil. Shales in the basin have attained the "oil-window" maturation in most parts of the basin.

6. Hydrocarbons are highly paraffinic and derived from the same maturation level.

TABLE 5. Organic matter type and distribution at different depth intervals in different wells of the Moncton Subbasin

Well	Depth (meters)	ORGANIC MATTER TYPE							
		Amorphous Terres.	Grey	Struct. aqueous	Pollen and Spores	Struct. Terrest.	Inert-inite	Biodegraded Terrest.	Resinoids
Irving Chevron Stoney Creek-1	437	5	-	10	30	35	10	15	-
	789	5	-	5	25	35	10	20	-
	955	40	10	10	5	10	5	20	-
	988	40	5	10	10	15	5	15	-
Irving Chevron Hillsborough-1	1916	35	20	10	-	10	10	10	-
	1920	30	20	10	-	10	15	10	5
	2364	5	5	10	5	20	40	15	-
	3010.50	5	5	10	10	15	40	15	-
	3012.00	10	5	10	5	20	35	15	-
Irving Chevron Lee Brook-1	802.80	25	10	10	20	10	5	20	-
	989.86	15	-	10	15	15	5	25	5
	997.87	5	-	5	20	30	20	20	-
	1696.00	10	5	10	5	20	10	40	-
Gulf Lower Millstream	180	5	-	-	25	25	30	15	-
Arco Dover-1A	37	55	5	10	15	5	5	5	-
	185.07	45	10	10	15	5	10	5	-
Arco Albert Mines - 1A	25.90	55	5	10	10	10	5	5	-
	64.00	55	5	10	10	10	5	5	-

TABLE 6. Source rock quality, maturity and organic mattery type at different depth intervals in different wells in the Moncton subbasin.

Well	Depth (m)	Source Rock Quality	Maturity	Organic Matter Type
Irving Chevron Stoney Creek-1	320-820	Generally poor	Immature/ Mature	Type III/I
	820-1340	Good	Mature	Type I
	1340-1590	Poor	Mature	Type I
Irving Chevron East Stoney Creek-1	240-680	Poor	Mature	Type III/I
	680-980	Good	Mature	Type I
	980-1280	Poor	Mature	Type I
Irving Chevron Hillsborough-1	1350-3000	Poor	Mature/ slightly overmature	Mainly Type III
McLeod Brook-1	470-5280 feet	Fair-Good	Mature/ slightly overmature	Type III
Shell Apohaqui-1	190-1300 feet	Fair-Good	Mature	Type III
Irving Chevron Lee Brook-1	770-1180	Poor	Mature	Type III
	1180-1500	Good	Mature	Type III
	1500-2100	Fair	Mature/ slightly overmature	Type III
Gulf Lower Millstream-1	182-197	Poor	Poor	Type III

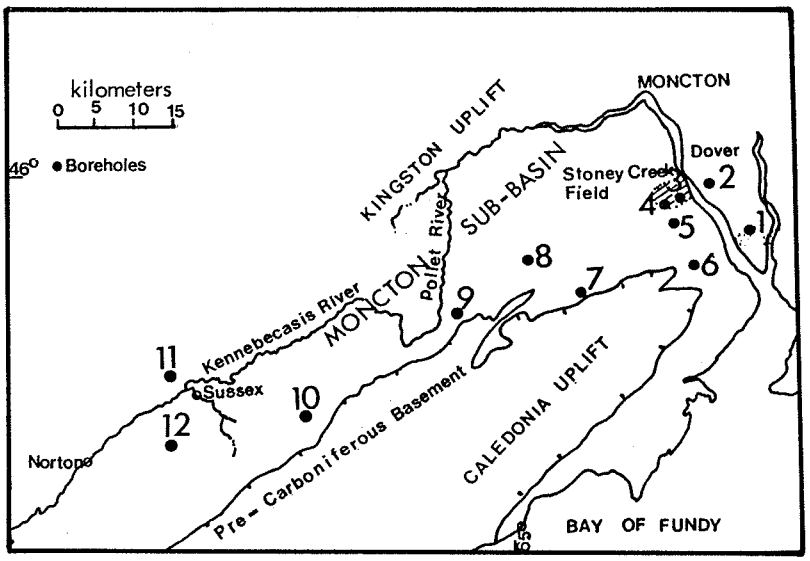

Location of wells incorporated in this study

4 □ IRVING-CHEVRON Stoney Creek-1

11 ▼ GULF Lower Millstream-1

5 △ IRVING-CHEVRON Hillsborough-1

3 ○ IRVING-CHEVRON East Stoney Creek-1

8 ◆ IRVING-CHEVRON Little River-1

7 ▣ ARCO Rosevale-1

1 ◇ ARCO Boudreau-1

6 ● ARCO Albert Mines-1

2 ■ ARCO Dover-1

10 ⊙ KERR McKEE Urney-1

9 ⧋ SHELL Apohaqui-1

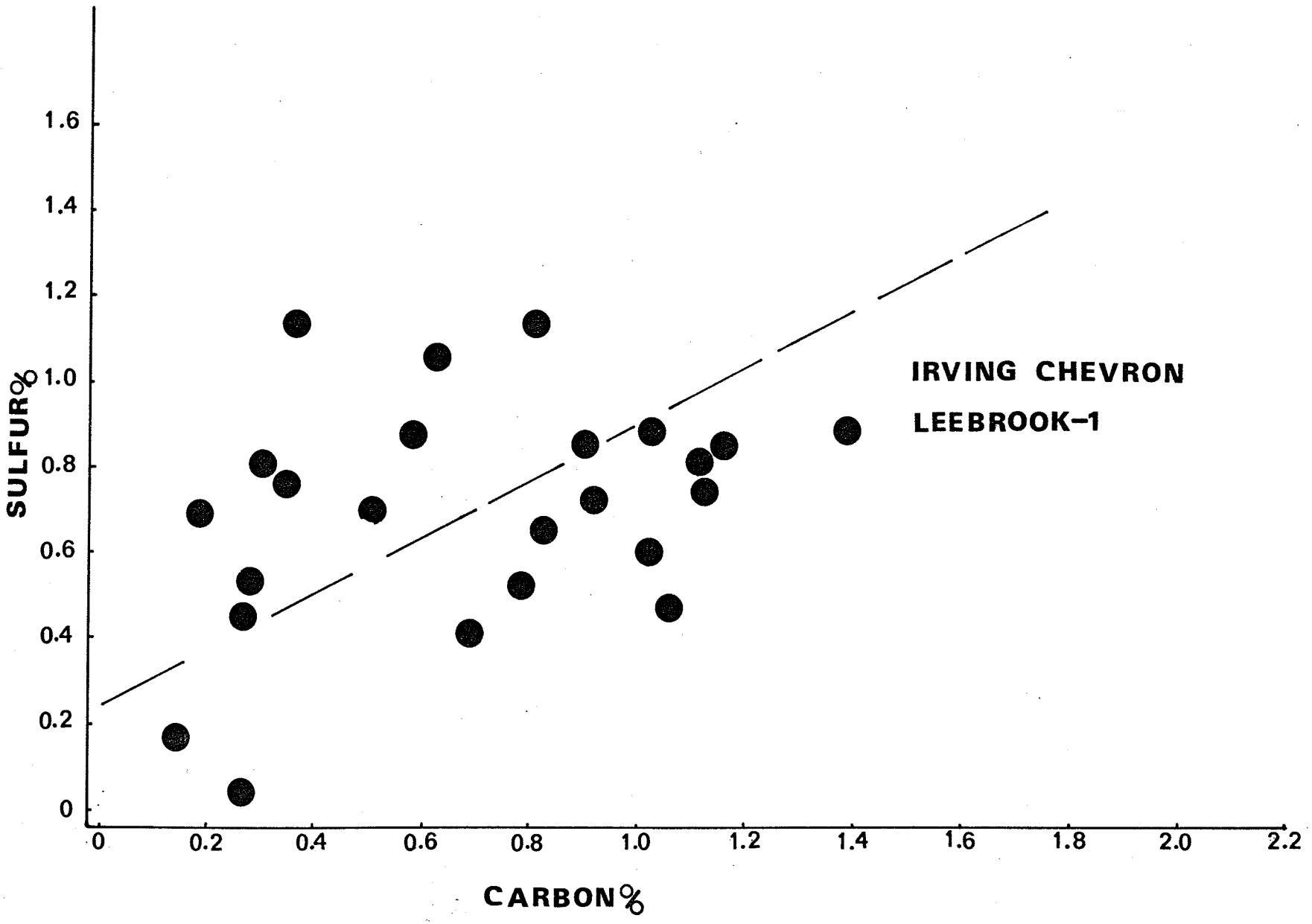

Figure 7: C/S plot of shale samples, Irving Chevron Lee Brook-1.

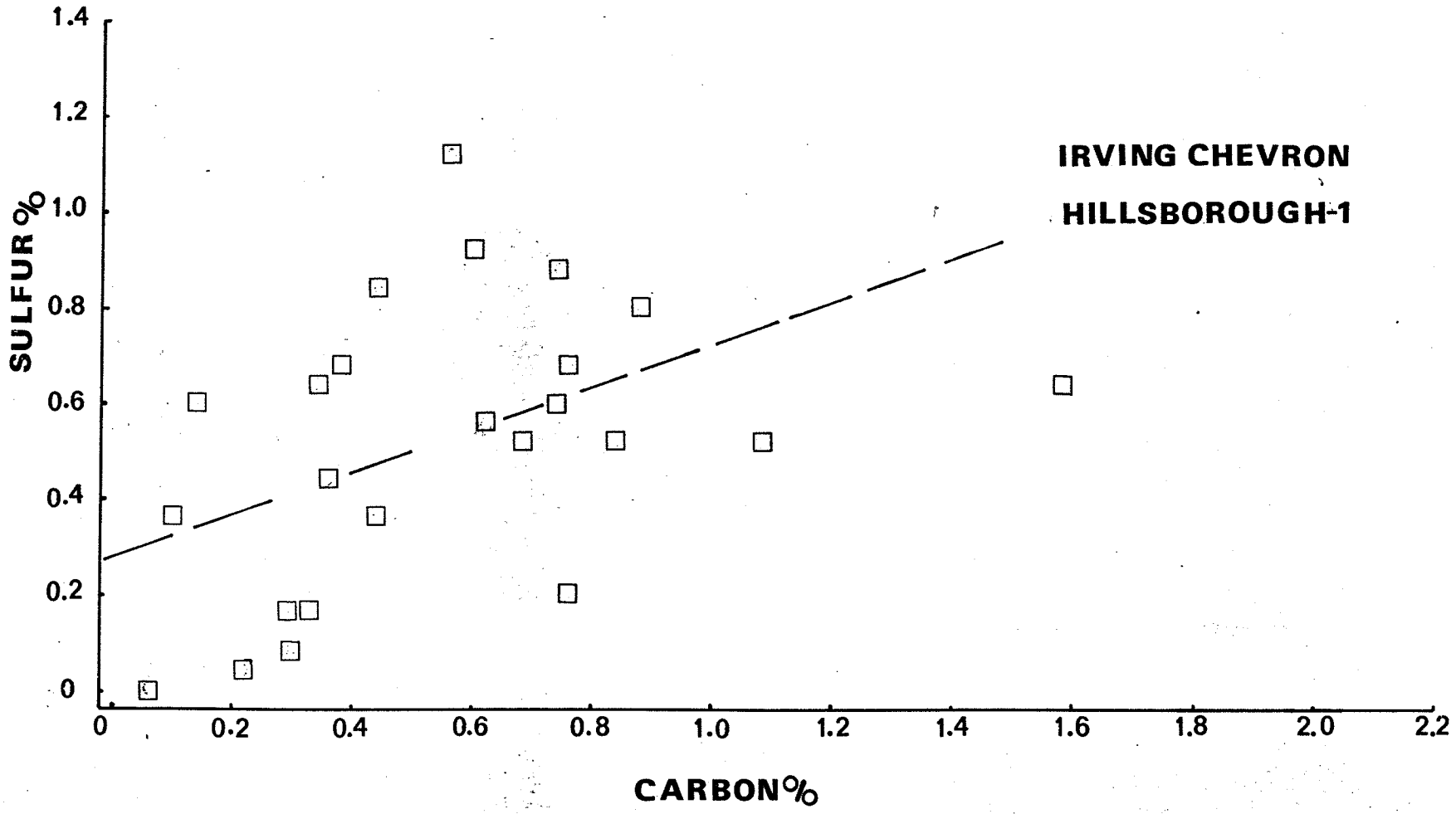

Figure 3: C/S plot of shale samples, Irving Chevron Hillsborough-1.

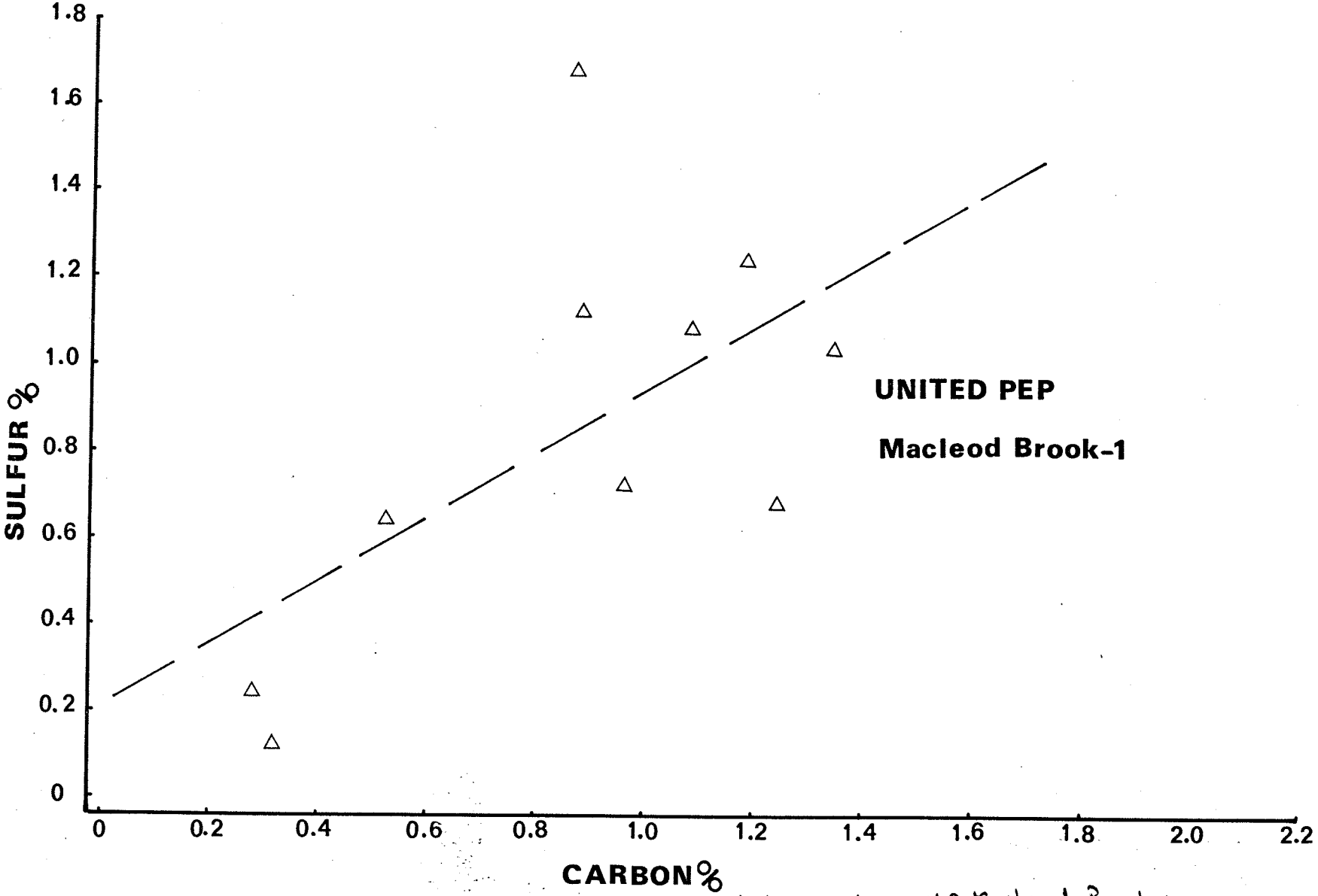

Figure 4: C/S plot of shale samples, UP Macleod Brook-1

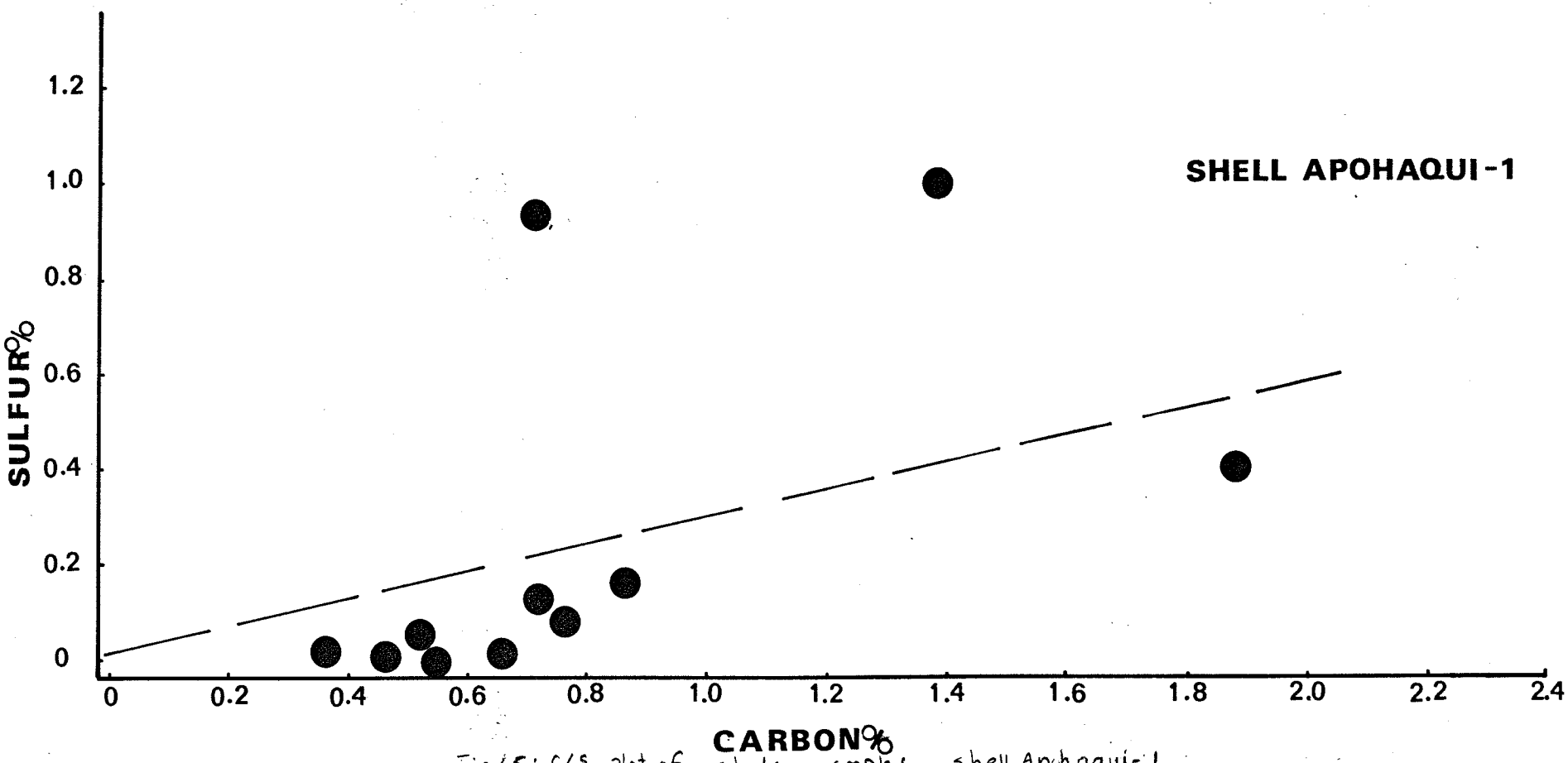

Fig 5: C/S plot of shale samples, Shell Apohaqui-1

Fig. 6.

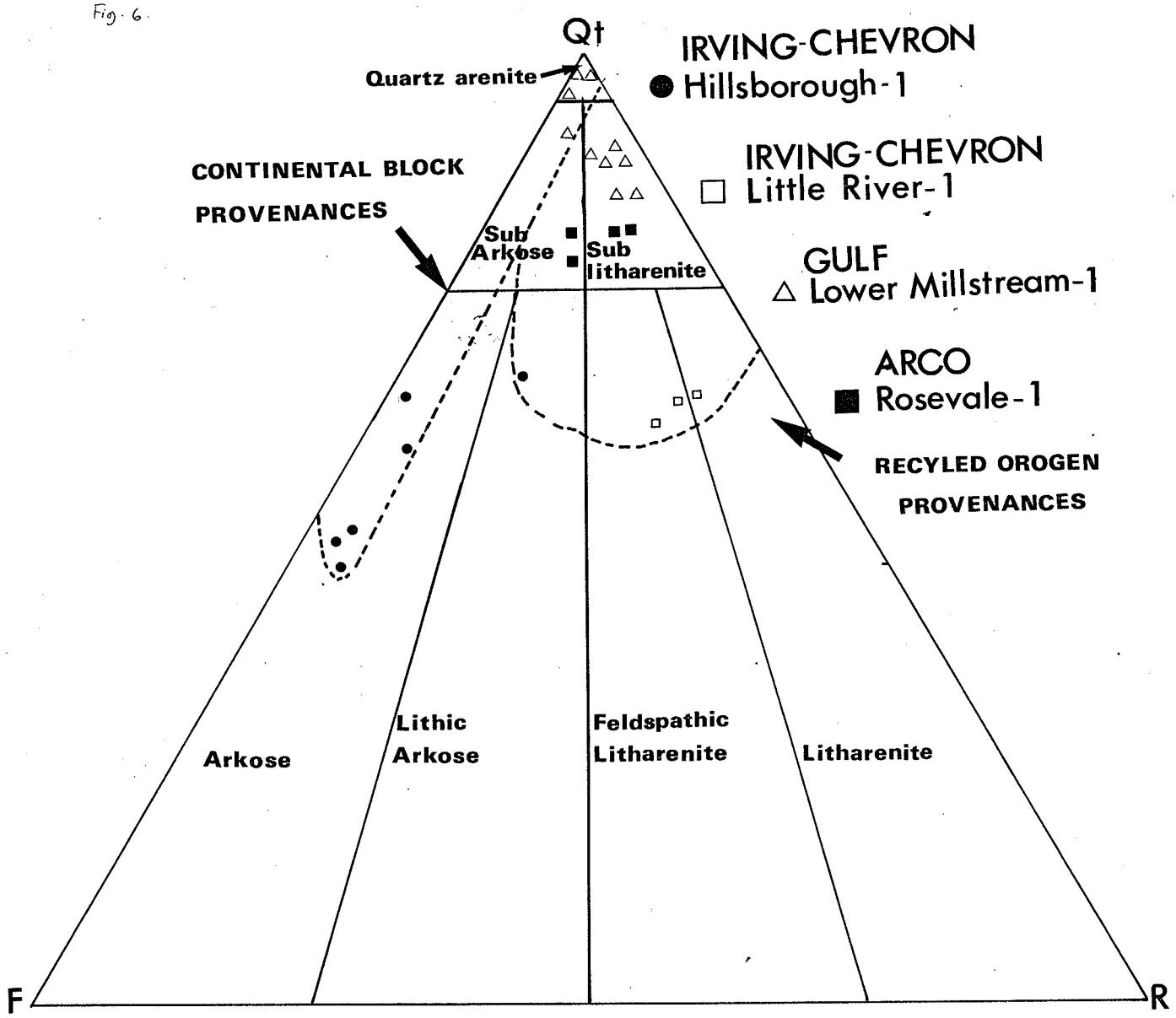

Fig. 6. QtFR triangular plot to illustrate composition and provenance of the Albert sandstones.

Fig. 7

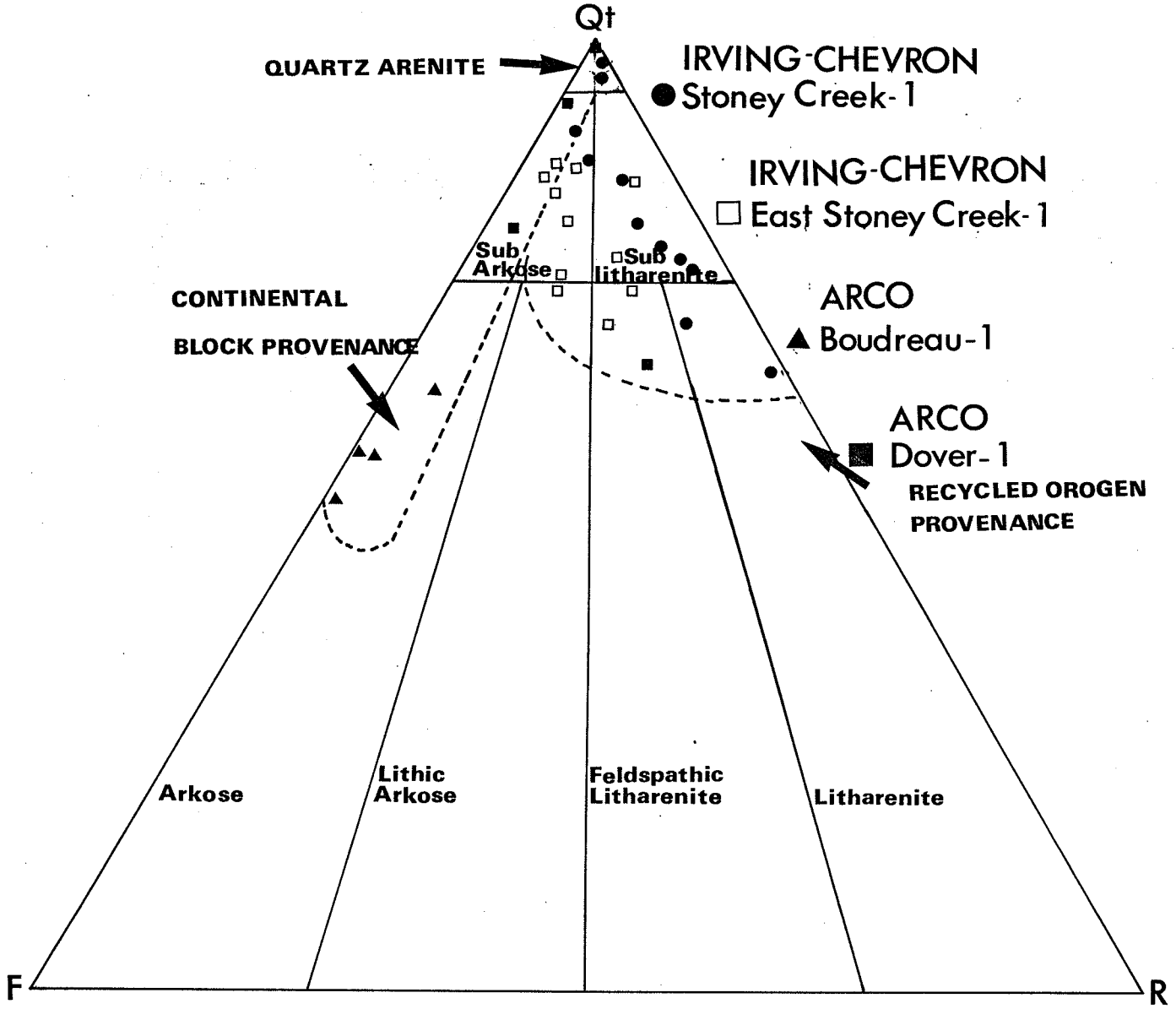

Fig. 7. QtFR triangular plot to illustrate composition and provenance of the Albert Formation sandstones.

Fig. 8

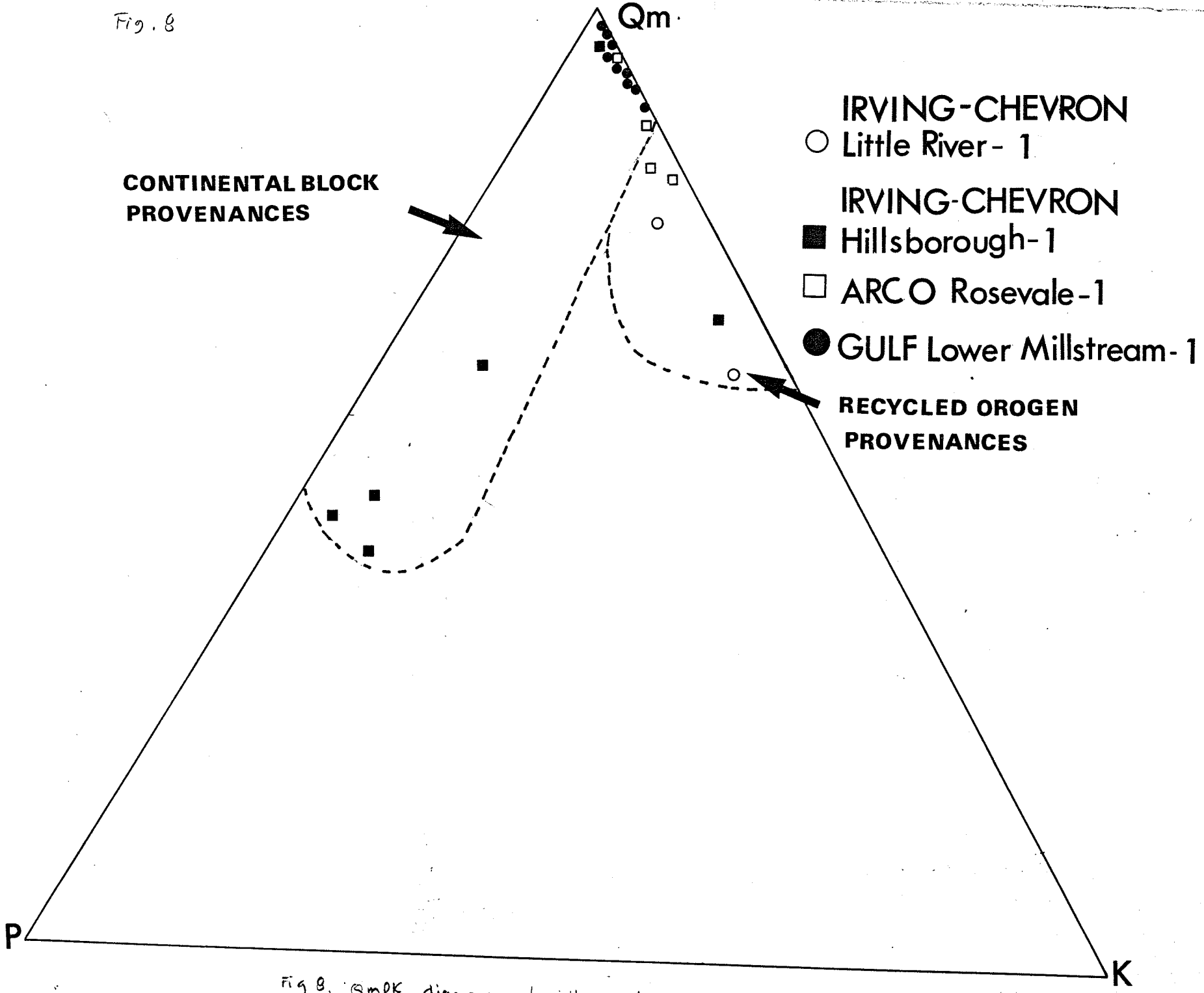

Fig 8. QmPK diagram to illustrate provenance.

Fig. 9.

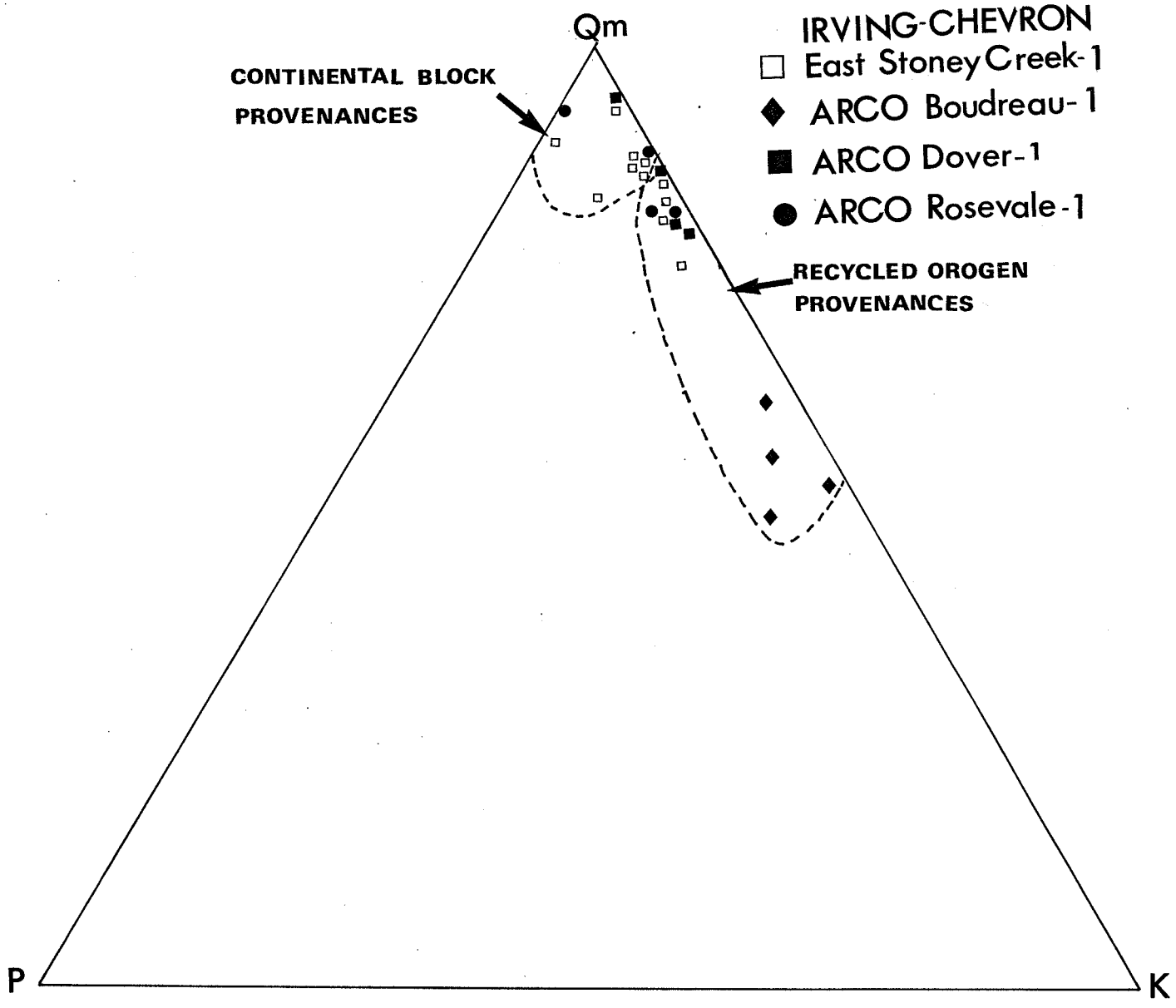

Fig. 9. QmPK diagram to illustrate provenance type.

Fig. 10

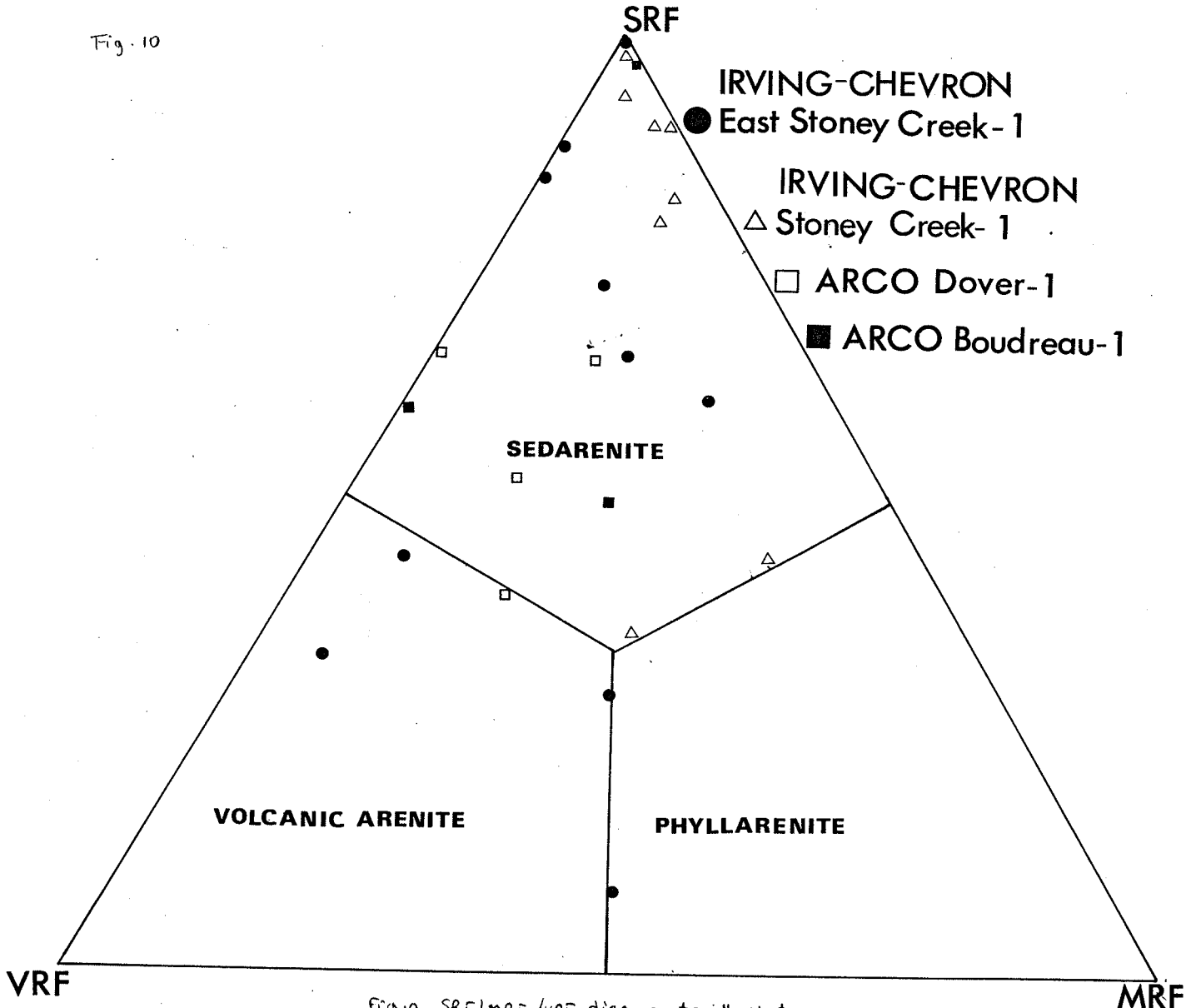

Fig 10. SRF/MRF/VRF diagram to illustrate rock fragment predominance in the studied sandstones.

Fig. 11

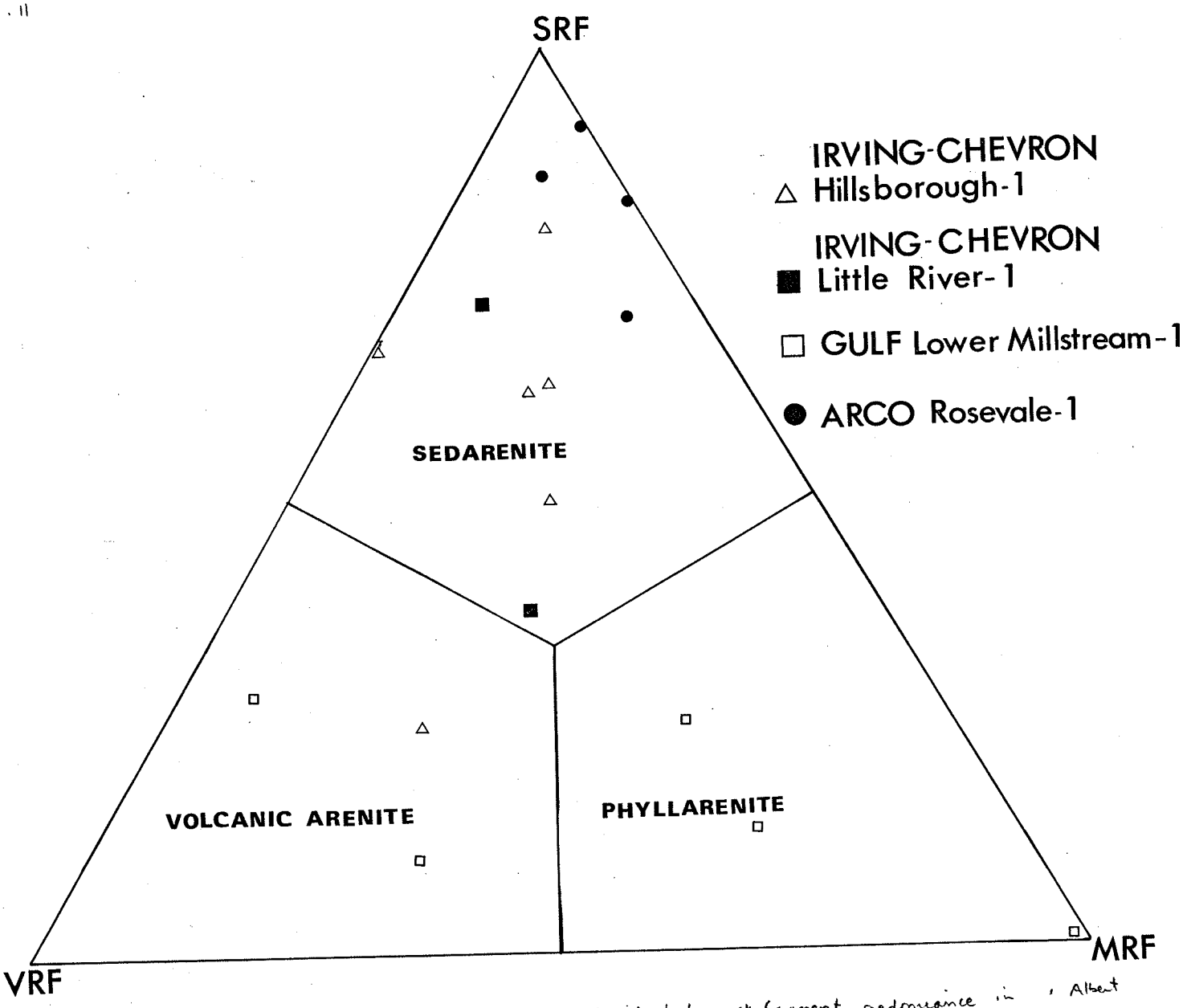

Fig. 11. SRF/MRF/VRF diagram to illustrate rock fragment predominance in Albert Formation sandstones

Fig. 12

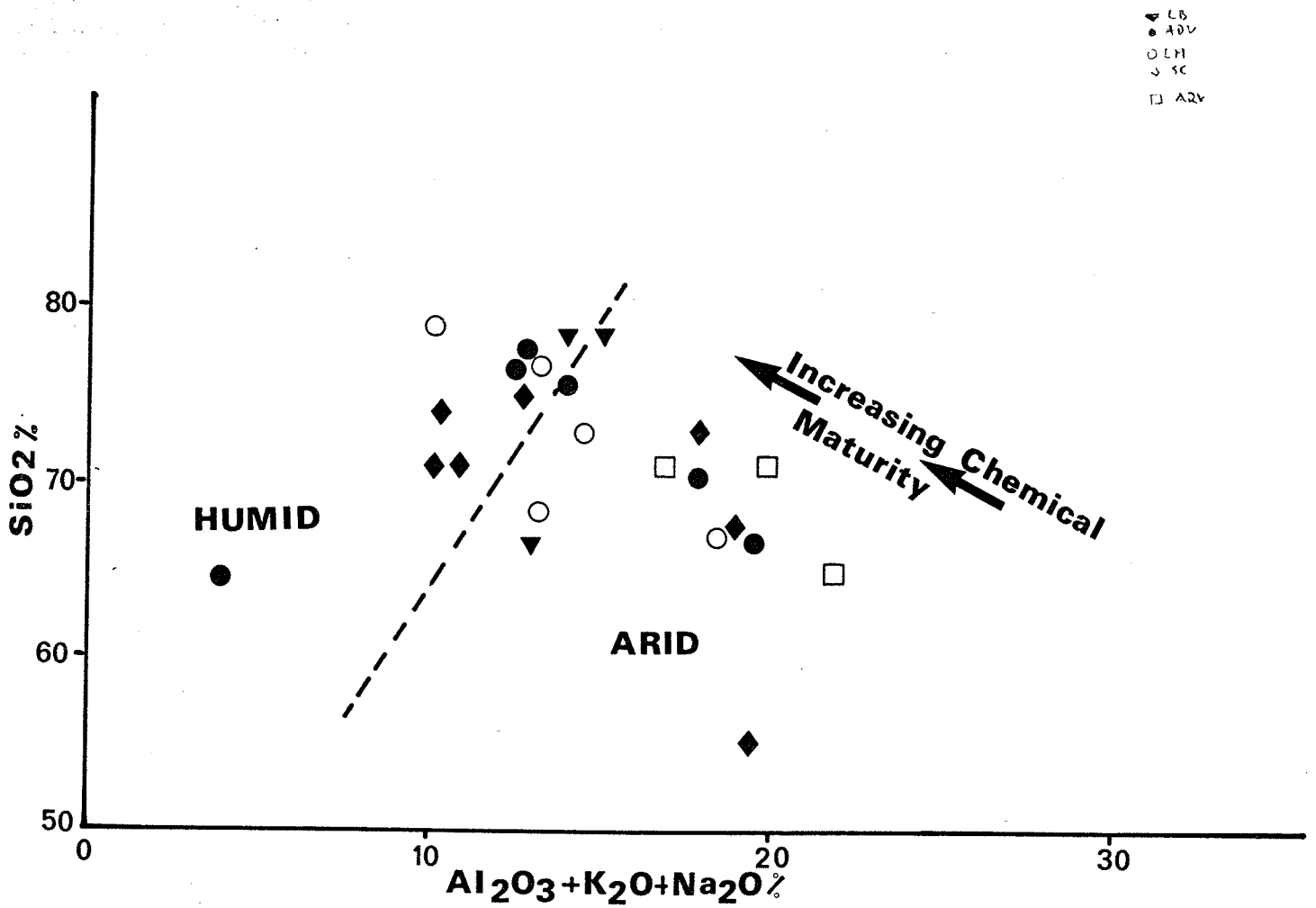

Fig 12. SiO_2% vs $Al_2O_3 + K_2O + Na_2O$% indicate both humid and arid climatic condition during Albert time.

Fig. 13.

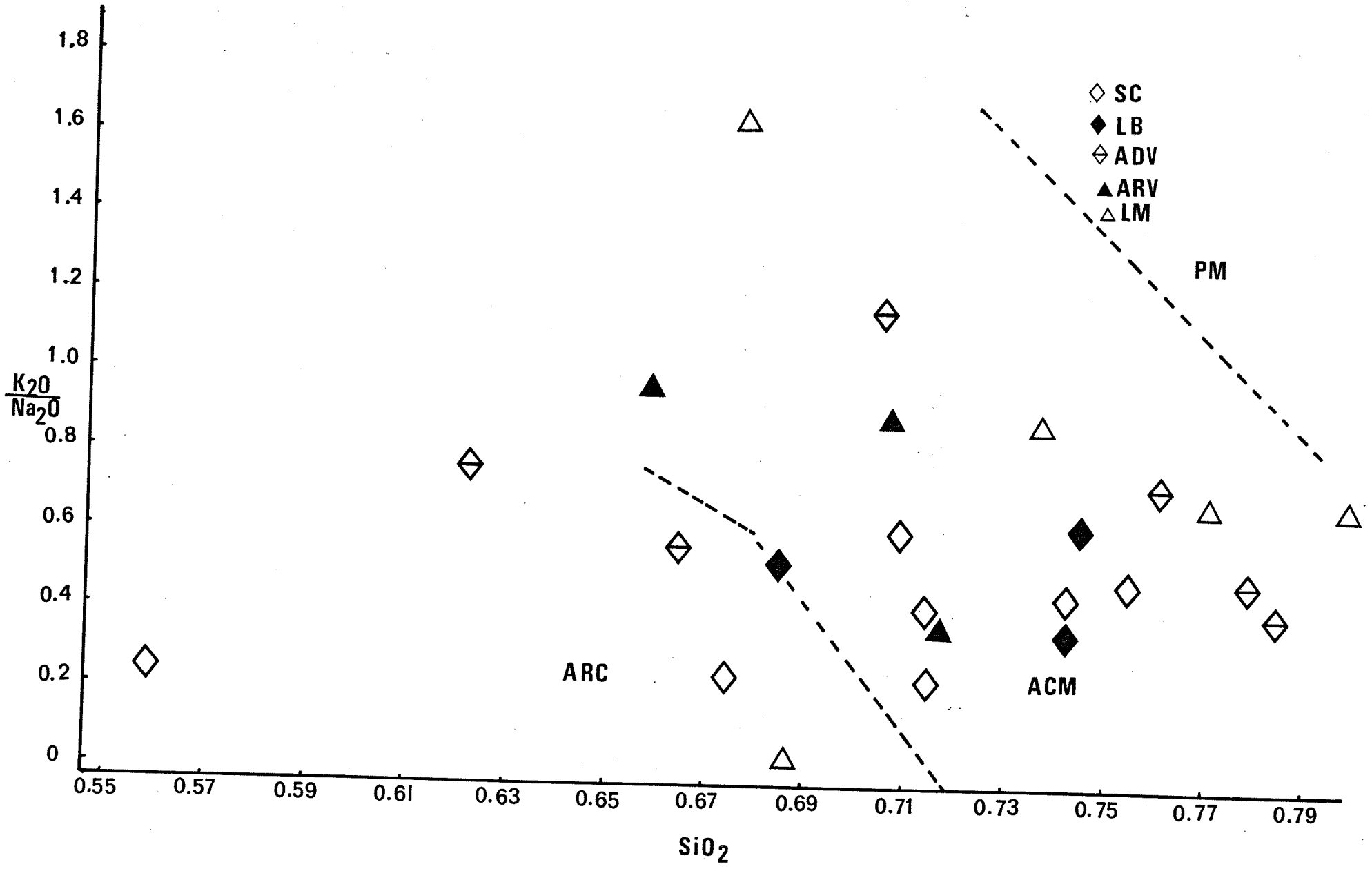

Fig 13. SiO_2 vs. K_2O/Na_2O diagram to illustrate the tectonic regime during Albian deposition.

Fig. 14

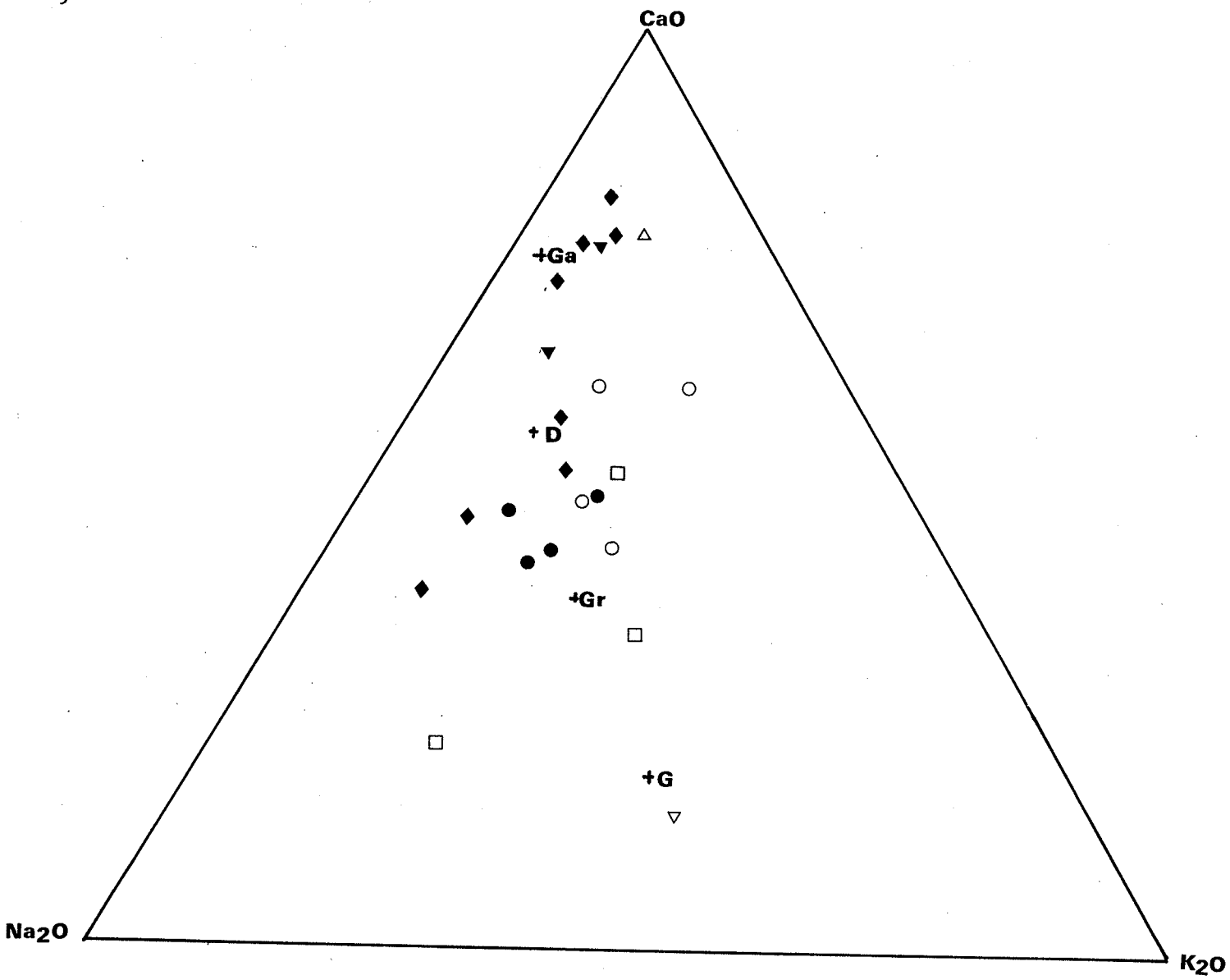

Frg. 14. CaO, Na_2O and K_2O diagram to compare Albert sandstone composition with Gabbro (Ga), Dacite (Da), Granodiorite (Gr) and Granite (G).

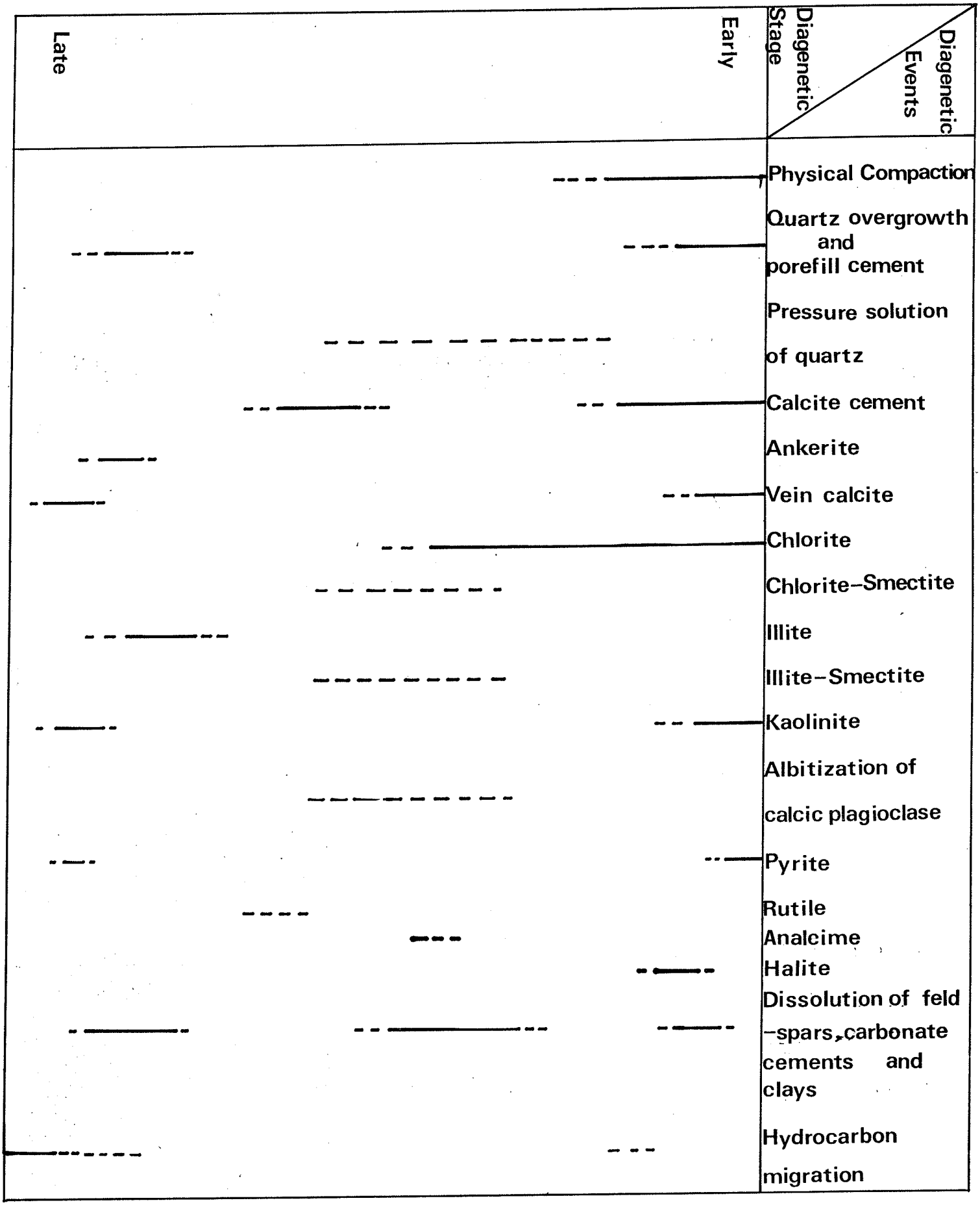

Fig. 15. Paragenetic sequence of diagenetic minerals.

Fig. 16

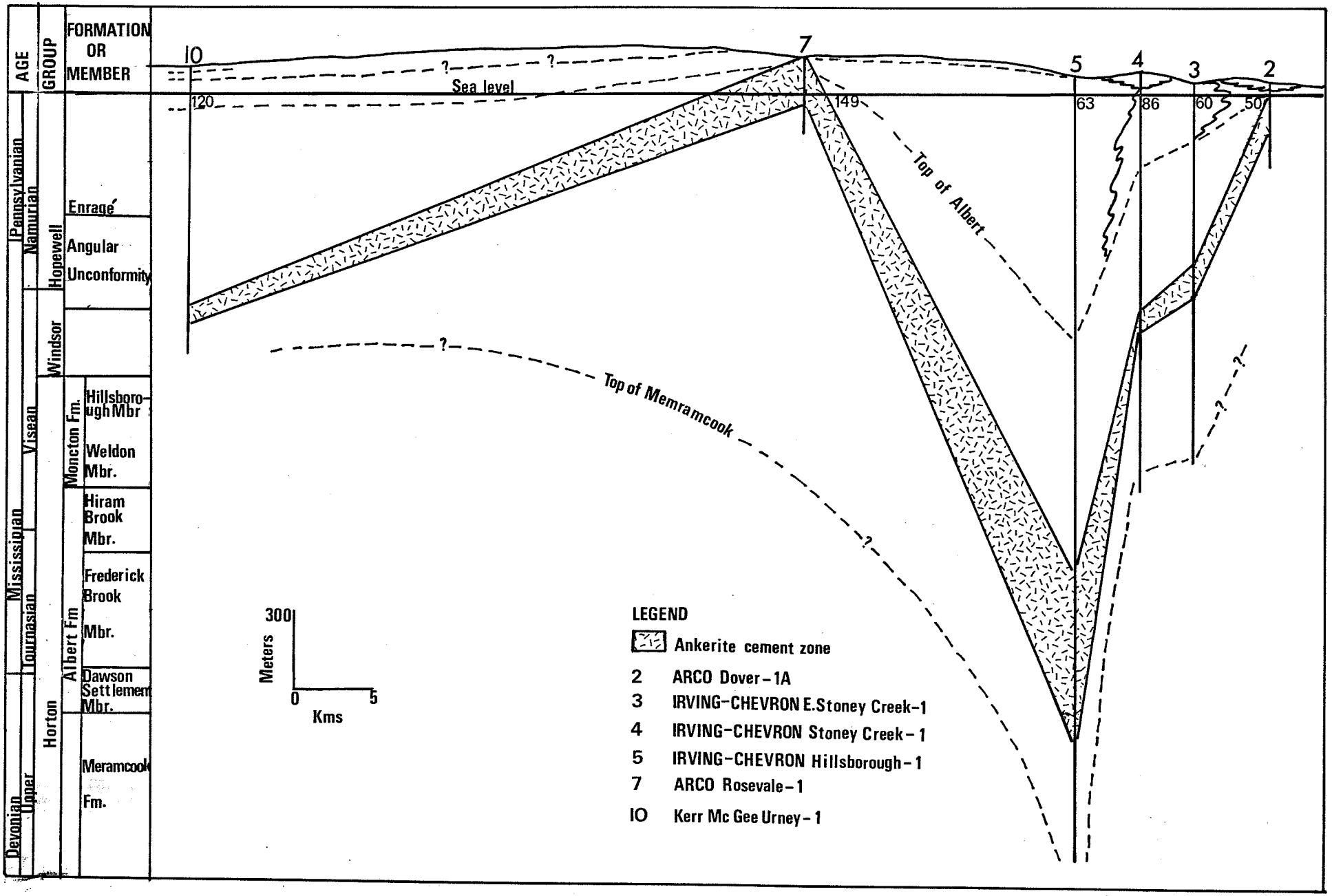
AGE
GROUP
FORMATION OR MEMBER
Pennsylvanian
Namurian
Mississipian
Visean
Tournasian
Devonian
Upper
Hopewell
Windsor
Horton
Albert Fm
Moncton Fm.
Enragé
Angular Unconformity
Hillsborough Mbr
Weldon Mbr.
Hiram Brook Mbr.
Frederick Brook Mbr.
Dawson Settlement Mbr.
Meramcook Fm.
10
7
5
4
3
2
Sea level
120
149
63
86
60
50
Top of Albert
Top of Memramcook
300
Meters
0
5
Kms
LEGEND
Ankerite cement zone
2 ARCO Dover-1A
3 IRVING-CHEVRON E.Stoney Creek-1
4 IRVING-CHEVRON Stoney Creek-1
5 IRVING-CHEVRON Hillsborough-1
7 ARCO Rosevale-1
10 Kerr Mc Gee Urney-1

Fig. 18

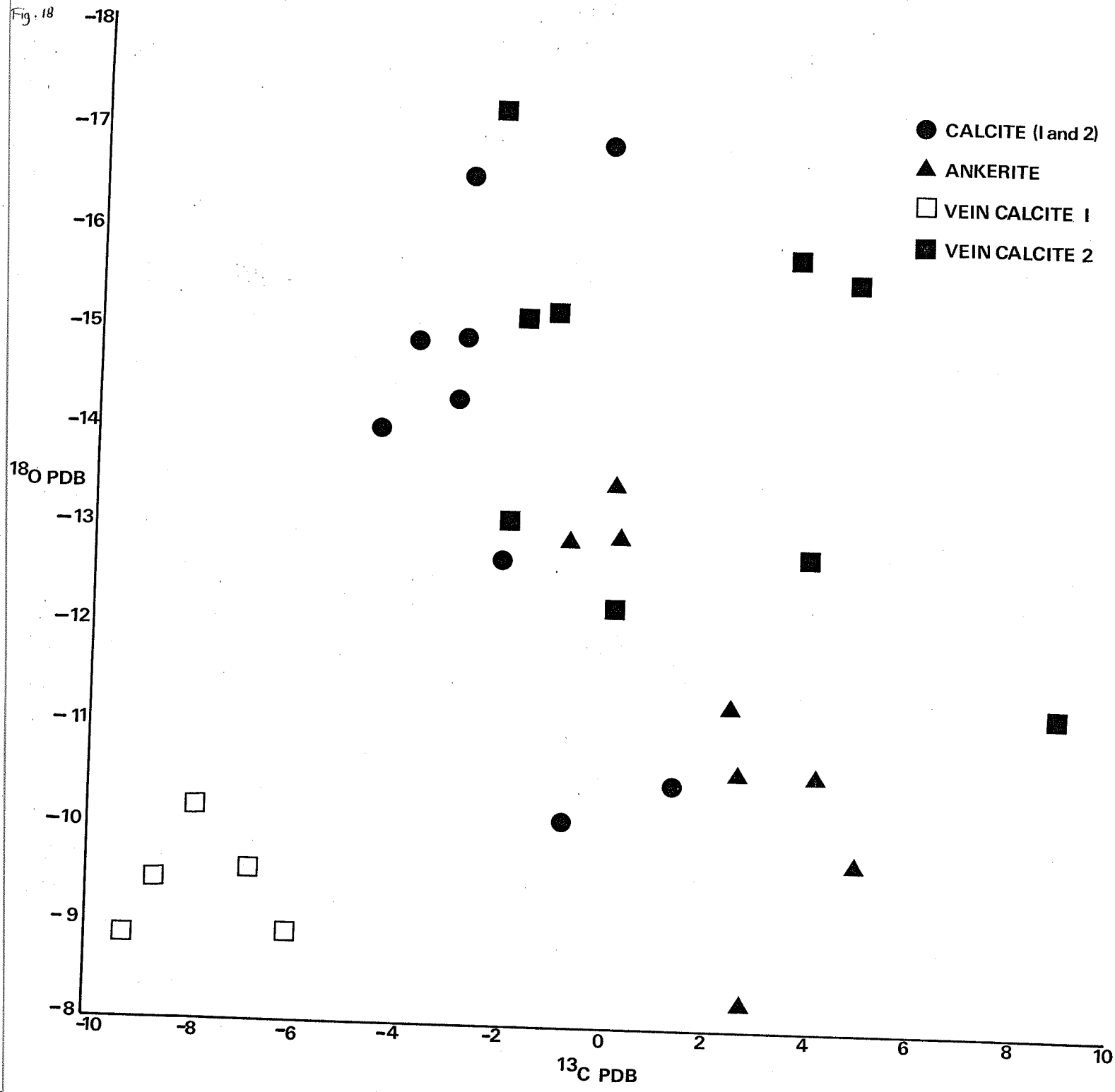

Fig. 18. ^{13}C vs. ^{18}O plot of carbonate cements and veins

Fig. 19.

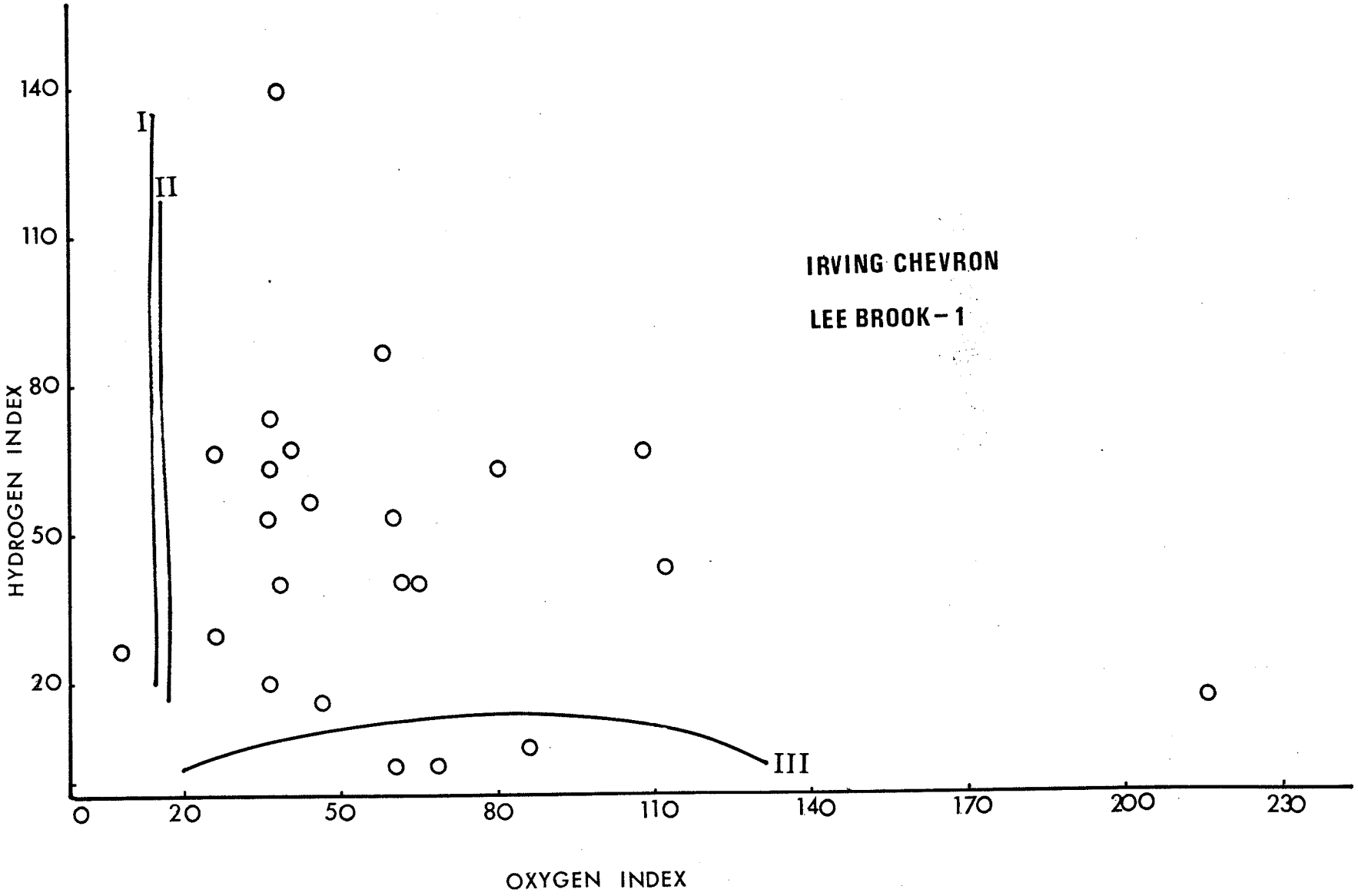

Fig. 19. Oxygen vs. Hydrogen index to characterise organic matter type.

Fig. 20

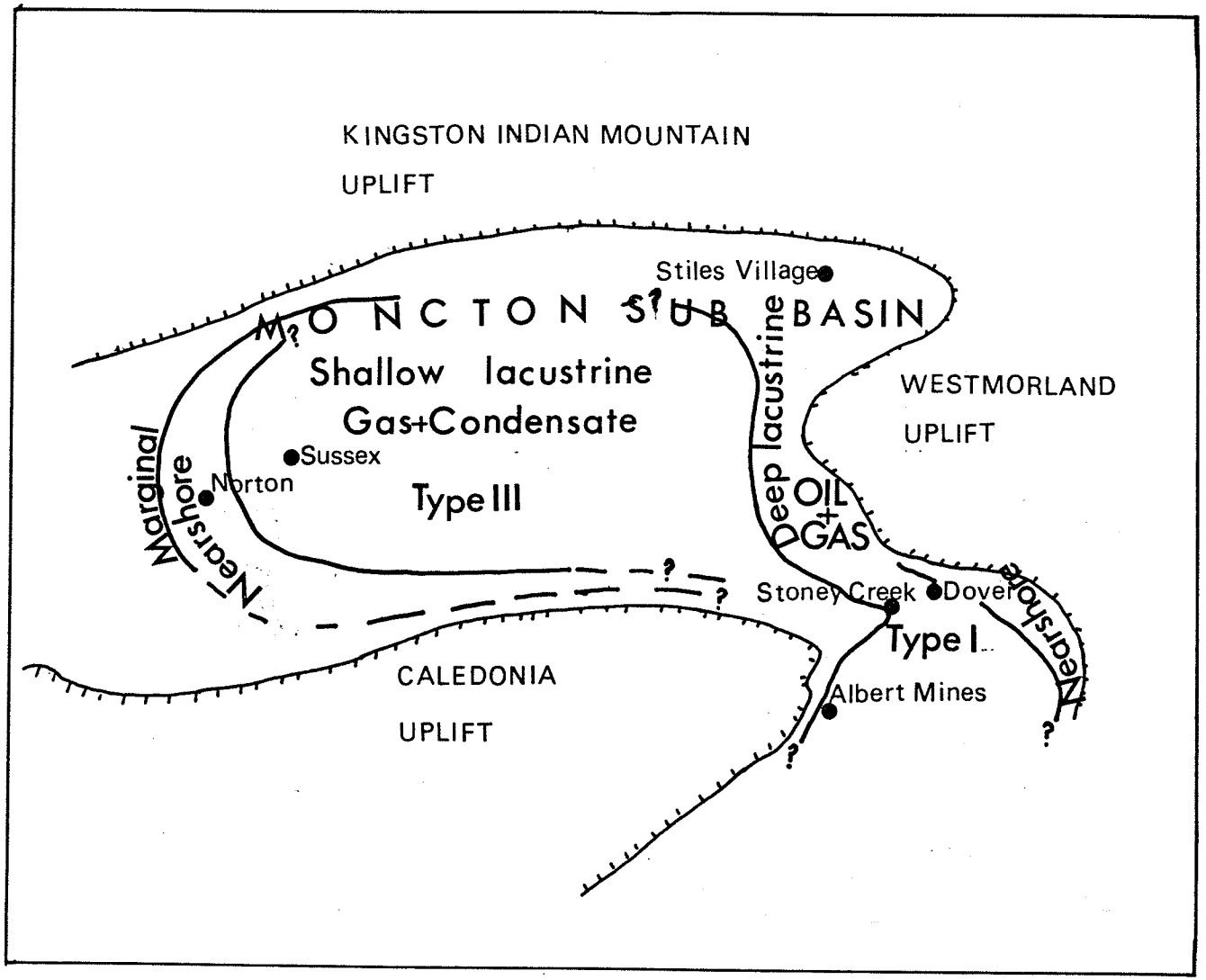

Fig. 20. Schematic representation of the lacustrine facies, organic matter distribution and oil and gas prospect in different parts of the subbasin.

Fig . 21

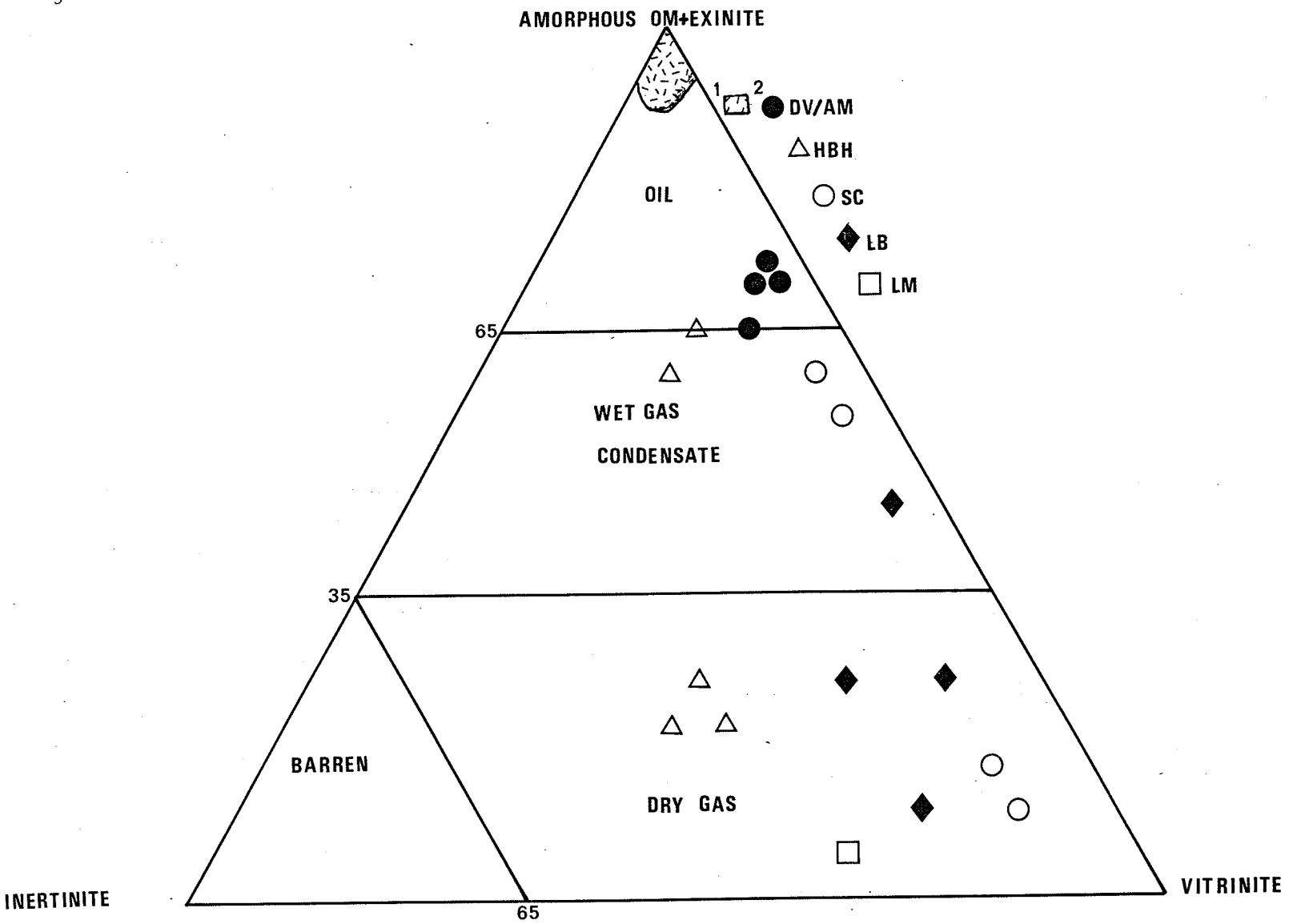

Fig. 21. Triangular diagrammatic representation of various organic matter type and hydrocarbon potential.

Fig. 22

● III
▲ ESCH
○ 56
△ PB

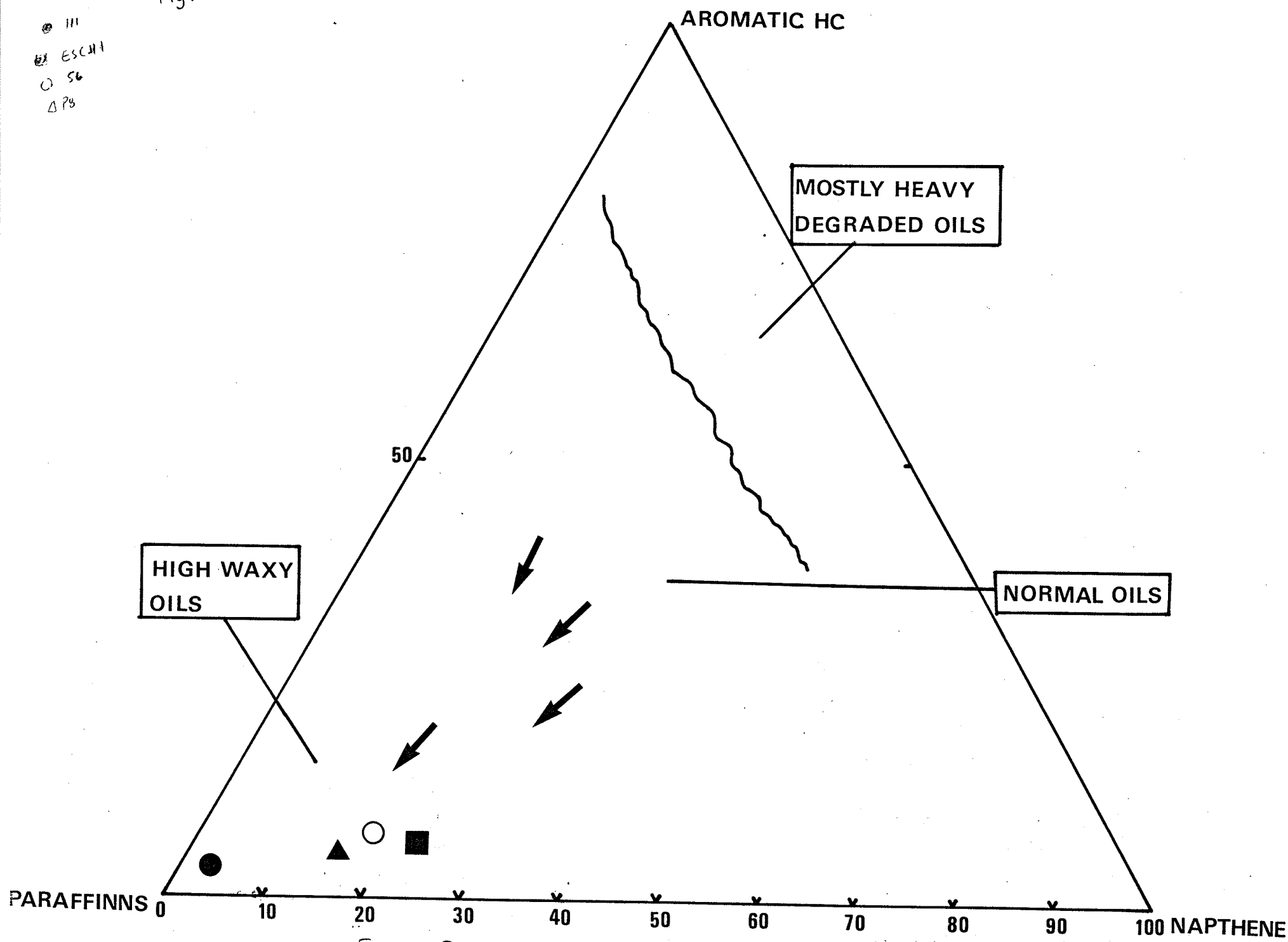

Fig. 22. Triangular diagram of hydrocarbon compounds in end members oils from Albert Fm. show high paraffinic

Fig. 23

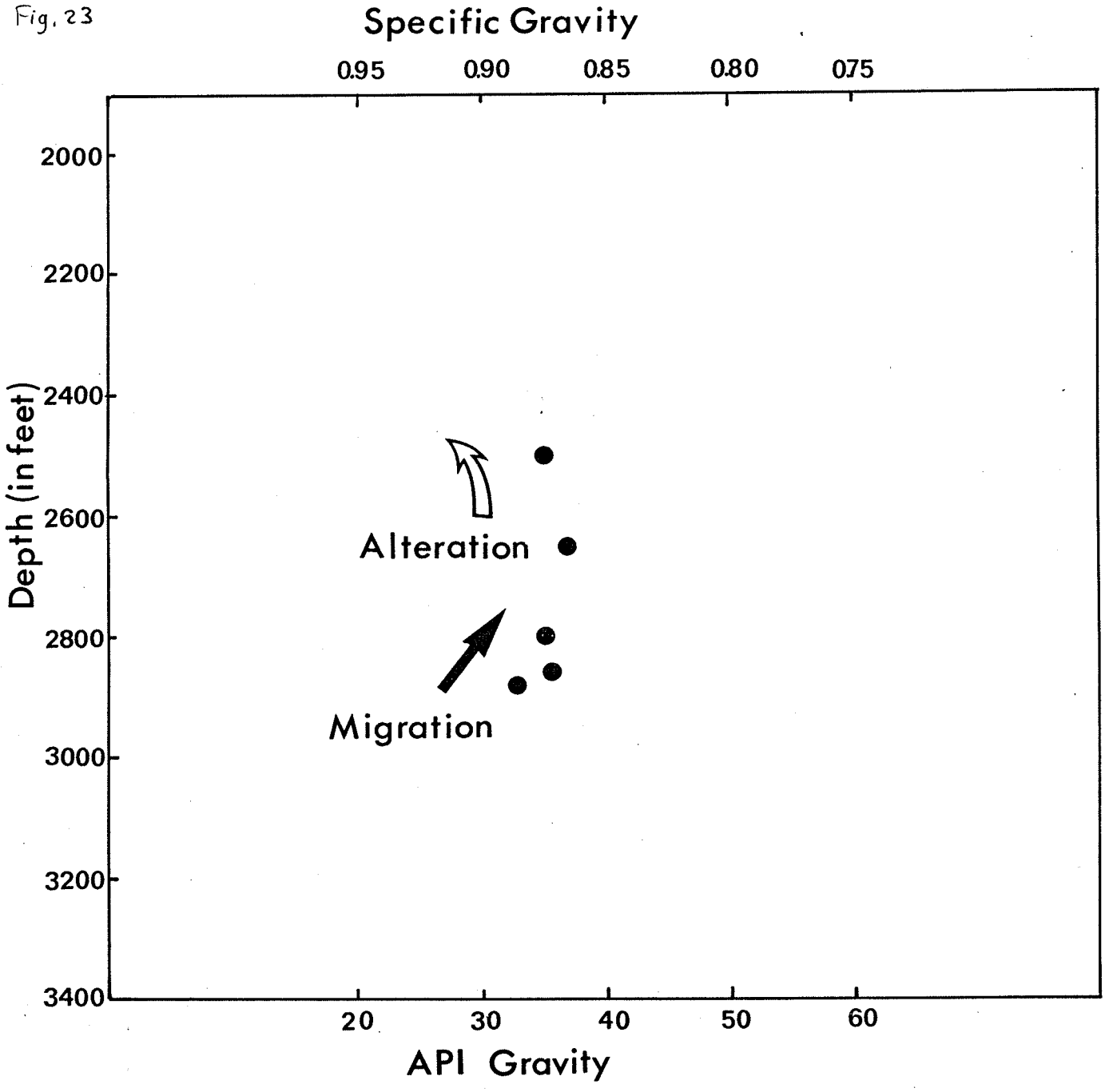
Specific Gravity
0.95
0.90
0.85
0.80
0.75
2000
2200
2400
2600
2800
3000
3200
3400
Depth (in feet)
Alteration
Migration
20
30
40
50
60
API Gravity

PLATE 1

A. Thin section photomicrograph to show fossiliferous and inorganic carbonate clast in an arkosic sandstone. Irving Chevron Stoney Creek-1, 443.14 meters.

B. Magnification of a carbonate clast shows two distinct petrofabric - a sparry calcite mosaic at the core is rimmed by pseudo-radiaxial fibrous (Rf) calcite.

C. Magnification of the above fibrous rim shows corrosion at the inter-growth contact of fibers, patchy inclusions and no replacement by later carbonate cementation events.

D. Thin section photomicrograph of a siltstone grain. Irving Chevron East Stoney Creek-1, 648 meters.

E. Thin section photomicrograph of oncolites in a micritic matrix. Dark patches of oil stain around the borders of the oncolites. Norton section.

F. Thin section photomicrograph of an void showing accretion of micrite around a K-feldspar nucleus. Boudreau section.

PLATE 2

A. Back Scattered Electron (BSE) photomicrograph of a quartz arenite showing profuse development of quartz overgrowths (Qo) into pore spaces (dark areas). ARCO Dover 1A, 100 meters.

B. Thin section photomicrograph to show enfacial junction (arrow) at the contact of two quartz overgrowths (Qo). Quartz overgrowth and the host grain is marked by a line of clay inclusions. P indicates porosity. ARCO Dover 1A, 120 meters.

C. Thin section photomicrograph of anhedral quartz cement (Q), Irving Chevron Stoney Creek-1, 450 meters.

D. SEM photomicrograph to show growth of numerous small quartz crystals in a pore. Irving Chevron East Stoney Creek-1, 770 meters.

PLATE 3

A. Thin section photomicrograph of displacive calcite within sheaves of biotite flakes. GULF Lower Millstream-1, 53 meters.

B. Magnification of the above to show pseudoanticlines formed by the injected pressure of displacive calcite.

C. Magnification of the above to show tenticular bodies of displacive calcite splitting a single biotite flake into multiples.

D. Thin section photomicrograph of a rip-up biotite clast rimmed by fibrous calcite cements (Fr) in a micrite matrix (M). GULF Lower Millstream-1, 53 meters.

E. Thin section photomicrograph of fractured framework grains floating in a micrite matrix. As above.

F. Thin section photomicrograph of an altered detrital K-feldspar grain showing fibrous calcite precipitation at only one side of the grain. As above.

PLATE 4

A. Thin section photomicrograph of poikilotopic early diagenetic pyrite (Py) cement. Quartz (Q) grains show corroded edges. Irving Chevron Stoney Creek-1, 457 meters.

B. SEM photomicrograph of framboid pyrites, Irving Chevron East Stoney Creek-1, 760 meters.

C. Back Scattered Electron (BSE) photomicrograph of fibrous calcite around an altered K-feldspar, GULF Lower Millstream-1, 53 meters.

D. Thin section photomicrograph of fibrous calcite showing corroded edges at the tip of the fibers, due to replacement by micrite. GULF Lower Millstream-1, 53 meters.

PLATE 5

A. Thin section photomicrograph of complete sparry calcite cement replacement of clasts (thick arrows) that retains well preserved grain boundaries. Irving Chevron Little River-1, 790 meters.

B. BSE photomicrograph of calcite cement (1) postdating early diagenetic chlorite (dark areas) and quartz overgrowth (Qo). Irving Chevron Stoney Creek-1, 450 meters.

C. SEM photomicrograph of calcisphere cements (Csp) resembling pyrite framboids, ARCO Dover-1A, 150 meters.

D. Thin section photomicrograph of calcite cement (Ca) and vein (V) from an outcrop sample. The continuity of the vein and the cement in thin section indicate same phase occurrence. At the lower left, clay lining (arrow) around quartz predate calcite. At the top center, calcite crosscutting quartz vein (thick arrow). Pollet River section.

E. Thin section photomicrograph of late diagenetic quartz overgrowth (Qo) in a porefill of lamellar twinned calcite. Irving Chevron Hillsborough-1, 2365 meters.

F. Thin section photomicrograph of poikilotopic calcite (1) cement (ca). At the bottom is an unaltered microcline. Irving Chevron Little River-1, 790 meters.

PLATE 6

A. Thin section photomicrograph of calcite (Ca) replacement of plagioclase (Pl) grain. Dissolution pore (Po) possibly postdates calcite replacement. Irving Chevron Stoney Creek-1, 450 meters.

B. Thin section photomicrograph of delicate calcite replacement morphology of plagioclase (Pl). Arrow shows a tiny plagioclase grain floating in replaced calcite (Ca). Irving Chevron East Stoney Creek-1, 700 meters.

C. Thin section photomicrograph of calcite replacement of polycrystalline quartz (Pq) and chert (C). Arrows show extent of replacement. Pollet River section.

D. Thin section photomicrograph of calcite replacement of polycrystalline quartz (Pq) and biotite (Bi). A fragment of the replaced biotite in calcite cement. At the bottom left (arrow), a thick wedge of replacement calcite onto the earlier phases. Long arrow indicates extent of replacement. Pollet River section.

PLATE 7

A. Back Scattered Electron (BSE) photomicrograph of stacks of late diagenetic ankerite rhombs (Ak) filling in a secondary pore. Ankerite postdate precipitation of albite overgrowths (Abo). Irving Chevron Hillsborough-1, 2364 meters.

B. Back Scattered Electron (BSE) photomicrograph of ankerite (Ak) cements showing abundant parallel solution pits, Irving Chevron Hillsborough-1, 1912 meters.

C. BSE photomicrograph of two isolated rhombs of ankerite nucleating around an extensively dissolved quartz grain (Q). Partially dissolved early clays (Cl) and albite (Ab). Irving Chevron Hillsborough-1, 1910.3 meters.

D. SEM photomicrograph of two phases of ankerite cements (1 and 2). Ankerite (1) is the precursor of ankerite (2) which is evidenced by partial dissolution of ankerite (1) and precipitation of ankerite (2) in close proximity to ankerite (1). Ankerite (1) occur as euhedral rhombs whereas ankerite (2) as irregular ovoids. Irving Chevron Hillsborogh-1, 2364 meters.

E. SEM photomicrograph of tiny rhombs of ankerite (1 and 2) precipitating on the surfaces of the detrital grains. As above.

PLATE 8

A. BSE photomicrograph of replacement dolomite in calcite cement (1). Irving Chevron Stoney Creek-1, 683.5 meters.

B. Magnification of the above to show rhombic characters of the dolomite and development of sucrosic porosity (P).

C. Siderisation (Si) of ankerite cement nucleus. At the lower center an authigenic albite (Ab) replacing ankerite (Ak). Siderite rhombs are partially indented into the albite grain (Ab) that indicate sideration postdating albite replacement. ARCO Rosevale-1, 147 meters.

D. SEM photomicrograph of albite (Ab) replacing anhedral calcite (1), Irving Chevron Stoney Creek-1, 683.5 meters.

E. SEM photomicrograph of calcite cement replacements by euhedral pyrite (Py) crystals occurring in patches. Authigenic albite (Ab) at the lower right. Calcite cement (1) riddled with inclusions, Irving Chevron Stoney Creek-1, 689.7 meters.

F. Thin section photomicrograph of large euhedral blocks of pyrite (Py) replacing calcite (1). Irving Chevron East Stoney Creek-1, 645.3 meters.

PLATE 9

A. SEM photomicrograph of porefill rutile needles (Ru) in association with authigenic chlorite (Chl). Flaky chlorites forming on the surfaces of the rutile needles indicating a later occurrence. Irving Chevron Stoney Creek-1, 600 meters.

B. Magnification of the above shows slight dissolution at the tip of the rutile needles. Pore space (Po) at the bottom and radial illites (Il) at the lower right.

C. SEM photomicrograph of delicate rutile needles (Ru) showing extensive dissolution as seen in the development of irregular corroded edges. Patches of irregular mussy illite (Il) precipitating on the rutiles. ARCO Boudreau-1, 54 meters.

D. SEM photomicrograph of "staircase" rutile (Ru) precipitating on a quartz grain. Arrows indicate stacks. Chlorite matrix indicated by chl. Irving Chevron East Stoney Creek-1, 700 meters.

PLATE 10

A. Thin section photomicrograph of rosette calcite as a secondary porefill in a calcite vein. Boudreau Section.

B. Magnification of a single rosette calcite. Dark areas are pore spaces.

C. Thin section photomicrograph microsparry calcite cement replacing larger poikilotopic vein calcites. Irish Town Quarry Section.

D. Thin section photomicrograph of a tapering form of vein calcite, Irving Chevron Hillsborough-1, 3000 meters.

E. Thin section photomicrograph of a brecciated vein, ARCO Albert Mines-1, 100 meters.

F. Thin section photomicrograph of two generations (1 and 2) of calcite veins in a dolomicrite. ARCO Rosevale-1, 80 meters.

PLATE 11

A, B. Thin section photomicrograph of two generations of calcites (1 and 2) in the vein. Irving Chevron Hillsborough-1, 2500 meters.

C, D. Thin section photomicrograph of reticulate irregular vein calcite, ARCO Dover-1A, 120 meters.

E, F. "Beef" calcite are composed of coarse to very fine fibers of calcite. From the fracture wall to the center, coarse fibers grade to sparry calcite. Fine fibers show concentrated inclusions at the contact between fibers. ARCO Rosevale-1, 120 meters.

PLATE 12

A. Thin section photomicrograph of vein calcite paragenesis and their morphology. Three generations of vein calcites (1, 2, 3) have been observed. Phase (1) is fibrous in form, Phase (2) is as tiny rhombic crystals followed by Phase (3) cornflake calcite. ARCO Rosevale-1, 80 meters.

B. Magnification of the above to show morphology of cornflakes.

C. Thin section photomicrograph of calcite vein infill (Ca) postdating dissolution of quartz (Q). Relict quartz (Q) veinfill showing irregular jagged edges at the right along the wall of the vein. ARCO Dover-1A, 90 meters.

D. Thin section photomicrograph of chalcedony (Ch) in a calcite vein. Formation of chalcedony postdates calcite (1) and predates calcite (2). ARCO Rosevale-1, 80 meters.

E. Thin section photomicrograph of barite (Ba) replacement in calcite vein, as above.

F. Thin section photomicrograph of spheroidal chalcedony in a calcite vein.

PLATE 13

A. Thin section photomicrograph of an irregular secondary vuggy porosity (P) formed as a result of dissolution of calcite cements (Ca) and chlorite (chl).

B. Thin section photomicrograph of secondary porosity (P) formed as a result of dissolution of diagenetic chlorite and plagioclase grain (Pl).

C. Thin section photomicrograph showing equal proportion of dissolution of both calcite (Ca) and plagioclase (Pl).

D. A narrow channelized pore (P) developed as a result of dissolution of clays. Rhombs of ankerite (Ak) occur as inclusions within quartz overgrowths (Qo).

PLATE 14

A, B. SEM photomicrograph of partly dissolved diagenetic albite (Ab) showing smooth parallel and corrugated irregular solution texture. Diagenetic albite (Ab) rests on a partly stripped quartz overgrowth (Qo). Phase (1) solution dissolved quartz overgrowths, Phase 2 solution event is recorded by smooth parallel dissolution of albite followed by the last phase of dissolution event which is irregularly corroded to the earlier formed texture.

C, D. SEM photomicrograph of partial dissolution of quartz overgrowth (Qo) which is later infilled by diagenetic chlorite.

E. SEM photomicrograph of partial dissolution of quartz overgrowths (Qo) which is later cemented by chlorite (chl).

F. SEM photomicrograph of dissolution of detrital quartz (Q) and diagenetic chlorite (chl) which indicates two phases of dissolution.

PLATE 15

A, B, C. SEM photomicrograph of K-feldspar solution texture showing parallel shallow to deep etch pits.

D, E. Patchy skeletal sheet removal texture of K-feldspars.

F. SEM photomicrograph of oligoclase dissolution texture marked by two dissolution events - chatter marks (1) and deep etch pits (2).

PLATE 16

A, B. SEM photomicrograph of incomplete curved dissolution texture of oligoclase.

C, D. Oligoclase dissolution texture as sheet removal resulting in parallel rod to flaky minerals.

PLATE 17

A, B, C. SEM photomicrograph of honeycomb K-feldspar dissolution texture. K-feldspar overgrowth (Ko) growing into porespace show no dissolution traces indicating that overgrowths postdate solution event.

D, E. Incomplete solution of a K-feldspar along parallel cleavage planes. Two phases of solution are recorded in the textures: Phase 1 is characterized by chatter marks followed by Phase 2 which show predominant deep etch pits. Rim overgrowth (Ro) is slightly dissolved.

F. Albite dissolution texture showing incomplete to complete dissolved rectangular etch pits stripped by stepwise sheet removals.

PLATE 18

A, B. Solution textures of oligoclase showing removal in sheets resulting in a stepwise patchy pore pattern. Deep etch pit is infilled by diagenetic chlorite (chl). Absence of diagenetic chlorite in the patchy pore pattern suggest solution postdating "deep etch pit". Chatter marks (chm) are also present on individual dissolved blocks which possibly are relicts of a third dissolution event.

C, D. Shallow parallel solution textures of K-feldspars occurring in stacks. Diagenetic chlorite (chl) partly infilling secondary pores. Quartz overgrowth (Qo) occluding available porespace (P).

E, F. SEM photomicrograph of dissolution of microcline resulting in floating irregular thin skins on the surfaces of the grain.

PLATE 19

A. Thin section photomicrograph of terrestrial organic matter (Type III), Hillsborough-1.

B. Thin section photomicrograph of predominantly amorphous organic matter, Albert Mines-1.

C. Magnification of one algal ball.

D. Thin section photomicrograph of predominantly amorphous with a few terrestrial organic matter. ARCO Dover-1A.

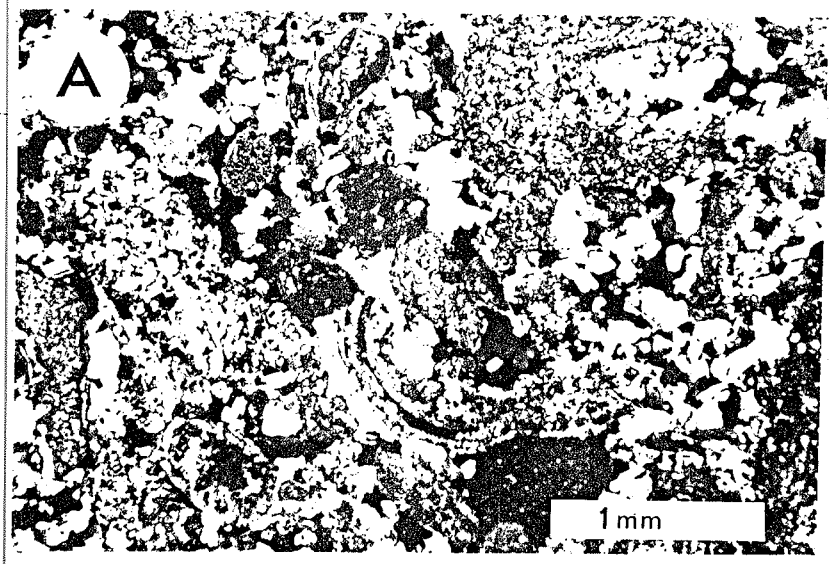
A
1 mm

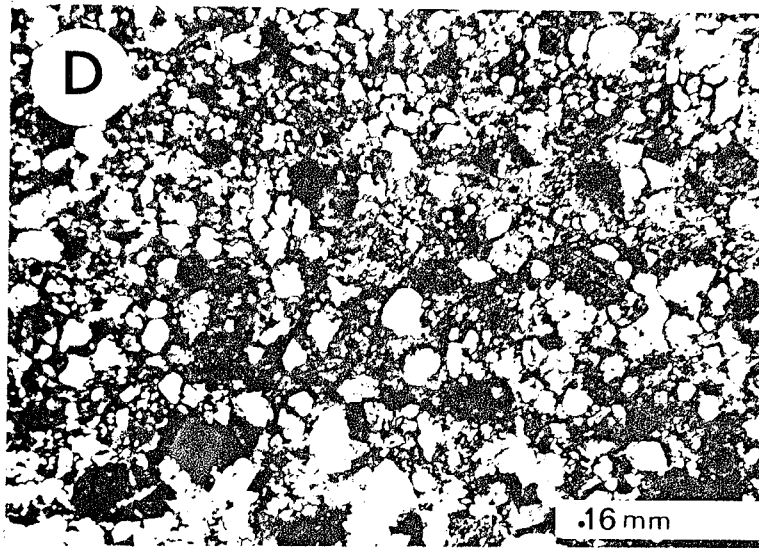
D
.16 mm

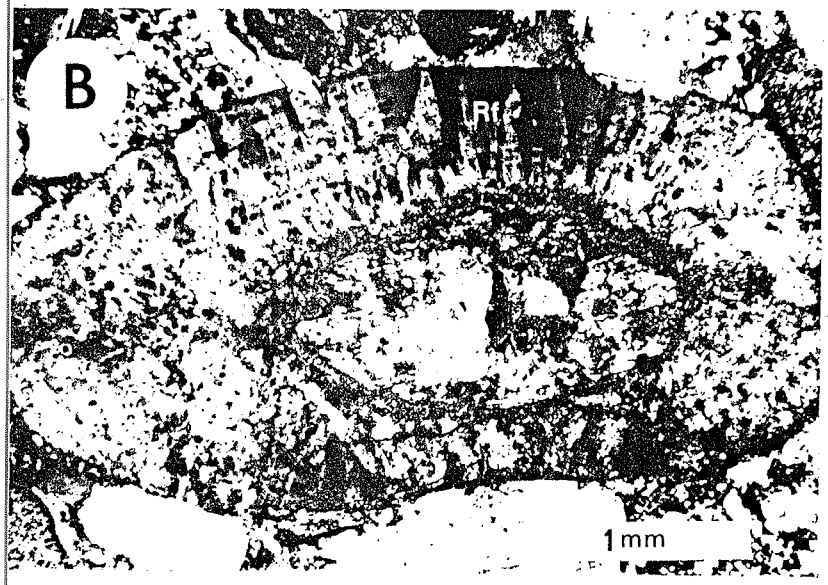
B
1 mm

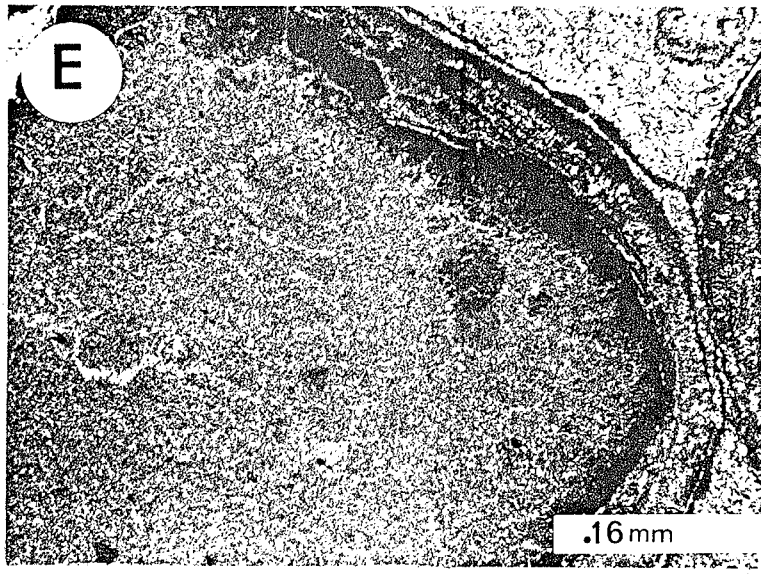
E
.16 mm

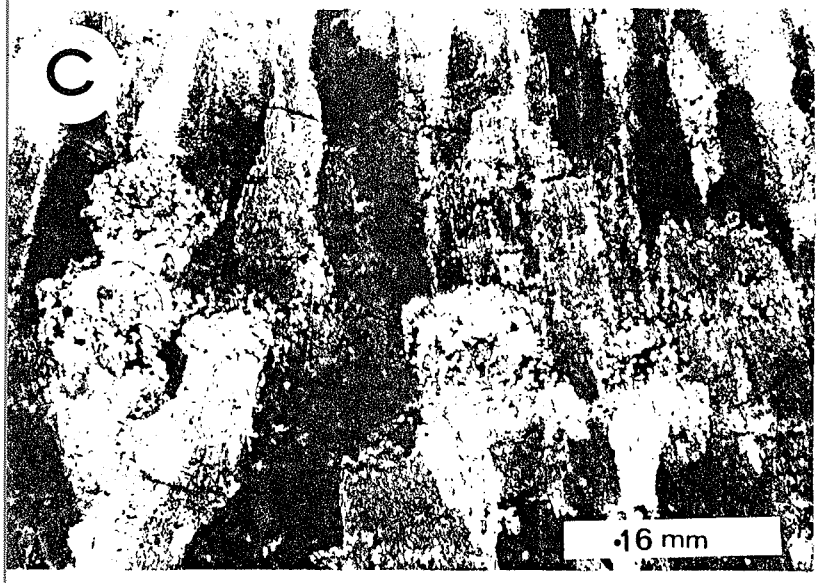
C
.16 mm

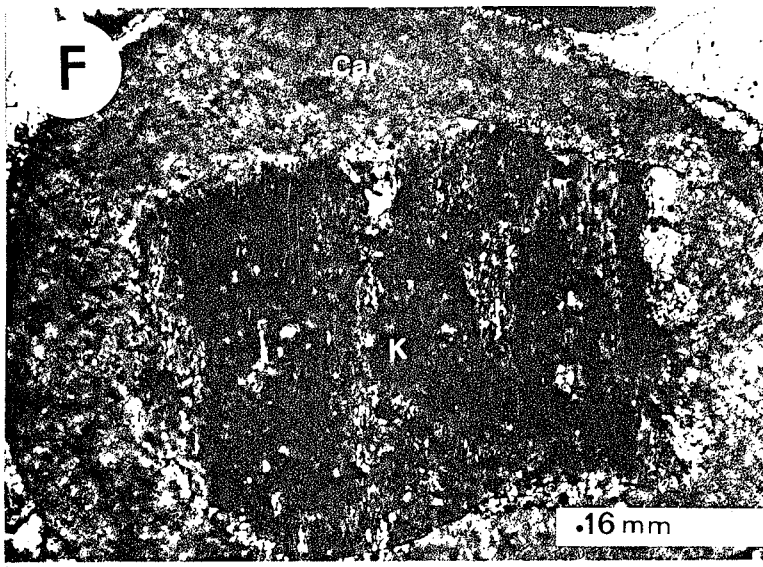
F
ca
K
.16 mm

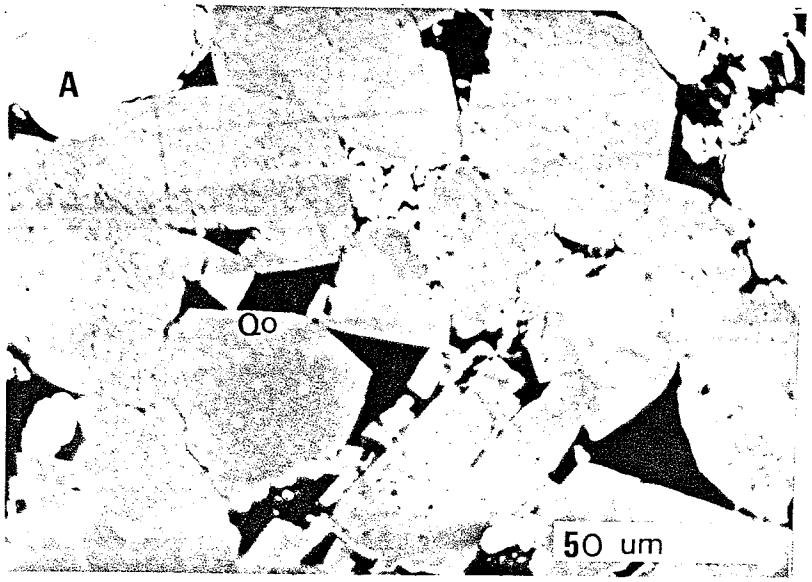
A
Qo
50 um

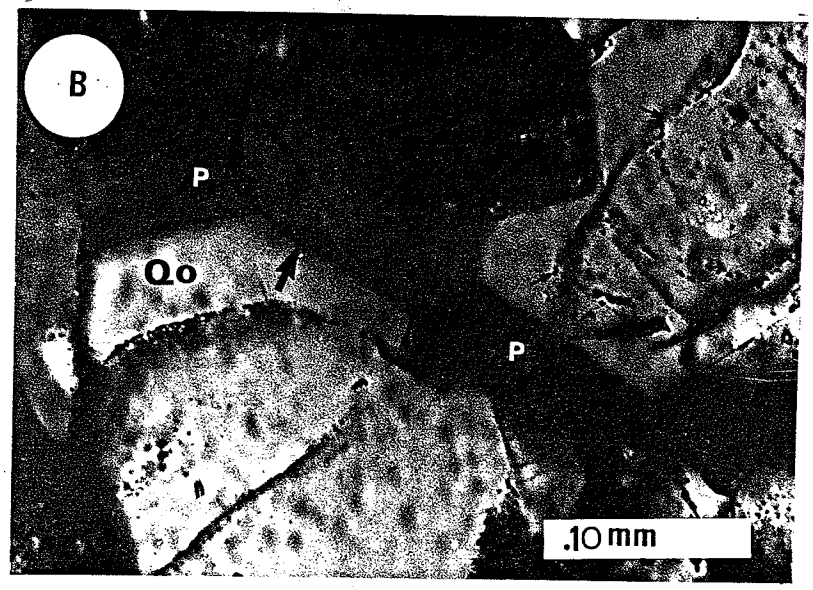
B
P
Qo
P
.10 mm

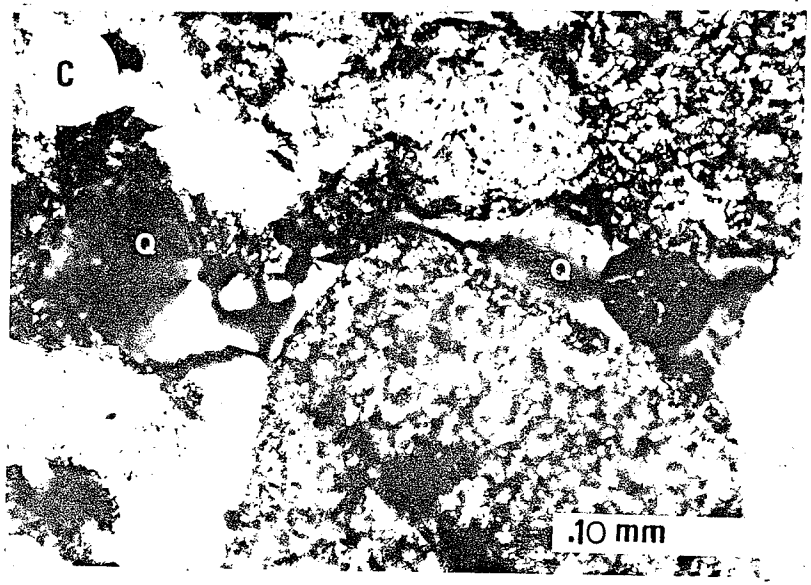
C
Q
Q
.10 mm

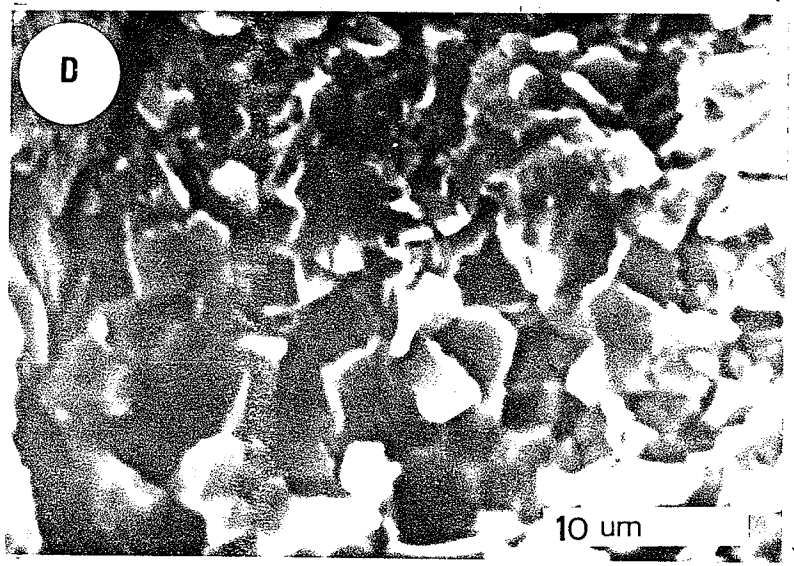
D
10 um

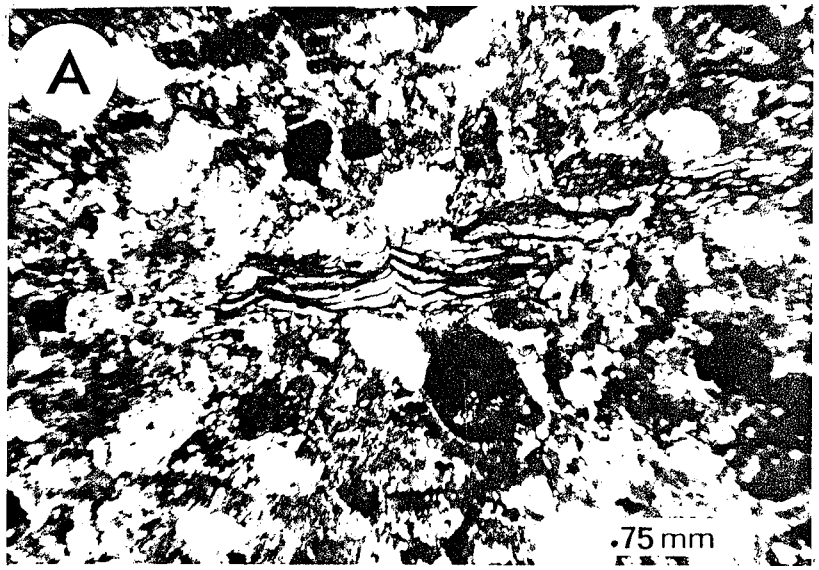
A
.75 mm

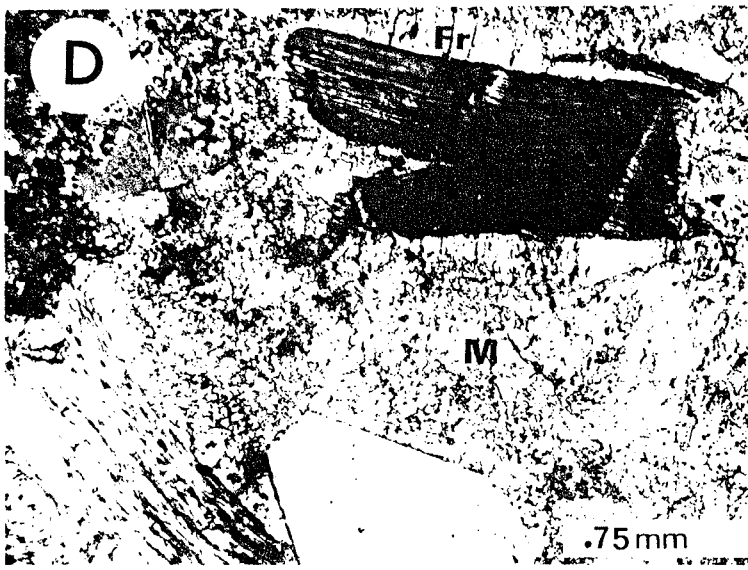
D
Fr
M
.75 mm

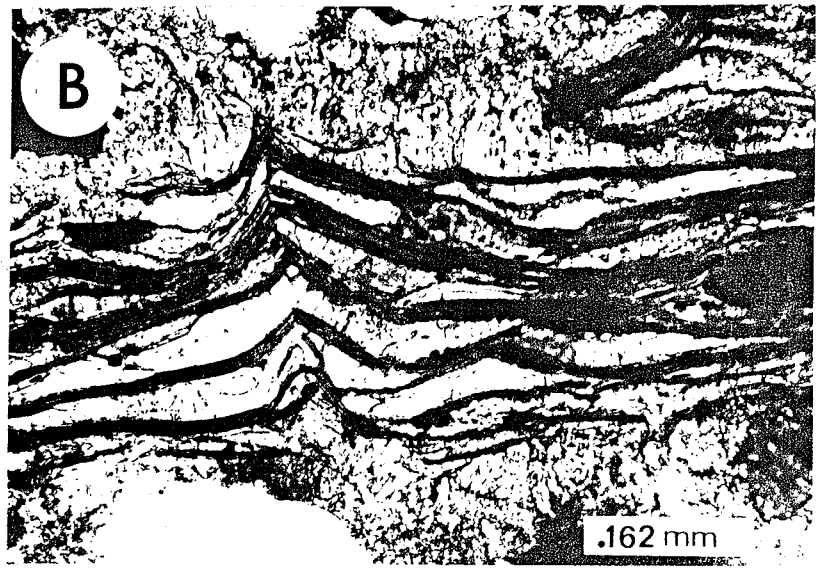
B
.162 mm

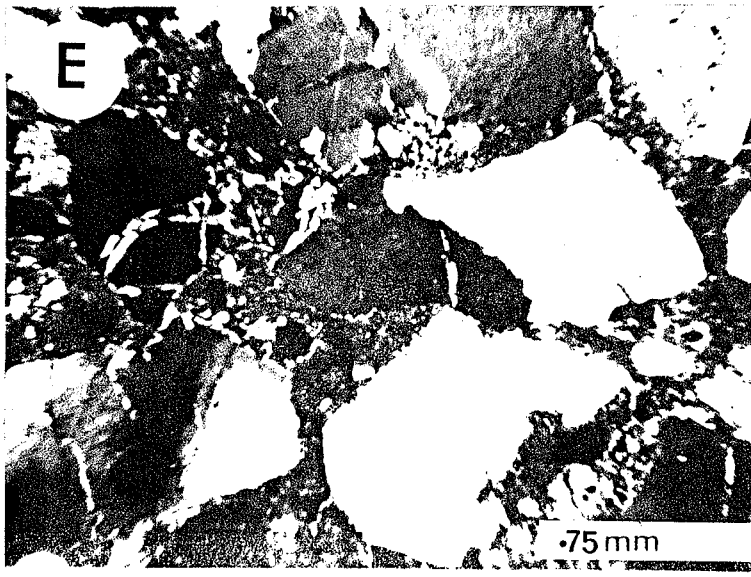
E
.75 mm

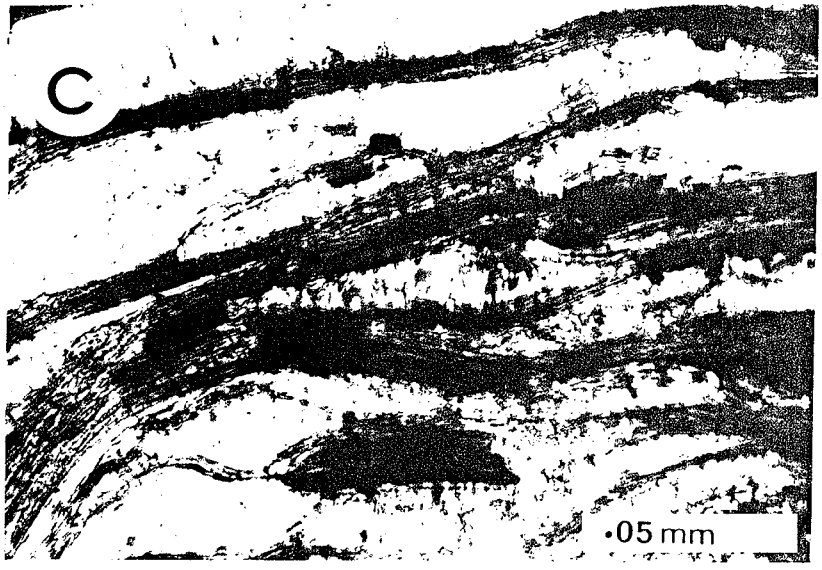
C
.05 mm

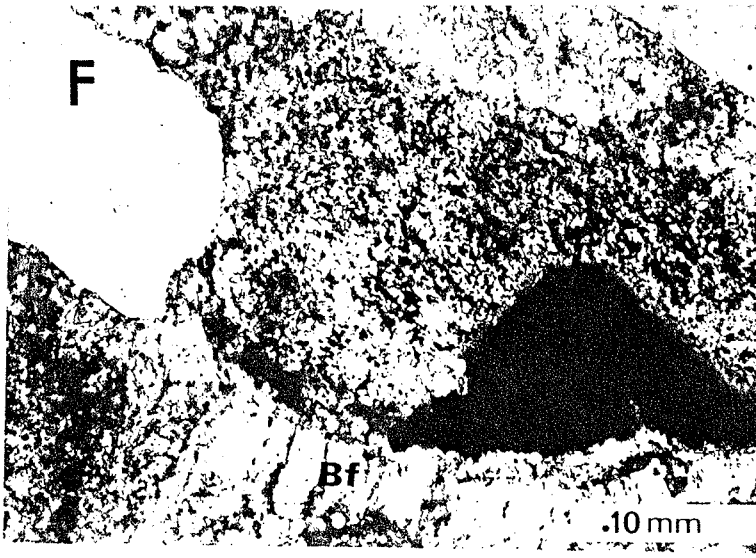
F
Bf
.10 mm

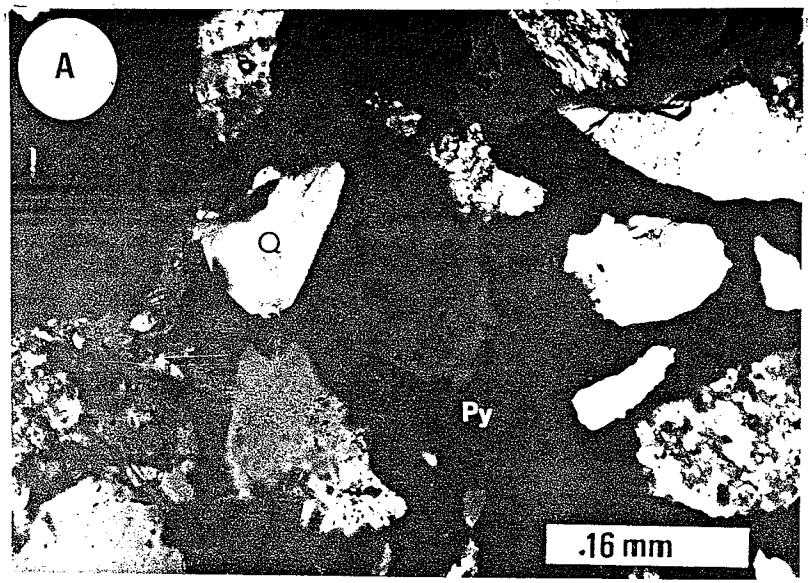
A
Q
Py
.16 mm

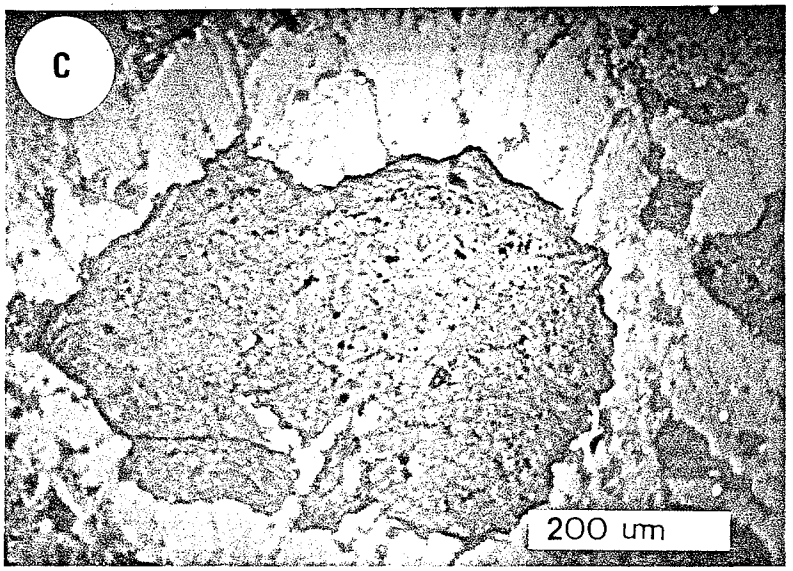
C
200 um

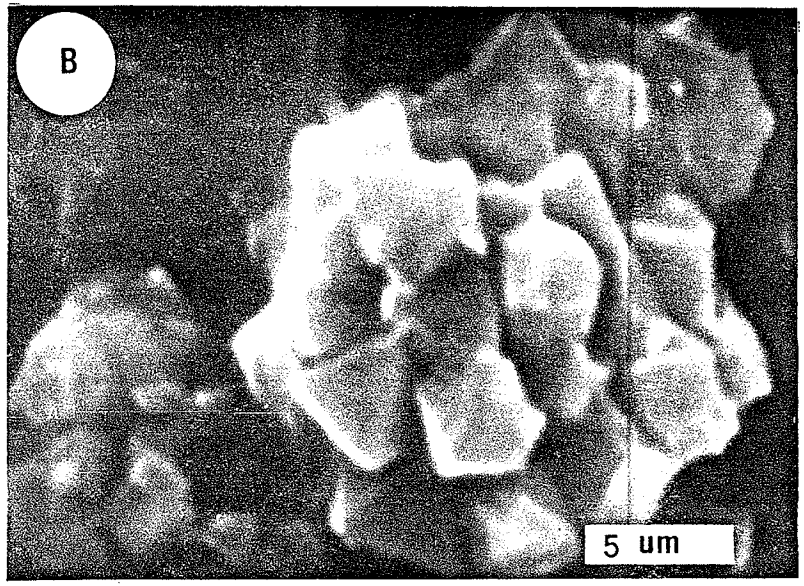
B
5 um

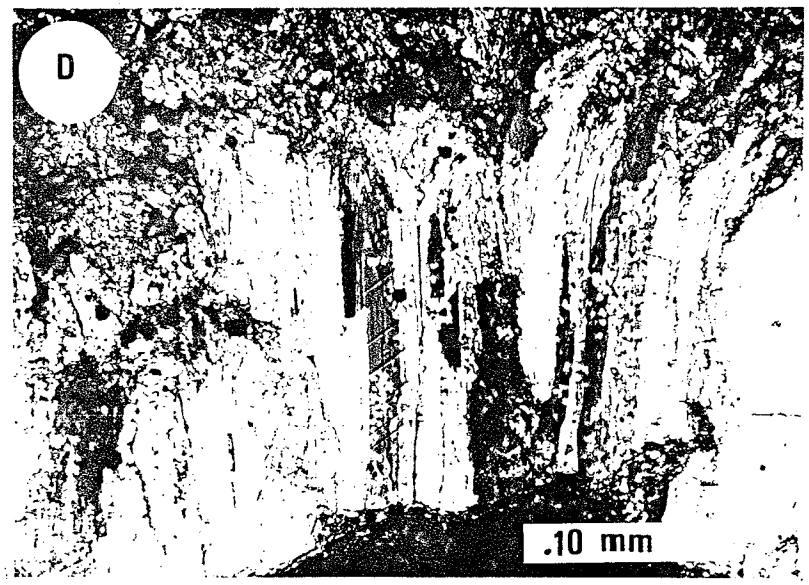
D
.10 mm

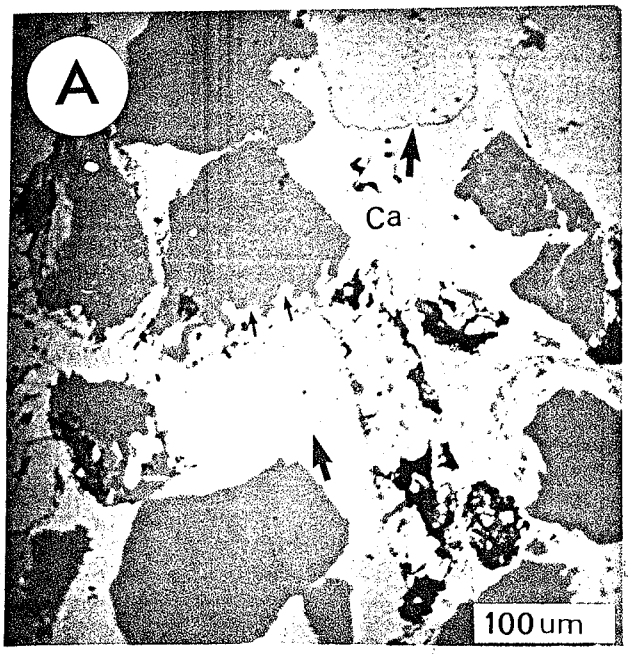
A
Ca
100 um

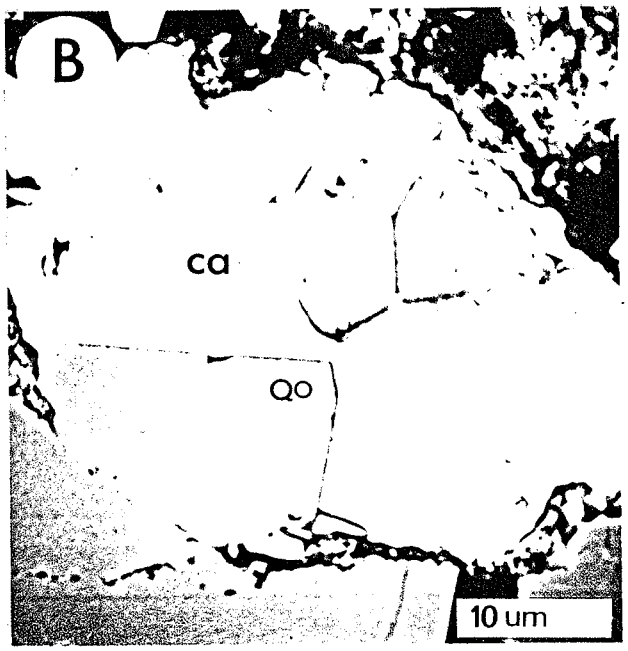
B
ca
Qo
10 um

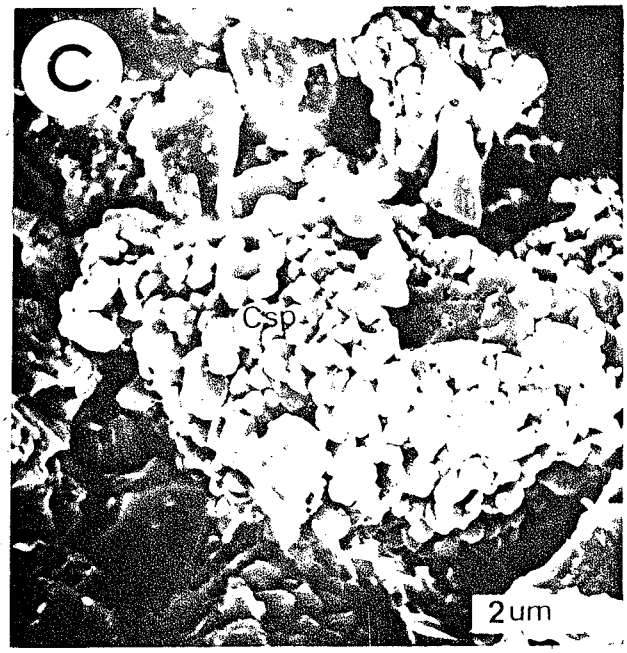
C
Csp
2 um

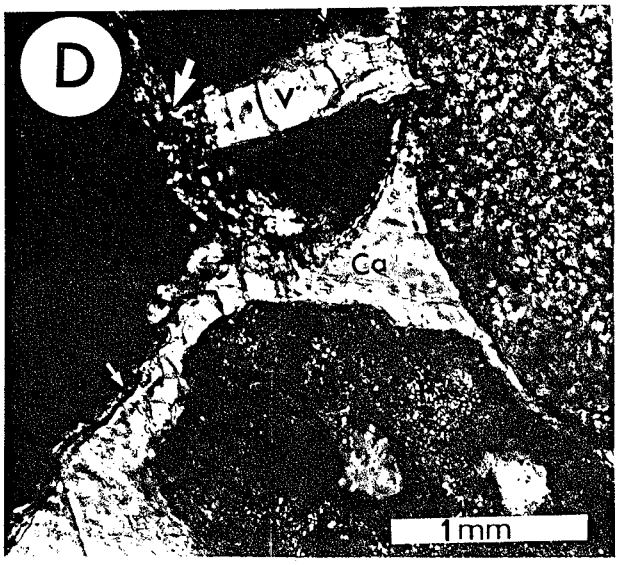
D
V
Ca
1 mm

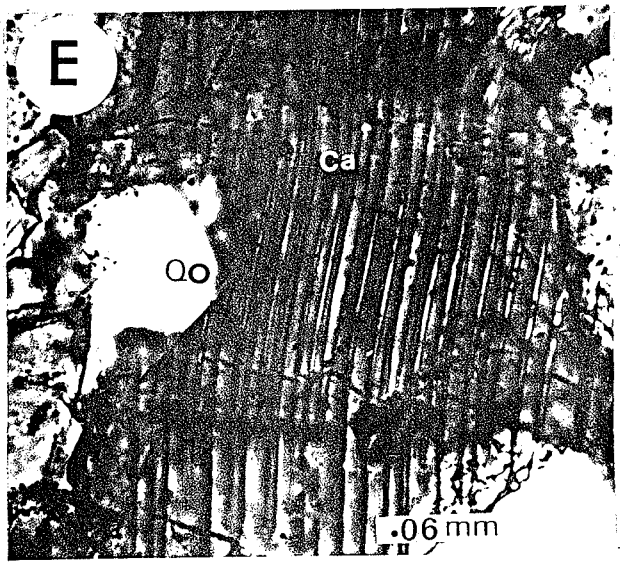
E
Ca
Qo
.06 mm

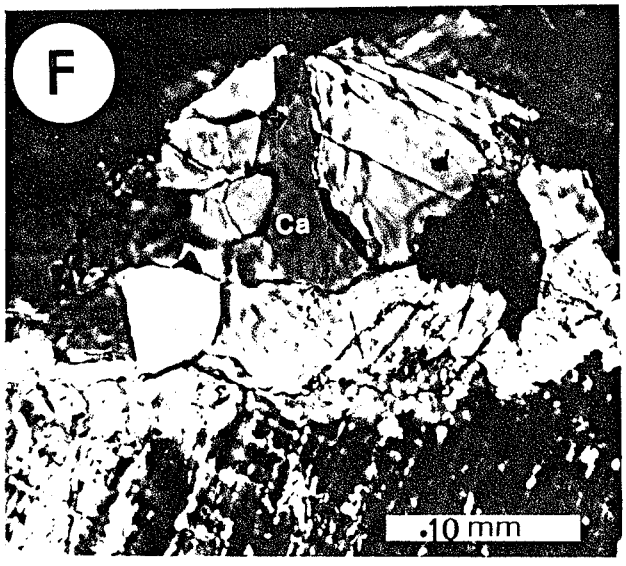
F
Ca
.10 mm

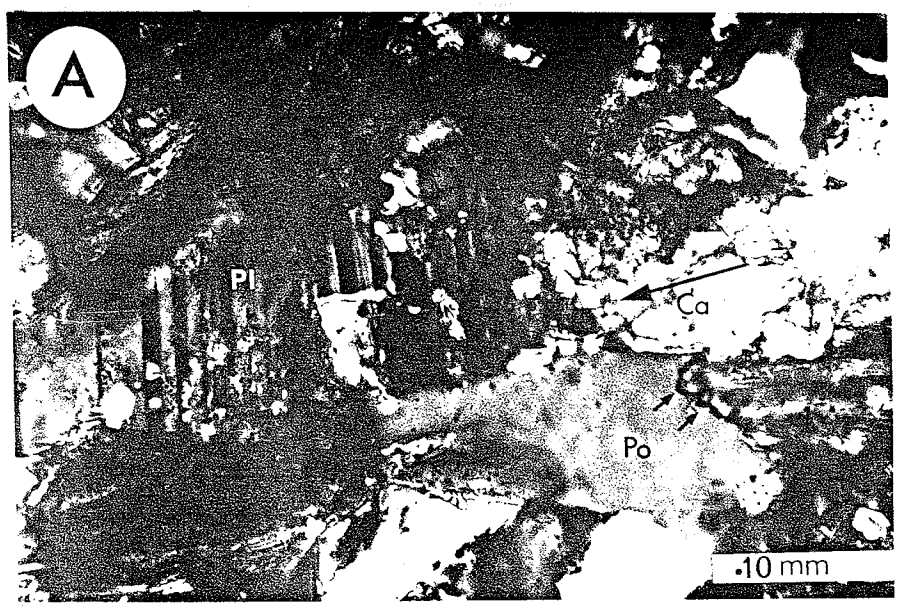
A
Pl
Ca
Po
.10 mm

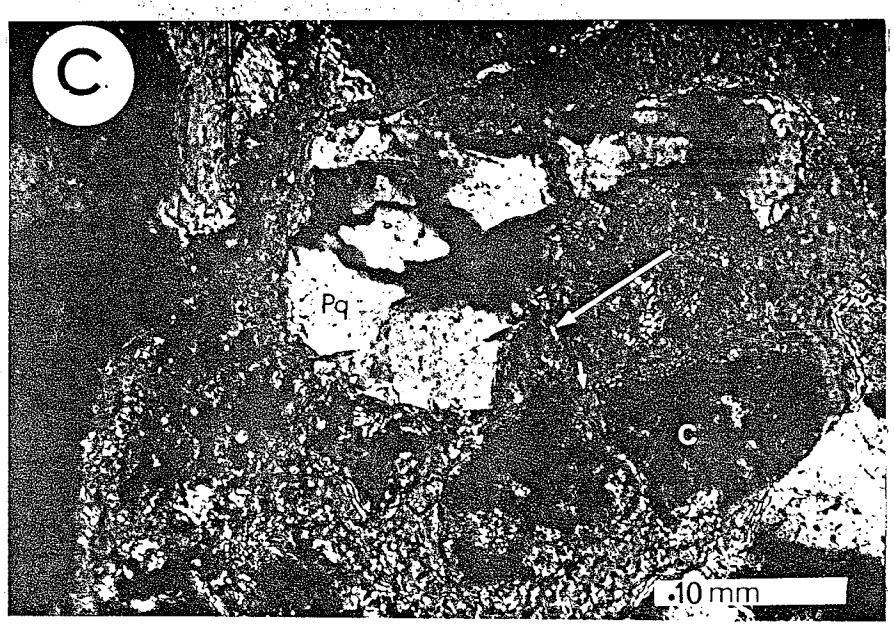
C
Pq
C
.10 mm

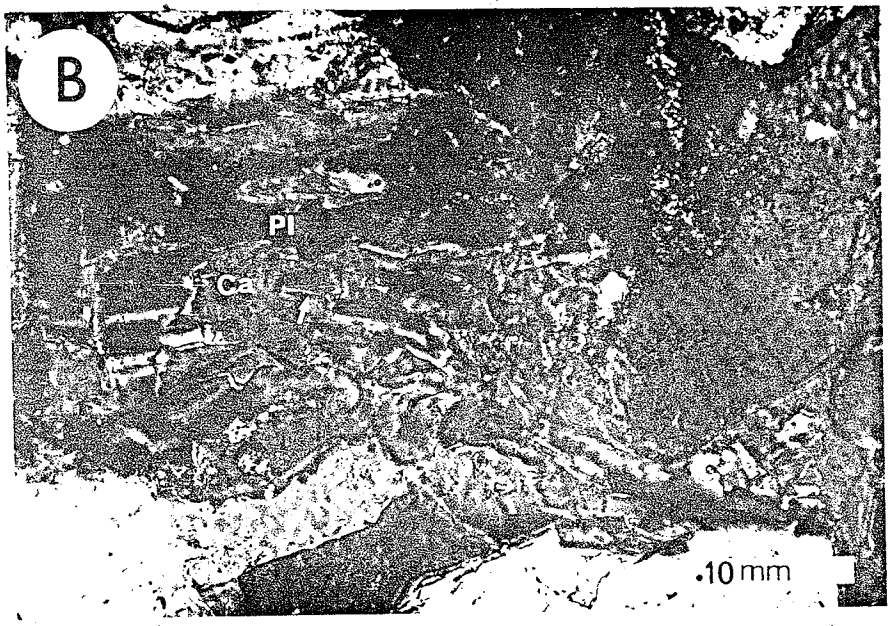
B
Pl
Ca
.10 mm


D
Bi
Pq
.16 mm
Fb

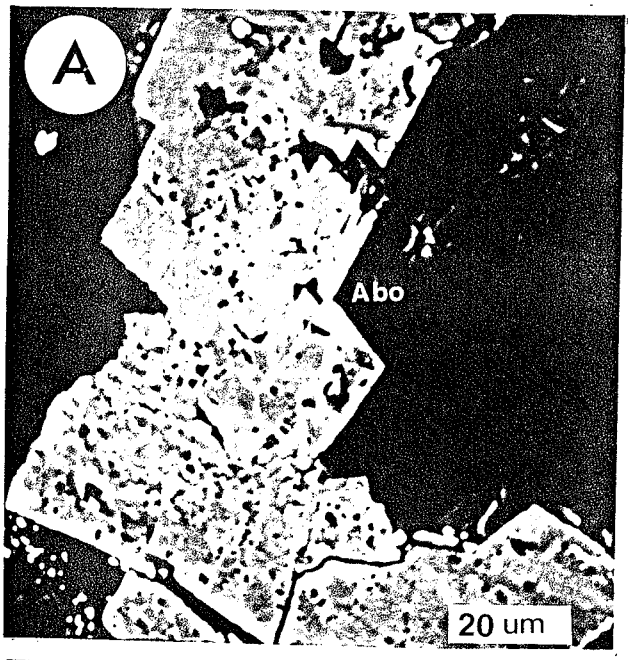
A
Abo
20 um

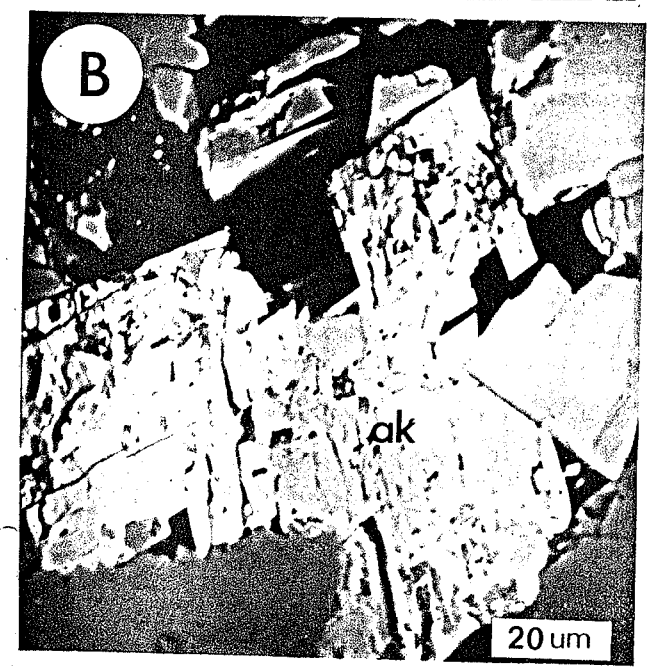
B
ak
20 um

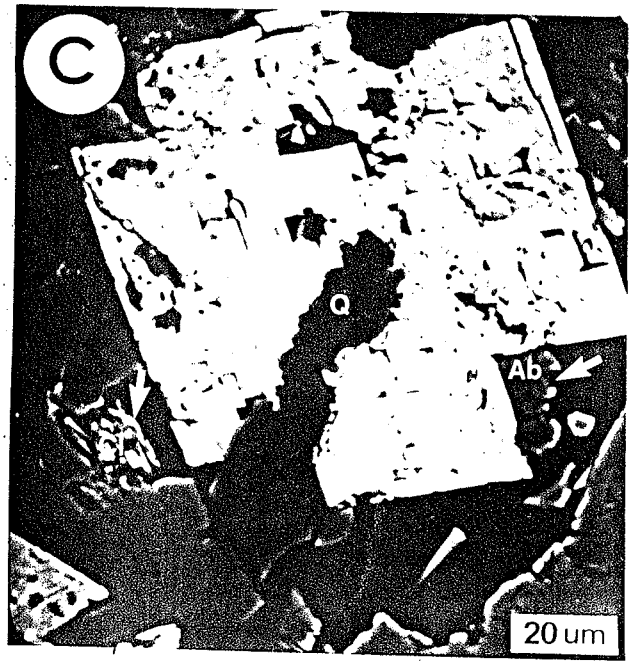
C
Q
Ab
20 um

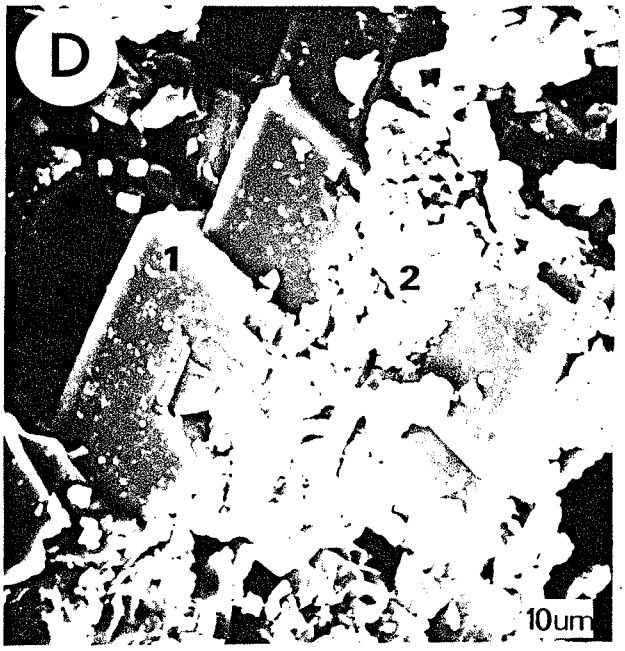
D
1
2
10um

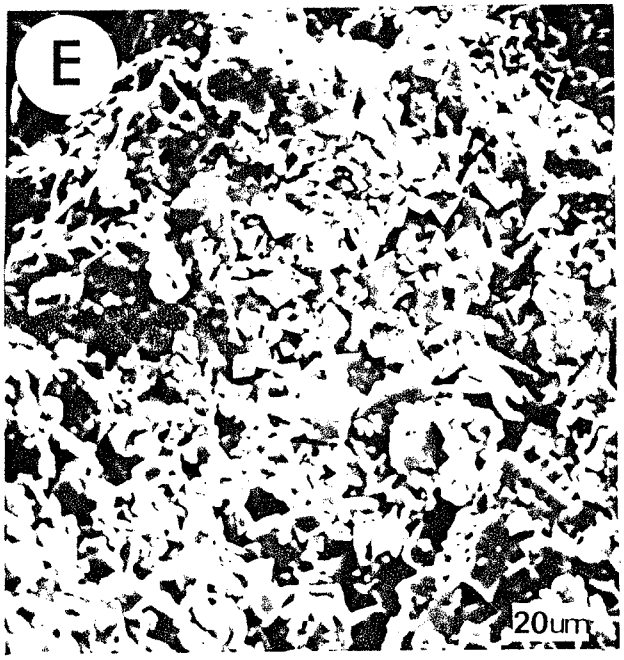
E
20um

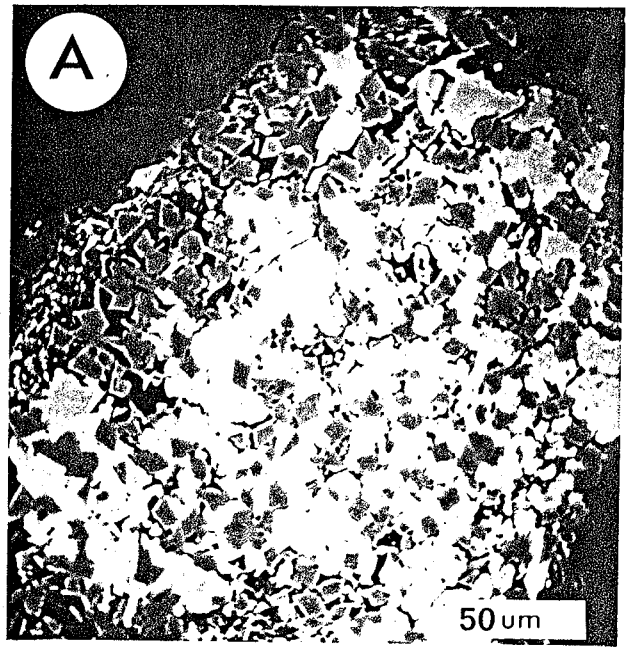
A
50 um

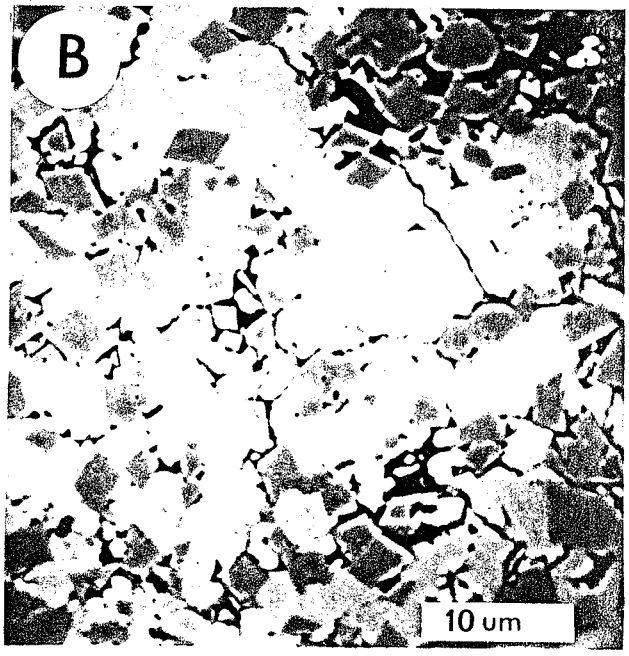
B
10 um

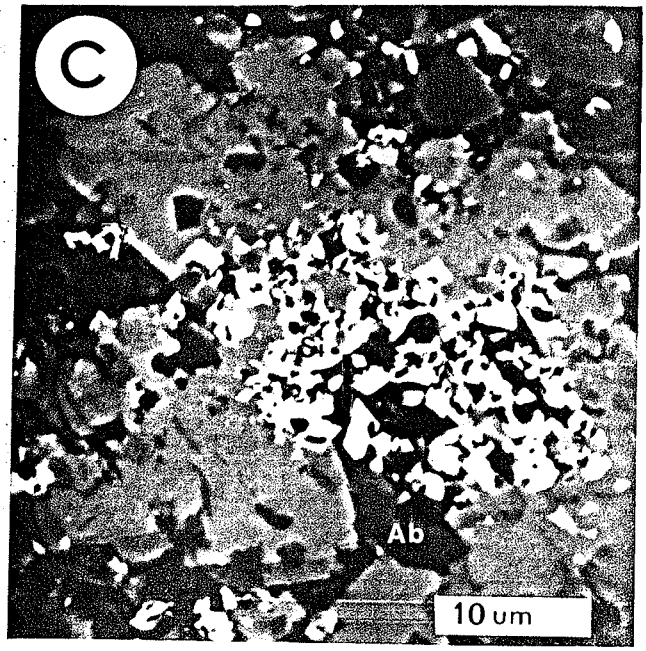
C
Ab
10 um

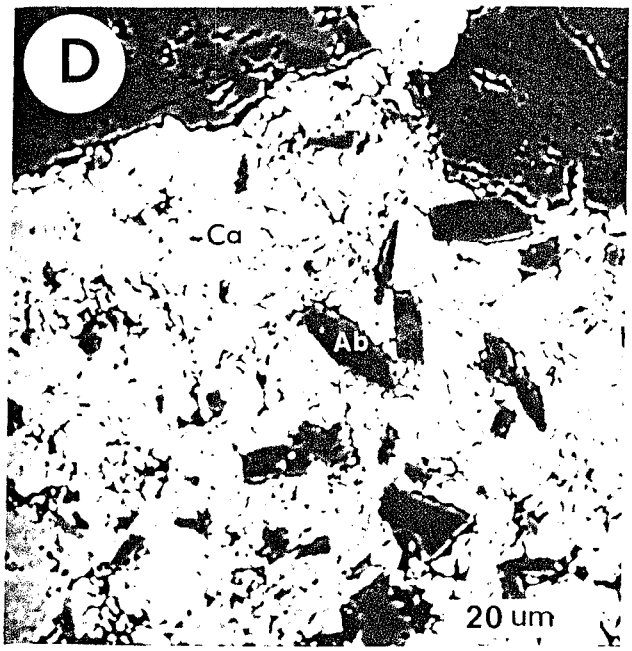
D
Ca
Ab
20 um

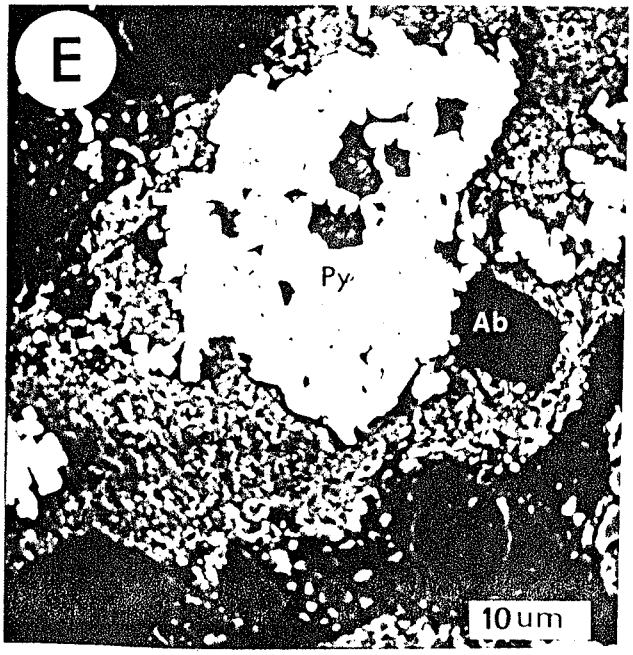
E
Py
Ab
10 um

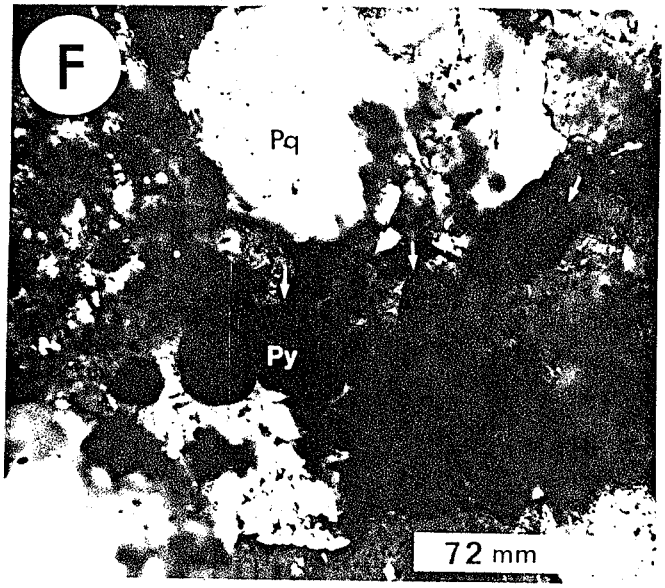
F
Pq
Py
72 mm

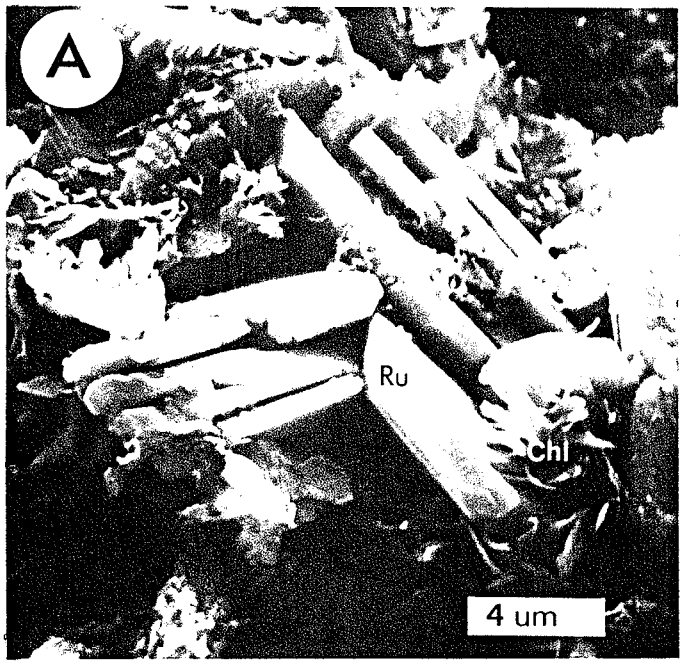
A
Ru
Chl
4 um

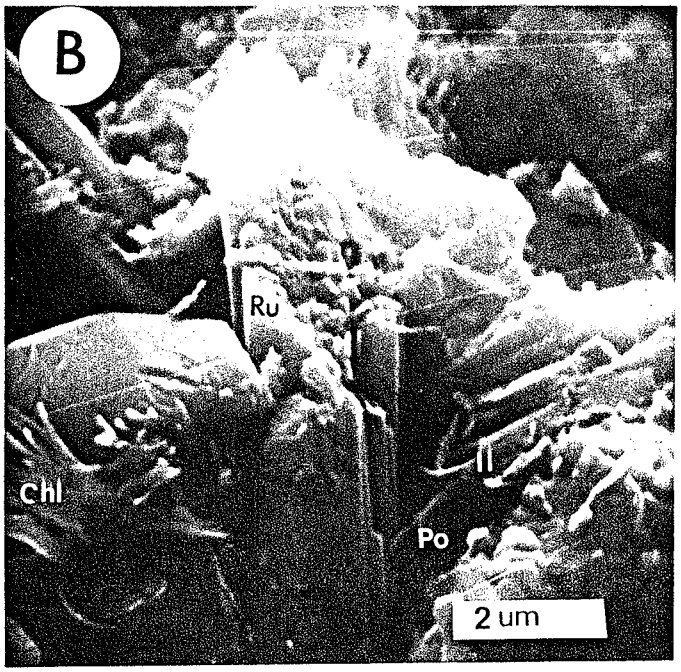
B
Ru
Chl
Il
Po
2 um

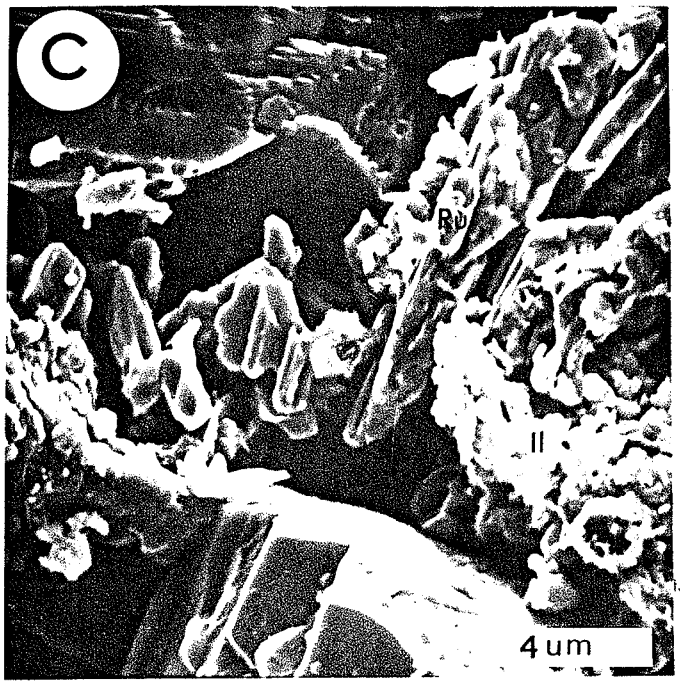
C
Ru
Il
4 um

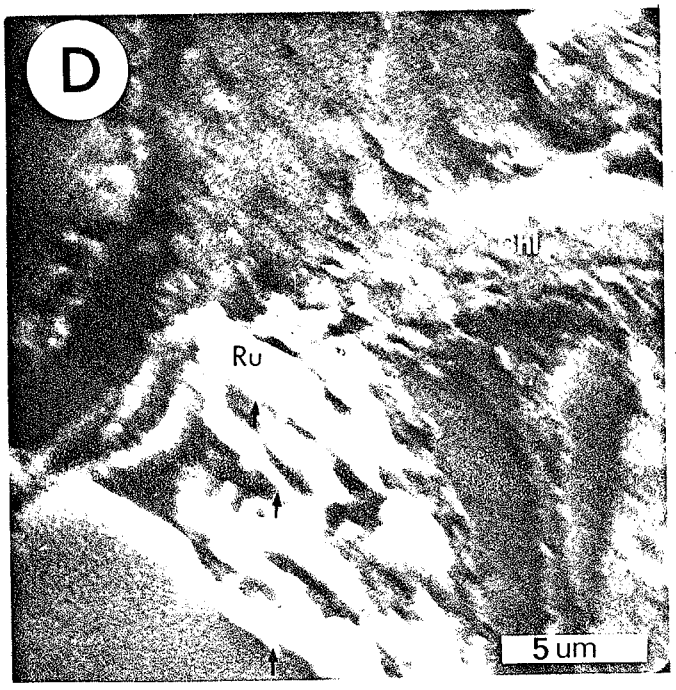
D
Ru
5 um

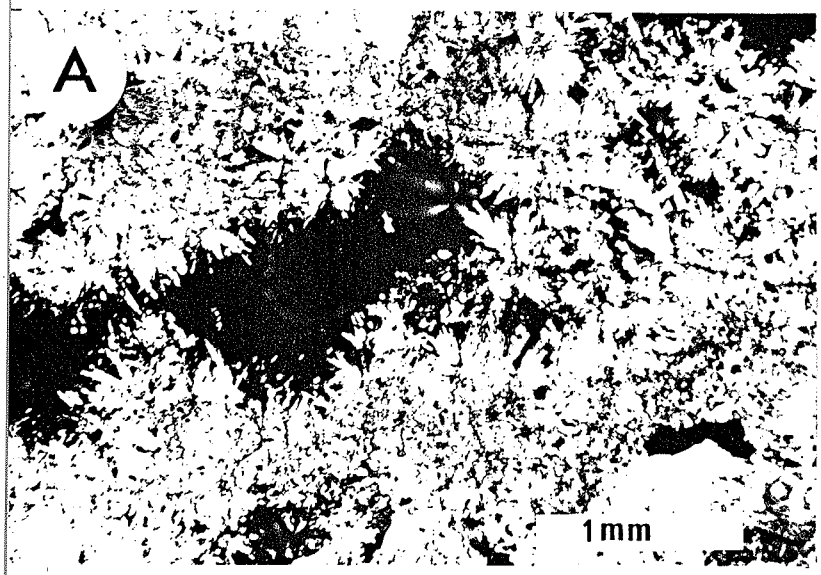
A
1mm

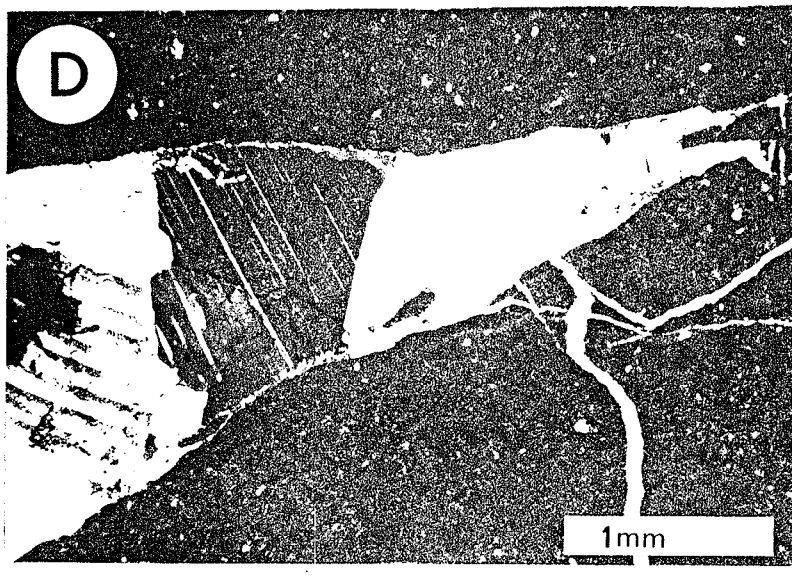
D
1mm

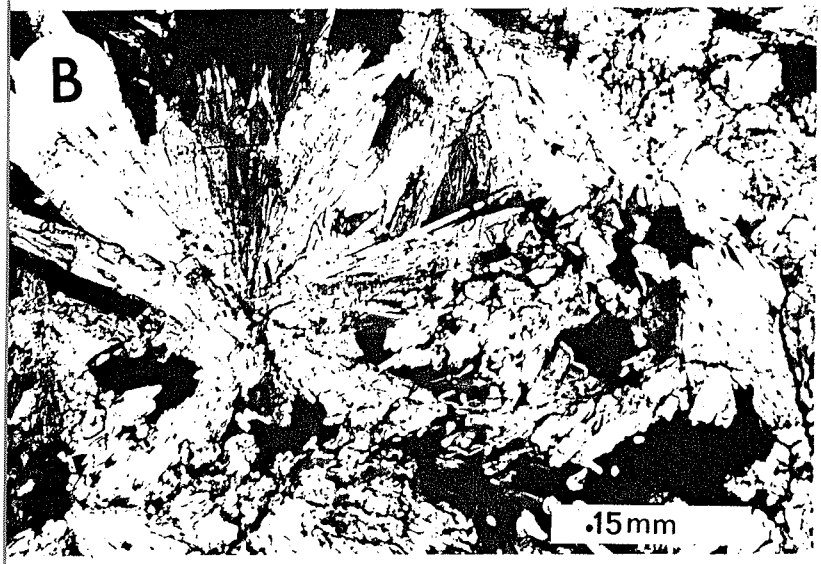
B
.15mm

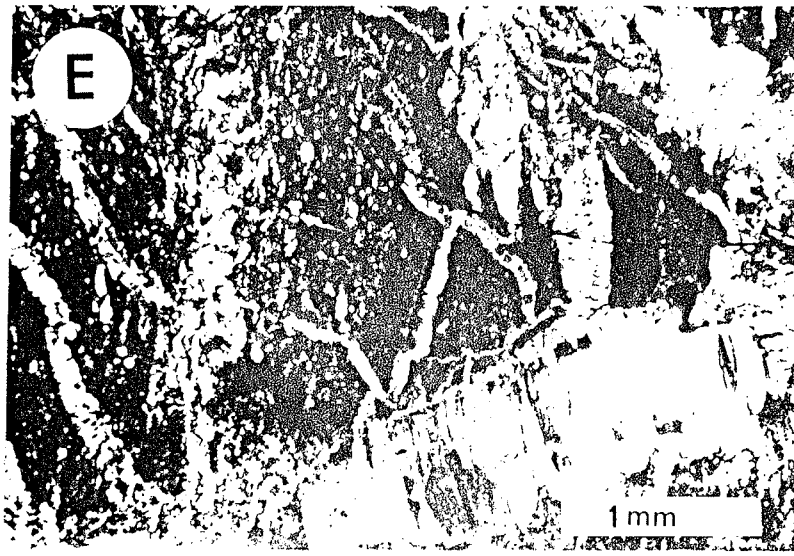
E
1mm

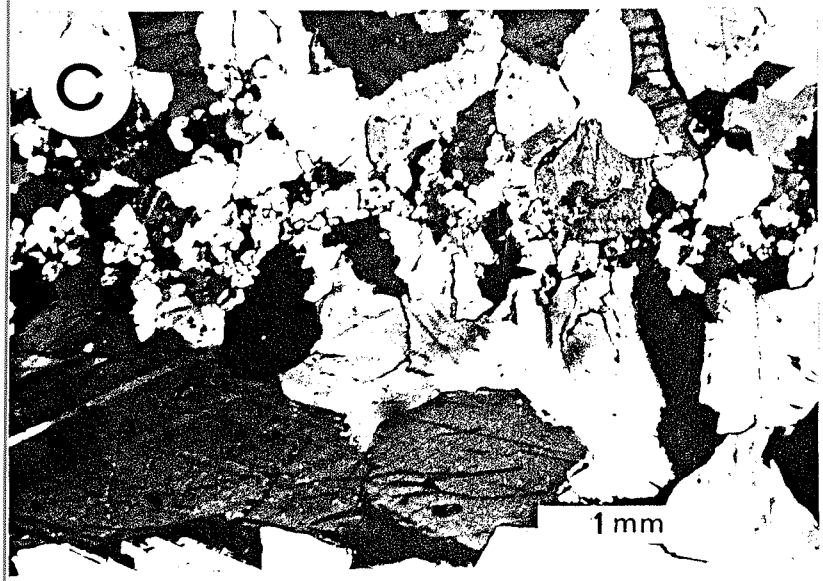
C
1mm

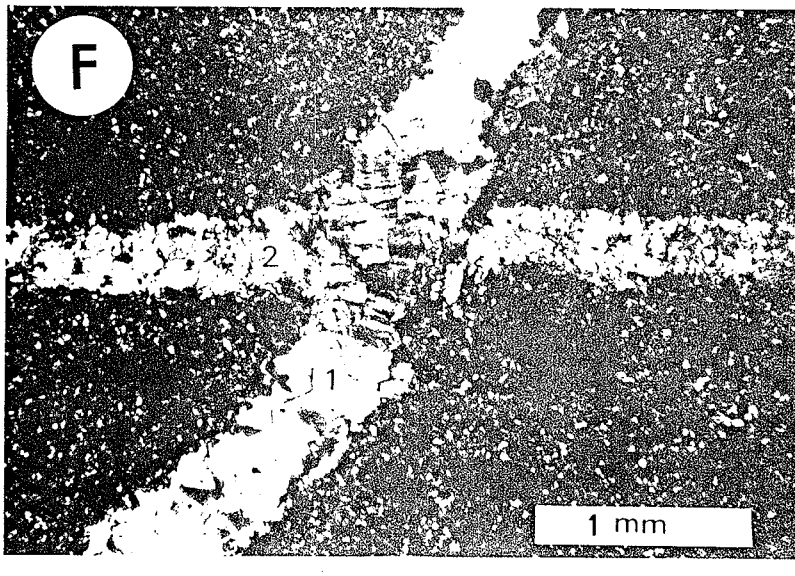
F
2
1
1 mm

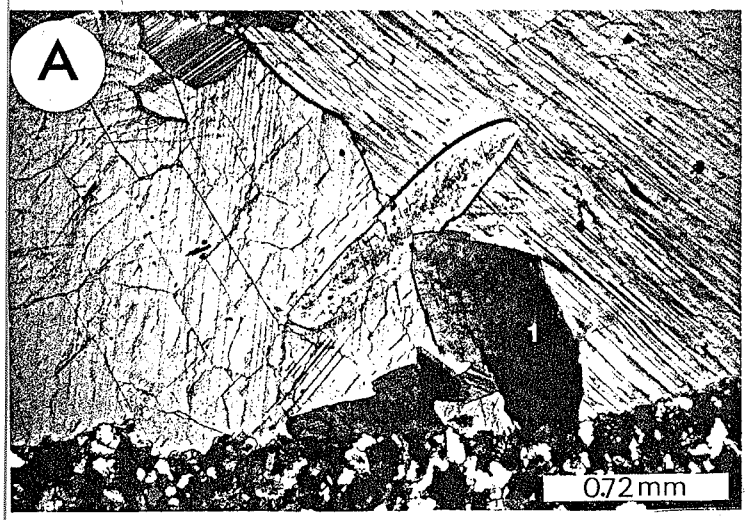
A
1
0.72 mm

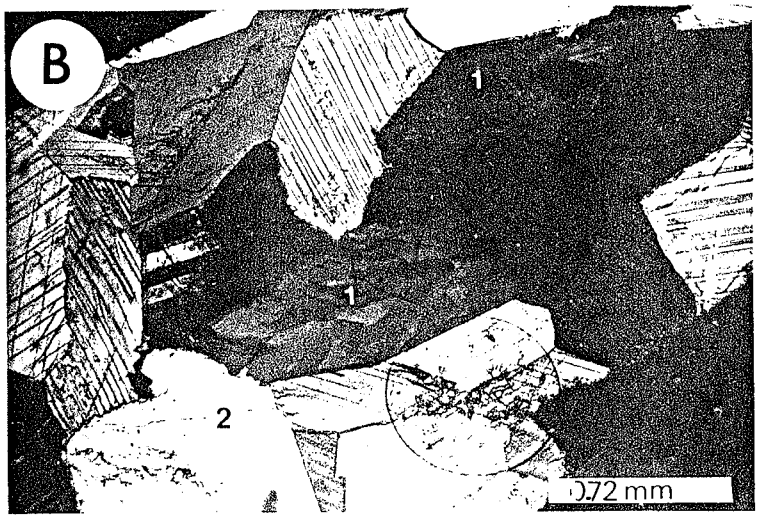
B
1
1
2
0.72 mm

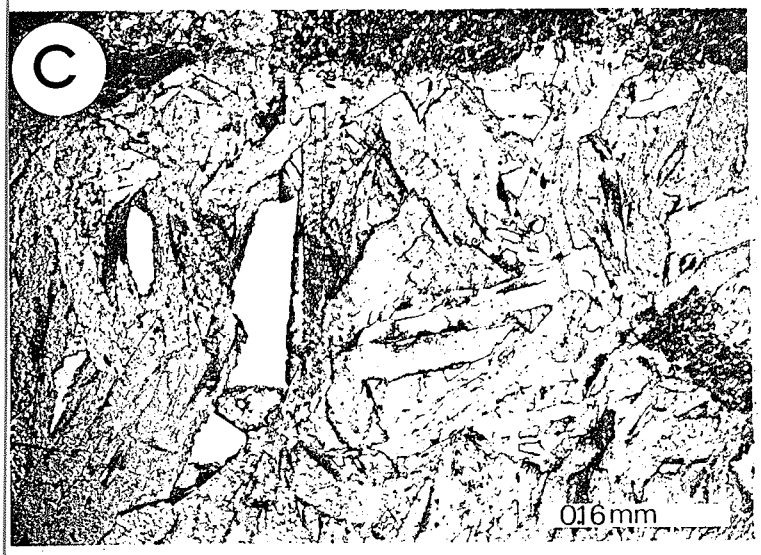
C
016 mm

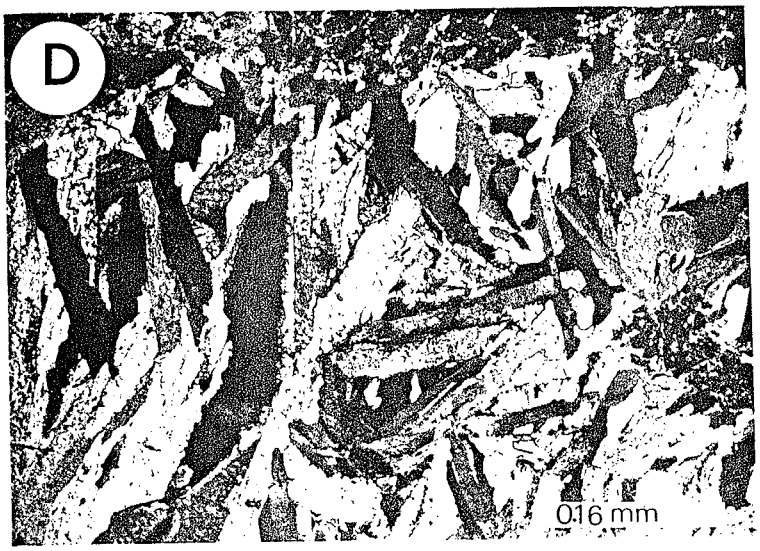
D
0.16 mm

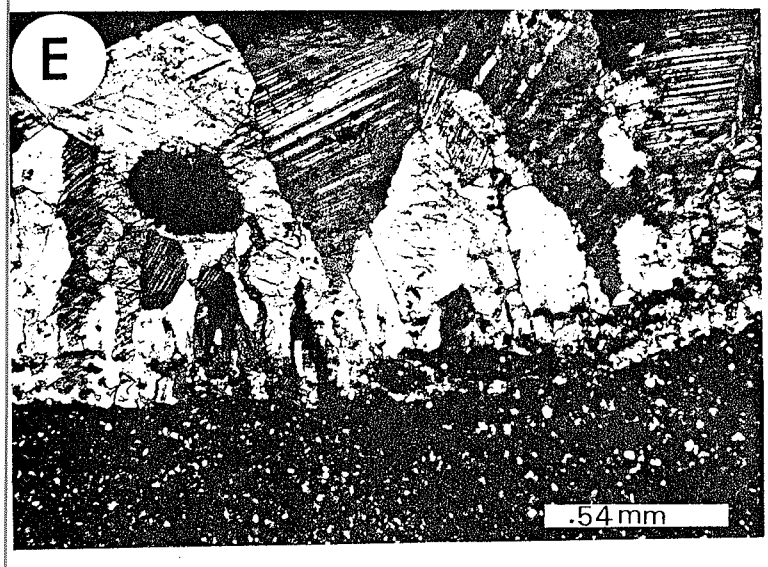
E
.54 mm

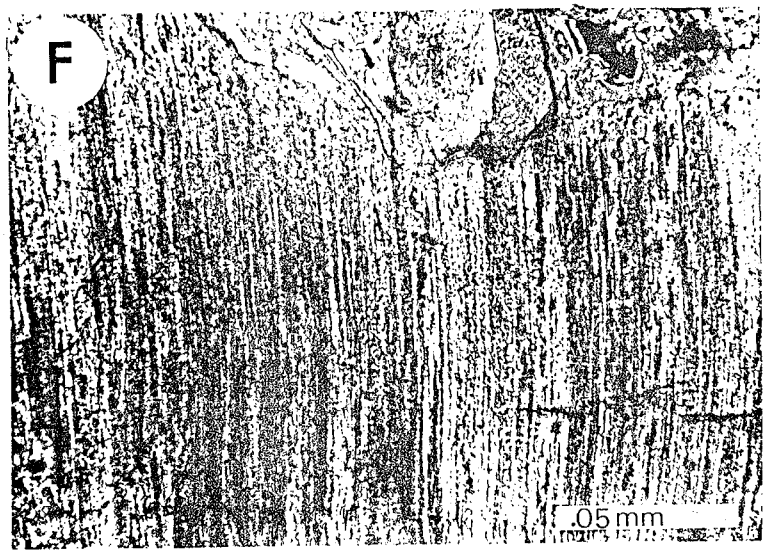
F
.05 mm

XII

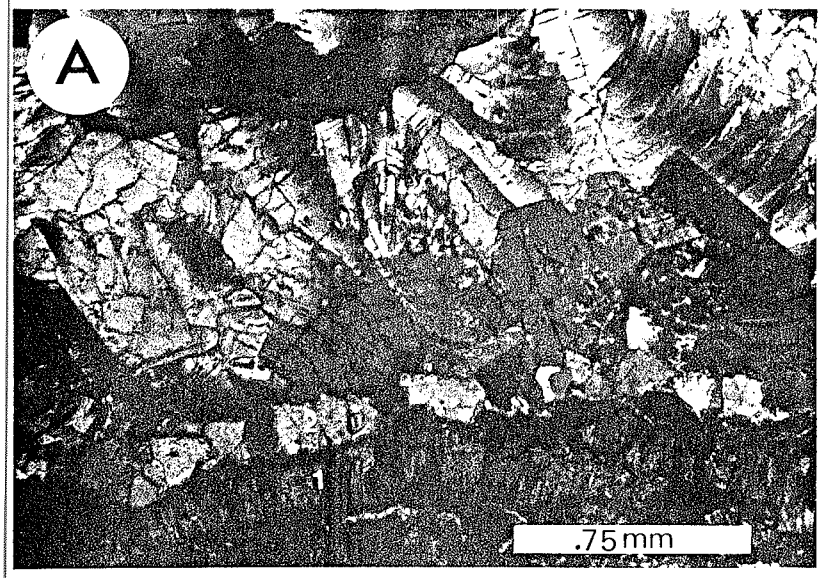

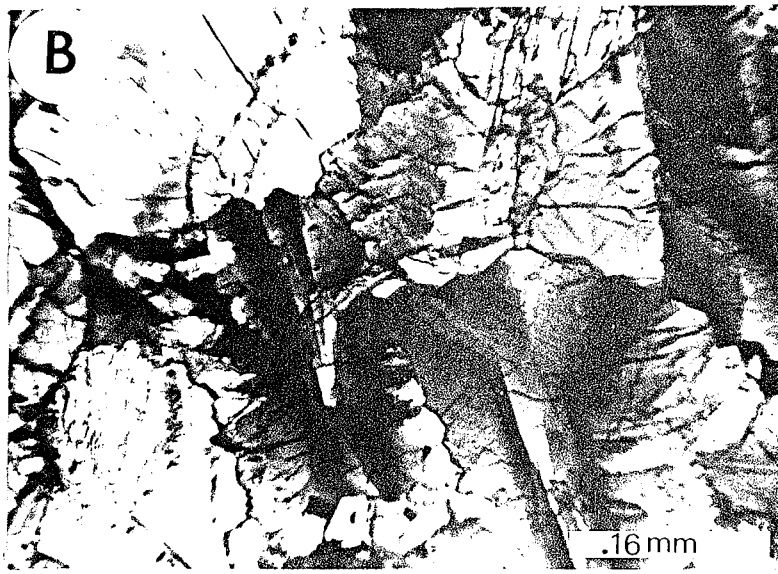

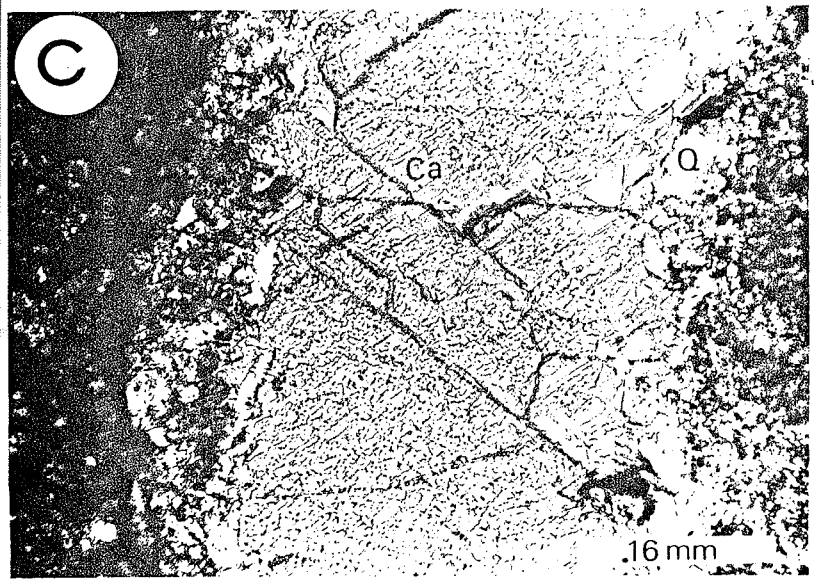

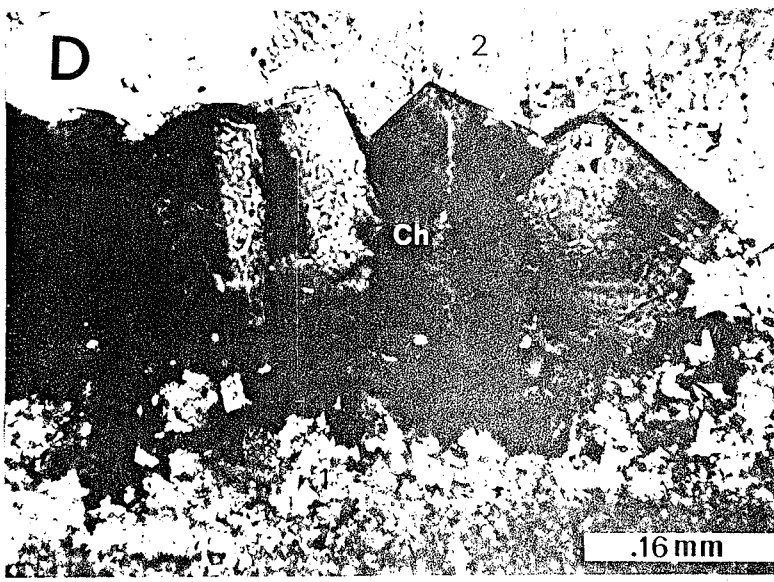

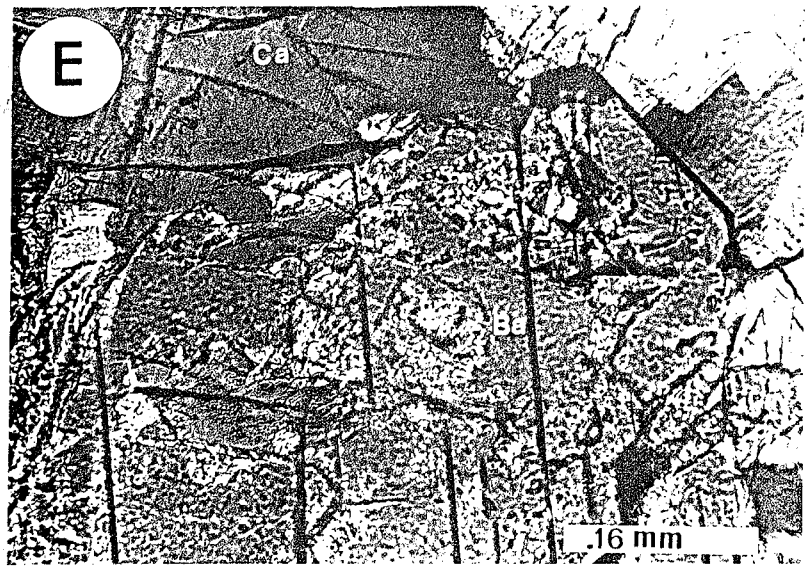

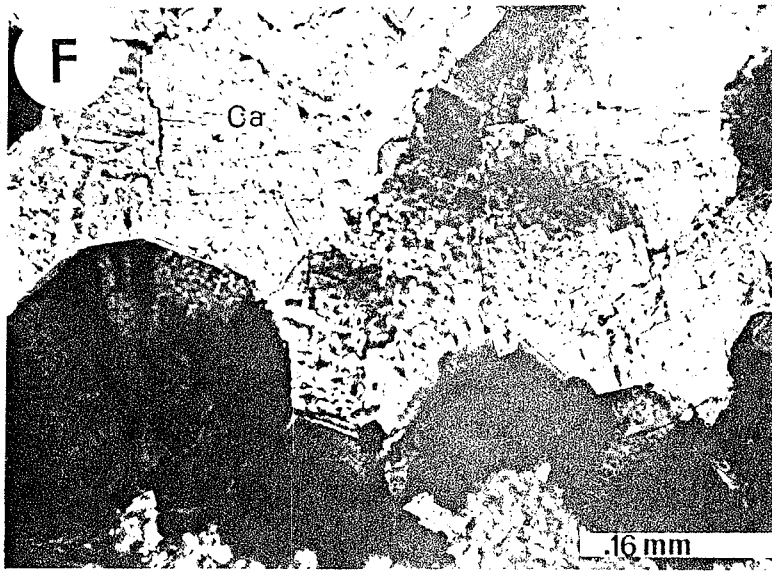

XII

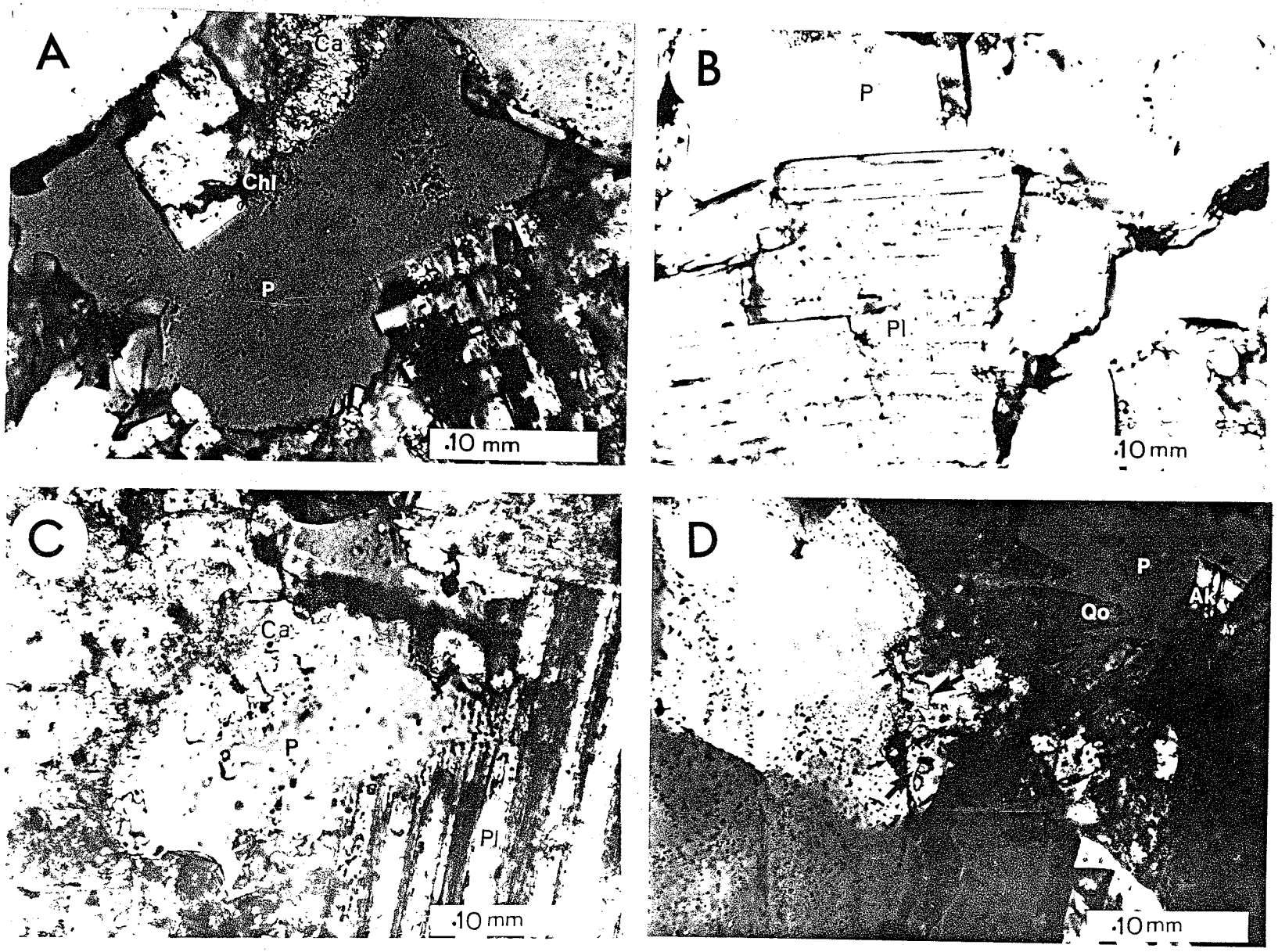

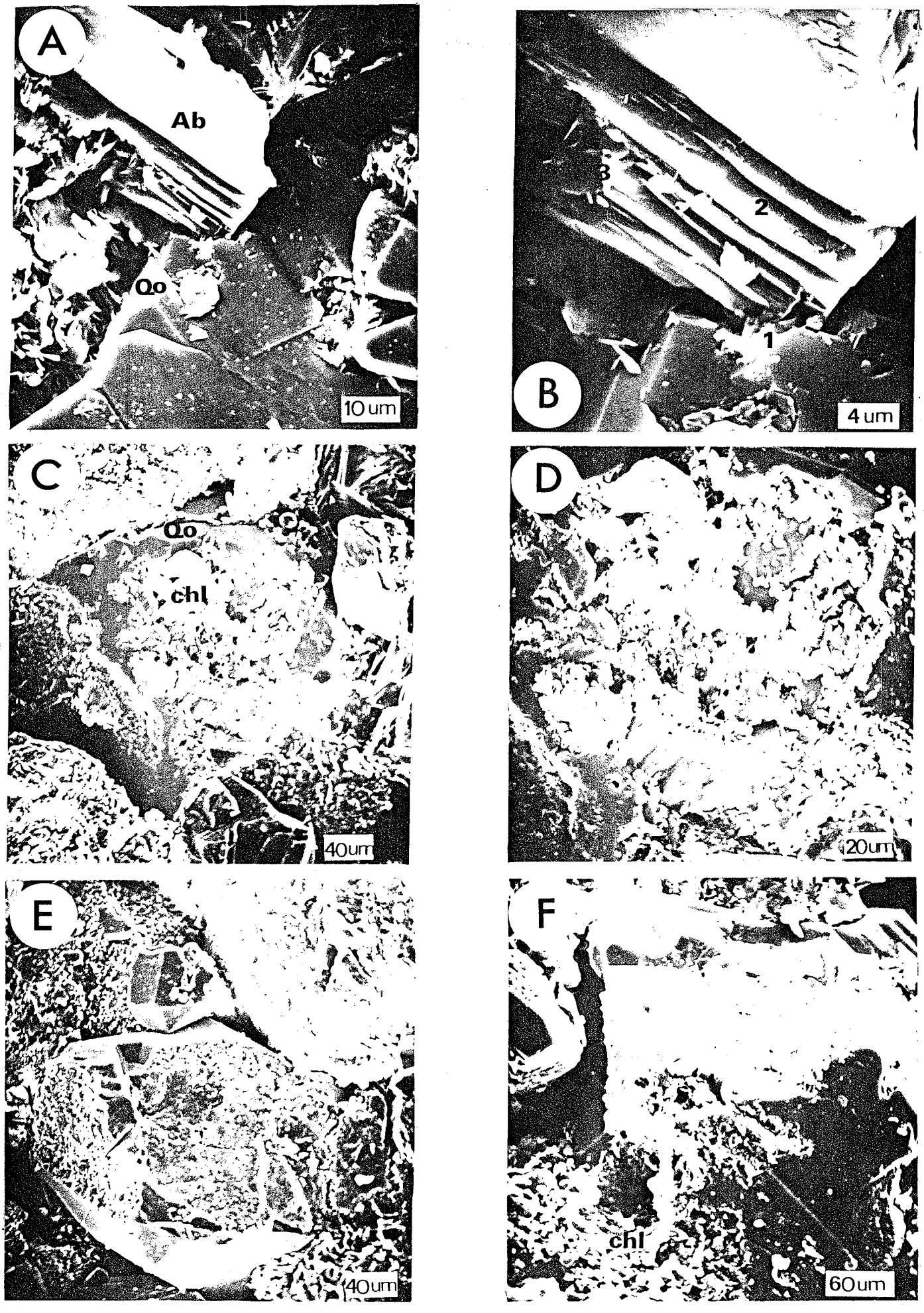
A
Ab
Qo
10 um
B
3
2
1
4 um
C
Qo
chl
40um
D
20um
E
40um
F
chl
60um

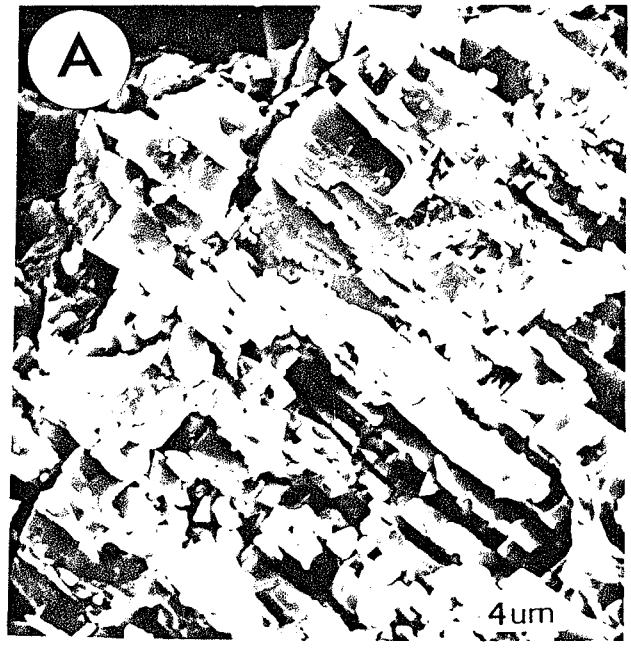
A
4um

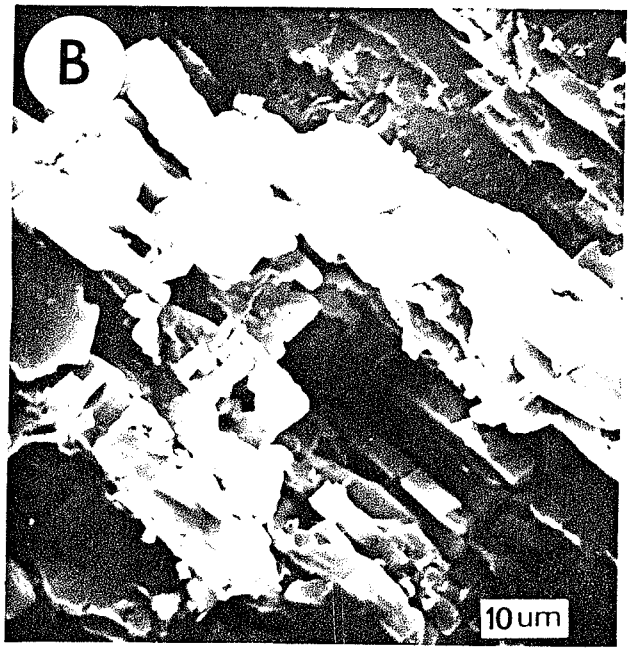
B
10um

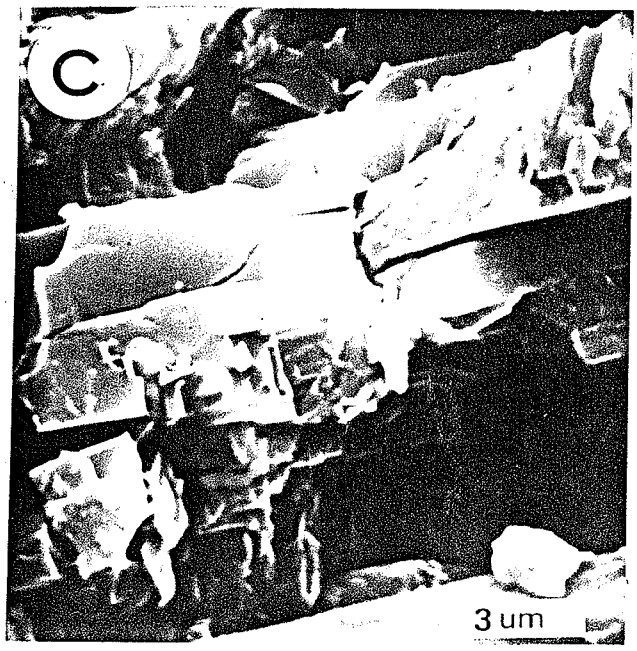
C
3 um

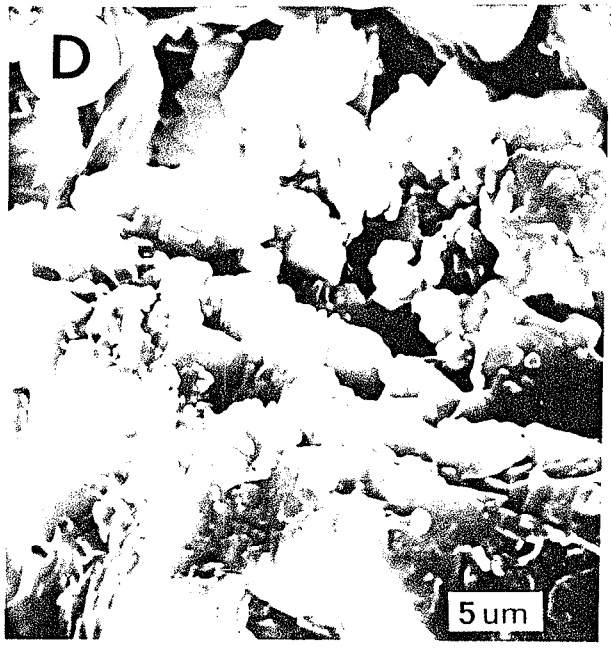
D
5 um

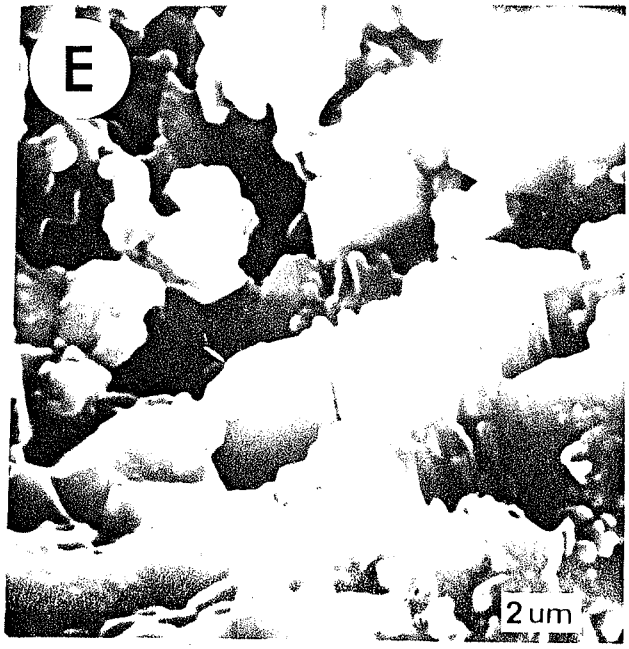
E
2 um


F
1
2
10 um

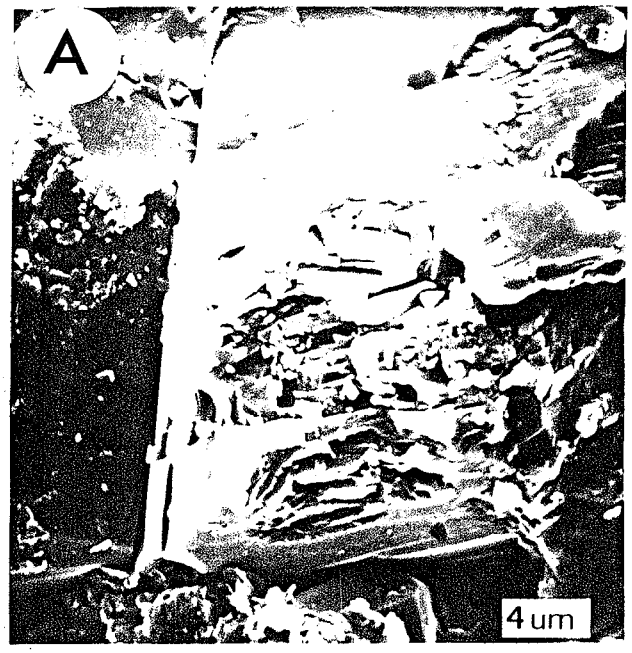
A
4 um

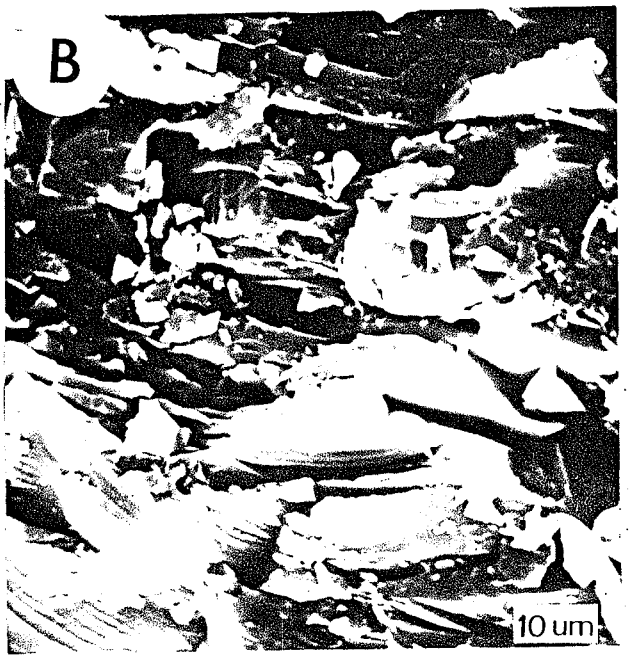
B
10 um

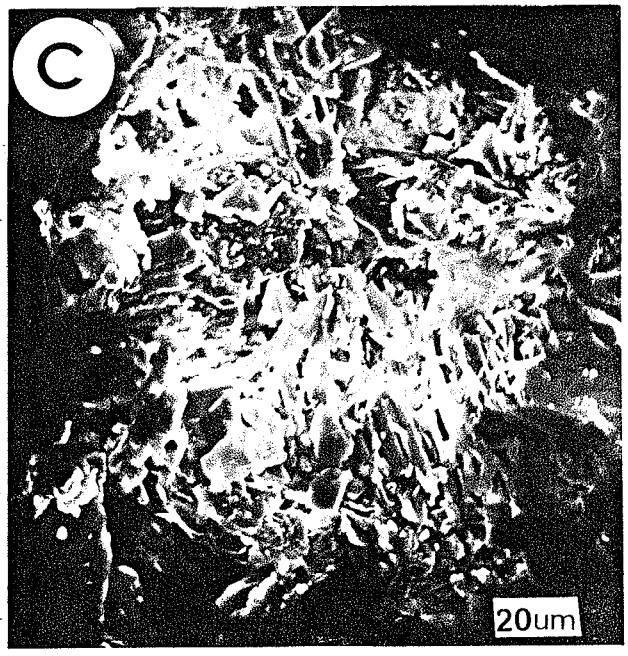
C
20um

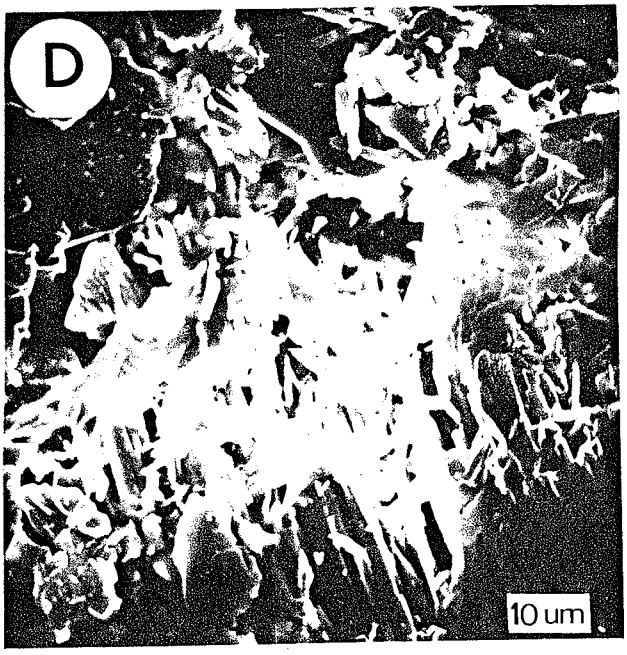
D
10 um


A
Ko
10um

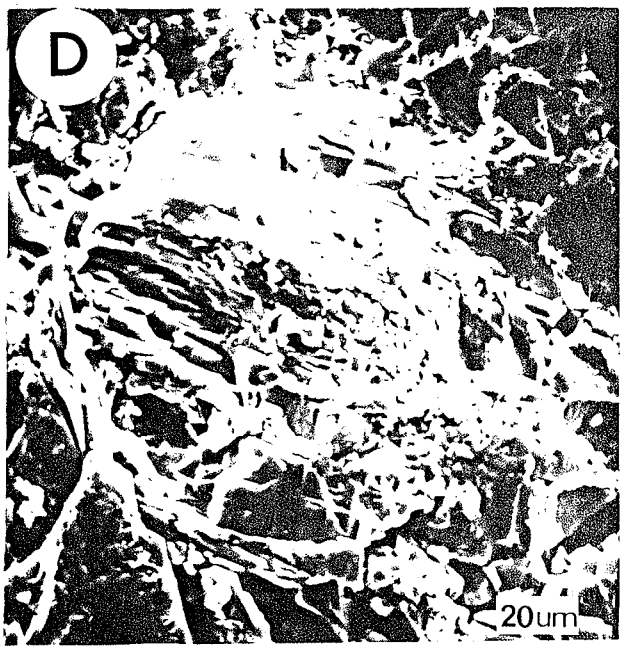
D
20um

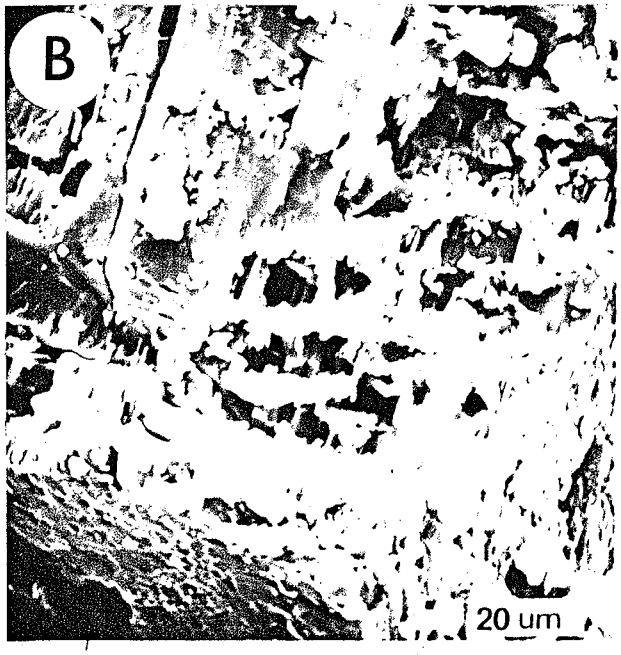
B
20 um

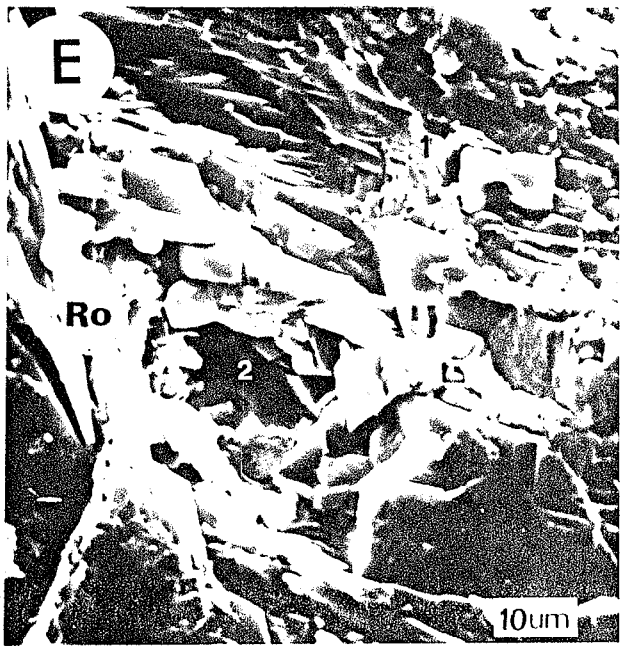
E
Ro
1
2
10um

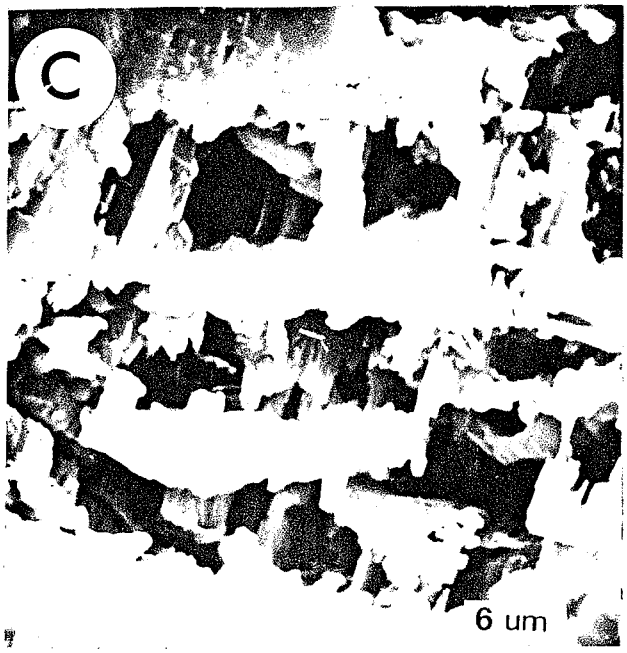
C
6 um

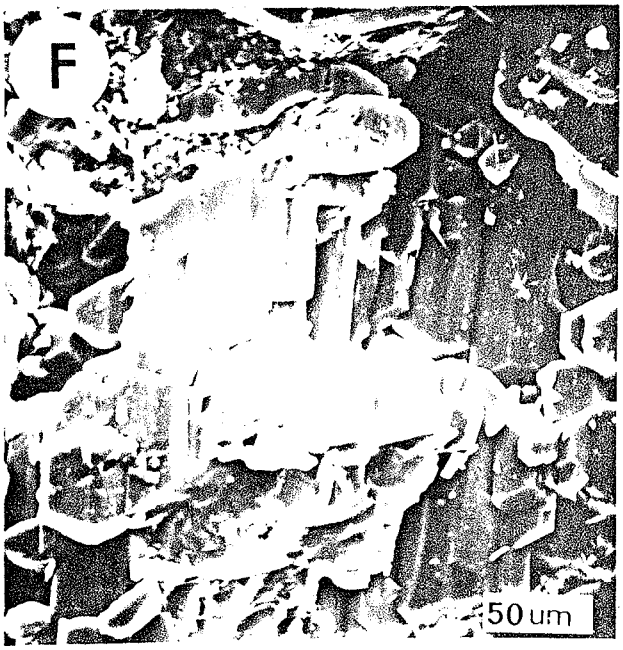
F
50 um

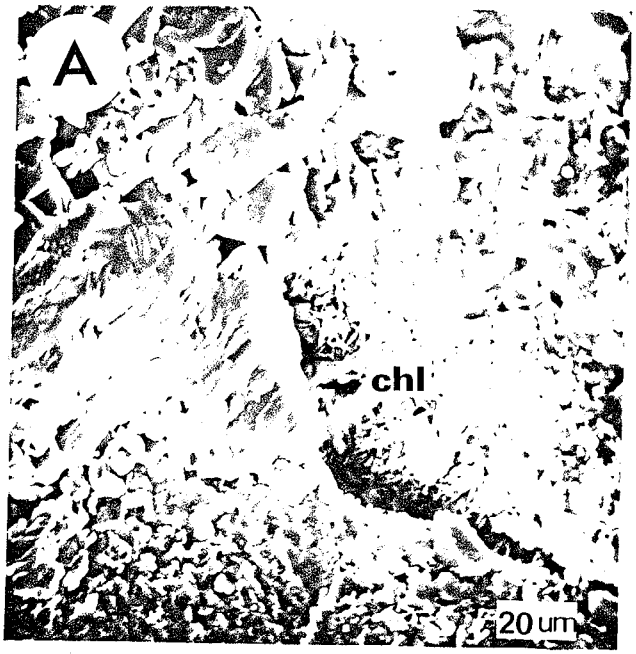
A
chl
20 um

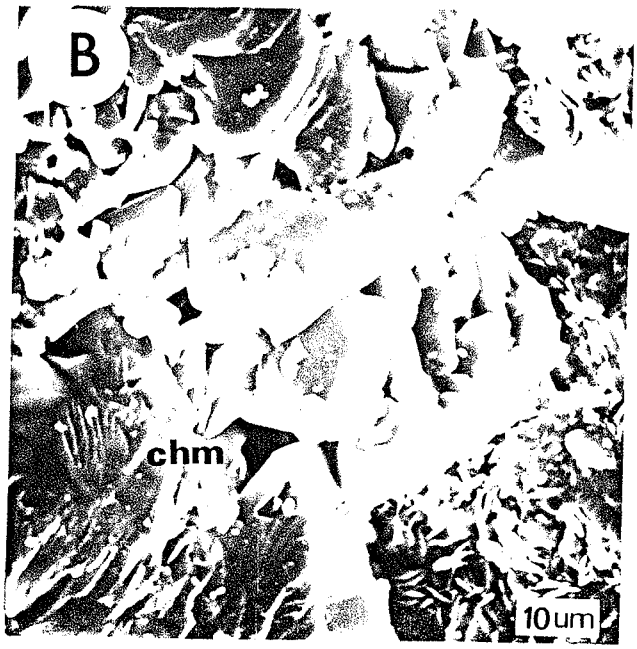
B
chm
10 um

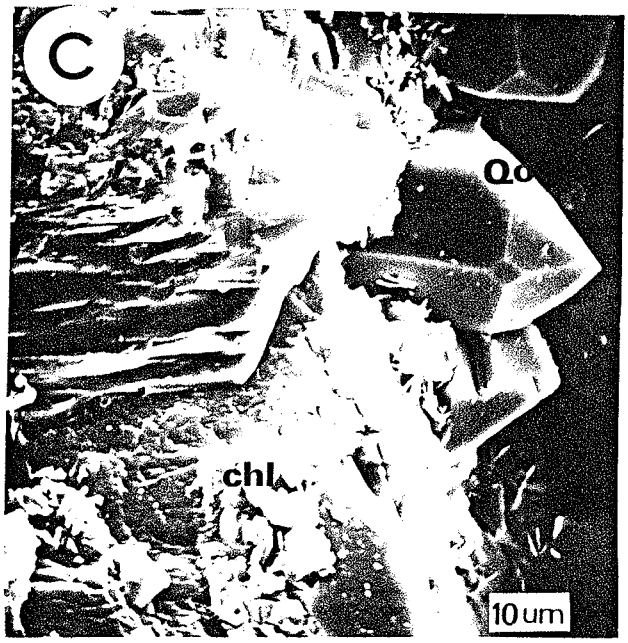
C
Qo
chl
10 um

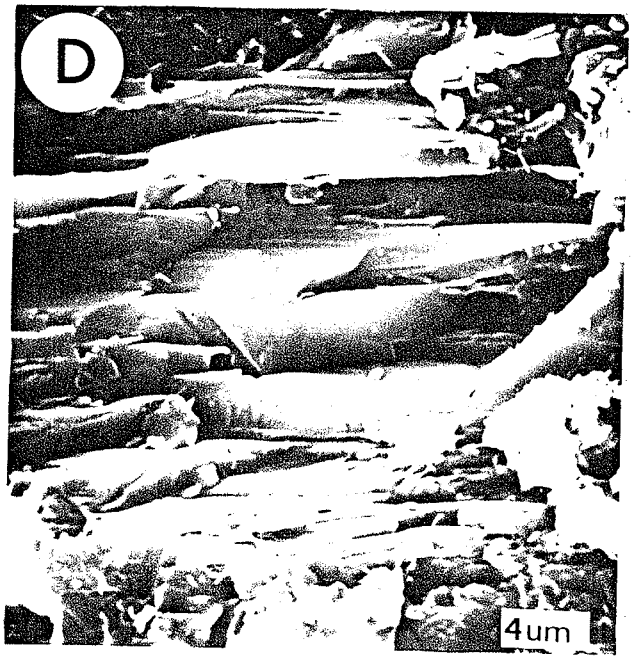
D
4 um

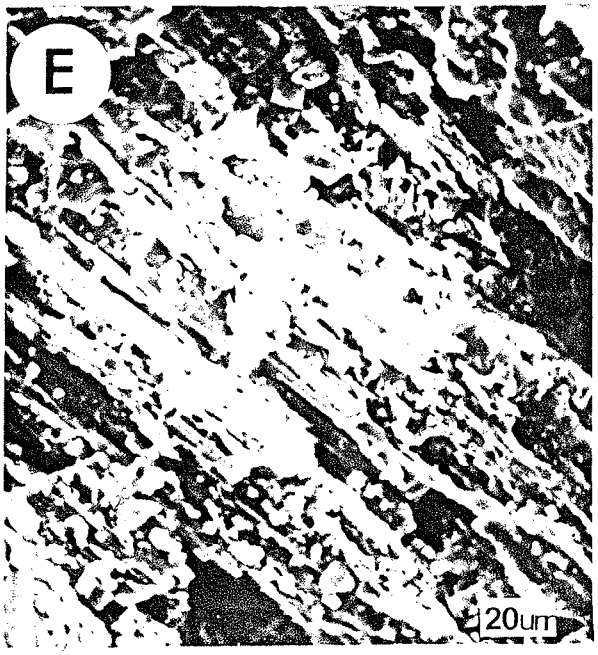
E
20 um

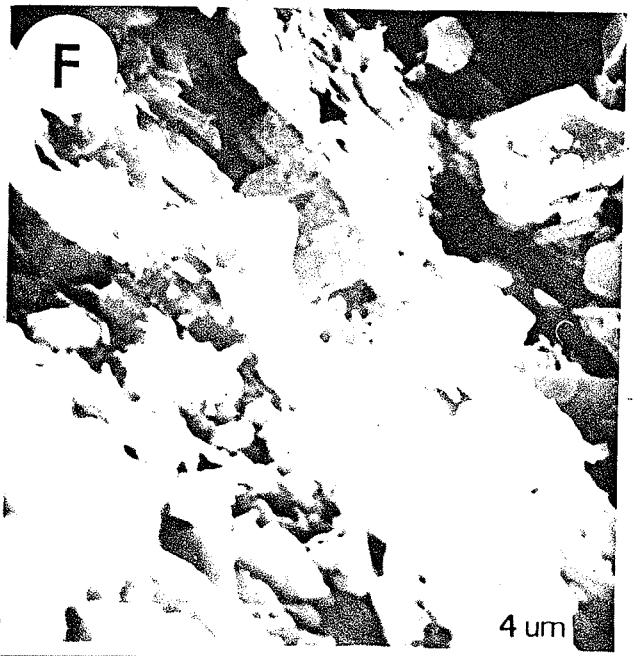
F
4 um

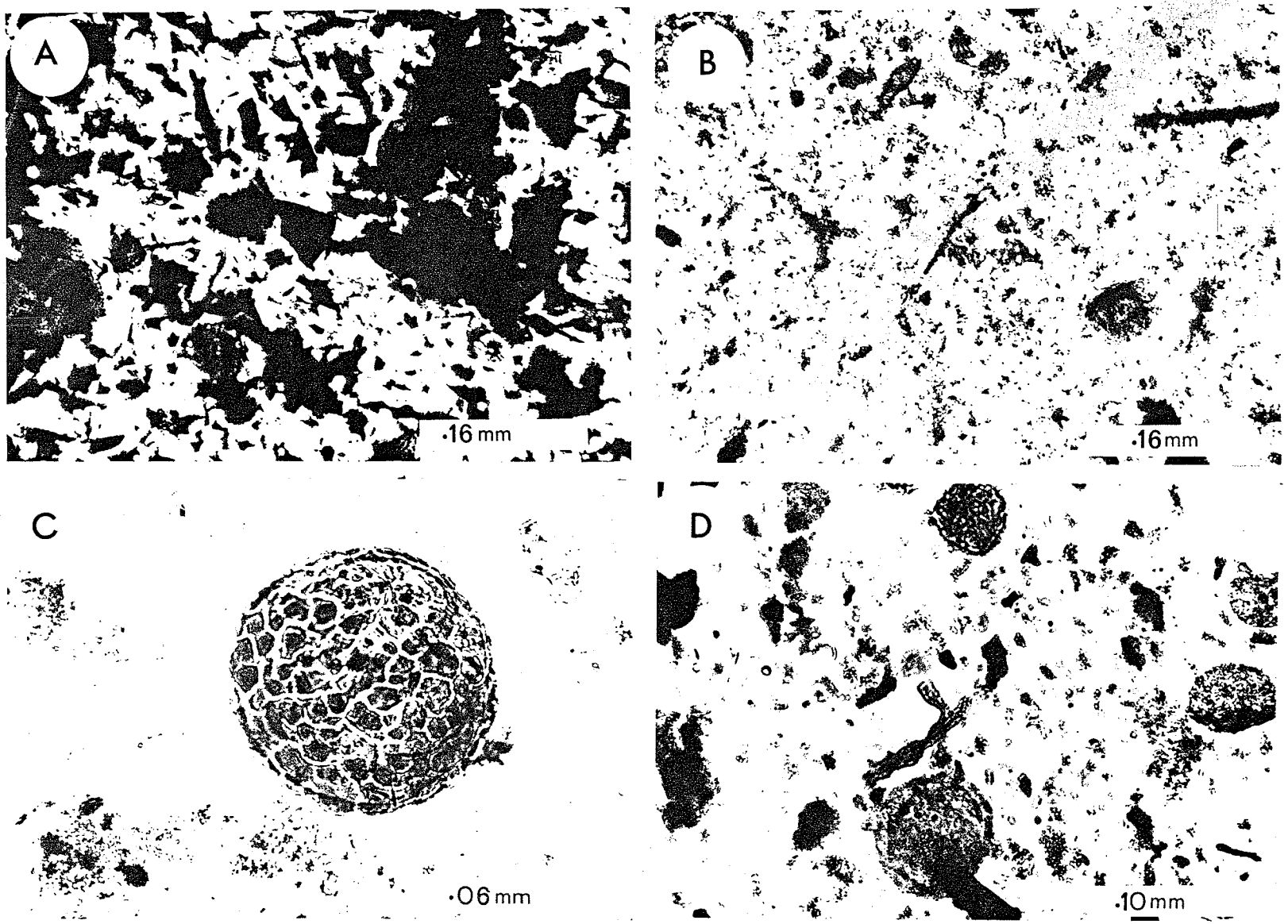
A
.16 mm
B
.16 mm
C
.06 mm
D
.10 mm